V/STOL DYNAMICS AND AEROELASTIC ROTOR-AIRFRAME TECHNOLOGY

Volume I. State-of-the-Art Review of V/STOL Rotor Technology

H. R. ALEXANDER

P. F. LEONE

THE BOEING COMPANY, VERTOL DIVISION

FOREWORD

This report was prepared by The Boeing Company, Vertol
Division of Philadelphia, Pennsylvania, for the Aerospace
Dynamics Branch, Vehicle Dynamics Division, Air Force Flight
Dynamics Laboratory, Wright-Patterson Air Force Base, Ohio,
under Contract F33615-71-C-1310. This research is part of a
continuing effort to develop new and improved techniques for
defining dynamic and aeroelastic phenomena for rotor/propeller-
powered V/STOL flight vehicles under the Air Force Systems
Command's exploratory development program. This contract was
initiated under Project 1370, "Dynamic Problems in Military
Flight Vehicles," Task 137005, "Prediction and Control of
Flight Vehicle Vibration." Mr. A. R. Basso of the Aerospace
Dynamics Branch was the Project Engineer.

The final report is presented in three volumes. The first
volume contains a state-of-the-art review of stability and
blade vibratory loads in V/STOL aircraft. The second volume
contains the development of the analytical methods, the corre-
lation of analytical results with experimental data, and the
results of parametric investigations. The third volume con-
tains a user's guide to the digital computer programs including
input and output formats. The third volume is not being
distributed; however, it is available upon request from the
Air Force Flight Dynamics Laboratory/FYS, Wright-Patterson
Air Force Base, Ohio 45433.

Mr. H. R. Alexander was The Boeing Company, Vertol Division
Project Engineer.

This report covers work conducted from February 1971 through
February 1972. The manuscript was released by the authors in
February 1972 for publication as an AFFDL Technical Report.

This Technical Report has been reviewed and is approved.

WALTER J. MYKYTOW
Assistant for Research and
Technology
Vehicle Dynamics Division

ii

ABSTRACT

The aeroelastic phenomena associated with prop/rotor systems
are discussed and classified. It is concluded that an ac-
ceptable technology exists in several areas, including wing/
rotor divergence, whirl flutter, aeromechanical instability,
and air and ground resonance.

The technology is less successful in those areas where the
flow through the rotor is significantly nonaxial, e.g., tilt-
rotor transition regime and high-speed helicopter flight;
also when forms of intermodal blade coupling exist due to
finite deflections of the blades. It is believed that, in
addition to collective deflections, finite cyclical deflec-
tions of the blades produce destabilizing coupling
effects in some cases. Significantly large edgewise flow in
combination with nonzero blade steady-state deflections is
also seen to be destabilizing.

A minimum-complexity methodology which may be expected to
correlate with currently identified phenomena is defined.

TABLE OF CONTENTS

LIST OF ILLUSTRATIONS

ix

x

LIST OF TABLES

LIST OF SYMBOLS

a	arm from nacelle gimbal pivot to rotor hub
ac	aerodynamic center
C	wing chord
C_a	inertial coupling coefficient between flap and pitch
C_d	aerodynamic stiffness coefficient coupling flap and pitch
C_m, $C_{m\alpha}$	hub pitching moment derivative
C_N, $C_{N\alpha}$	normal force derivative, N_P/q_S
$C_{n\alpha}$	yawing moment derivative
C_T	thrust coefficient
C_v	aerodynamic damping coefficient coupling flap and pitch
$C_{Y\alpha}$	side force derivative
c	blade chord
cg	center of gravity
c_0	nacelle damping rate
D	rotor disc diameter
dC_L/d_α	lift curve slope
H_D	density altitude, feet
Hz	Hertz, cycles per second
I	moment of inertia about flap axis
I_r	product of inertia about pitch-flap axes
I_θ	moment of inertia about pitch axis
J	inflow ratio
K	reduced frequency parameter

K_θ	torsional stiffness of wing at rotor location
L	wing lift
M	Mach number
M_f	blade flap frequency
M_θ	blade pitch frequency
P	per blade revolution, i.e., 1P = one per rev
R	blade radius
r	radial distance from wing tilting line
rpm	revolutions per minute
r/R	radial station along blade length, ratio or percent
S	rotor disc area
S_θ	pitch stiffness
S_ψ	yaw stiffness
V	velocity
V_n	component of circulation velocity normal to disc
V_θ	circulation velocity
x	moment arm from rotor hub to torsional axis
$\dot{Z}$	blade velocity normal to relative wind
$1/2 \rho V^2$	dynamic pressure
α	angle of attack, degrees; elastic twist of wing
α_o	initial incidence of the wing
α_2	rate of change of blade pitch with respect to blade lag
Γ	strength of bound vortex of wing
γ	Lock number, $2\Pi \rho C R^4 / I$
$\Delta\alpha$	small change in wing angle

δ_3	rate of change of blade pitch with respect to blade flap
ζ	lead-lag freedom
η_f	flap frequency ratio
θ	nacelle pitch angle
θ_t	blade twist
Λ	angle between relative wind and blade chord
λ	advance ratio, V_{AXIAL}/V_{TIP}
μ	$V_{NORMAL\ TO\ SHAFT}/V_{TIP}$
ρ	density of air
σ	rotor solidity, total blade area/total disc area
ψ	blade azimuth position, degrees; nacelle yaw angle
Ω	angular velocity of the rotor shaft; rotor speed, rpm
ω_b	natural frequency of an individual blade
ω_F	flutter frequency
ω_h	wing-nacelle bending, torsion natural frequency
ω_L	rotating natural frequency of blade lead-lag mode
ω_R	rotating natural frequency of blade
ω_β	uncoupled rotating flap natural frequency
ω_θ	uncoupled rotating pitch natural frequency
ω_ψ	nacelle yaw natural frequency

Part I. Stability in V/STOL Aircraft

H. R. Alexander

INTRODUCTION

Until quite recently it was possible to regard the aeroelastic stability problems of helicopter rotor systems and those of fixed-wing aircraft as distinct areas of technology whose study could quite properly proceed independently. The first serious departure from this state of affairs occurred with the Electra accidents of 1959 in which the propeller dynamic effects specifically provided the unstable mechanism which led to wing failures. After certain fatigue failures in the engine mounting structure, a whirling oscillation of the propeller would occur in a mode similar to the retrograde motion of a gyroscope. In contrast to a gyroscope, which experiences only damping force, the propeller aerodynamic forces beyond a certain speed always tend to feed energy into the whirling motion, with catastrophic results in the case of the Electra.

As an outcome of these incidents, the phenomenon of propeller whirl, which had been previously recognized in the design of engine mountings, was reformulated for the total dynamic system consisting of the airframe, propeller, engine and mounting structure, including the propeller's aerodynamic forces and moments.

The helicopter phenomenon known as ground resonance was successfully formulated by Coleman (1) in terms of the interaction of the rotor system with fuselage degrees of freedom which provided significant amplitudes of vibration in the plane of rotation of the rotor. Prior to that time the aeroelastic behavior of helicopter blades had been considered independently of the rest of the system. It now became apparent that fuselage and landing gear properties could interact with the rotor to exhibit overall system instabilities. While the propeller whirl phenomenon encountered on the Electra involved propeller blades, adequate predictions could be made assuming that the blades were structurally rigid. Prediction of ground resonance behavior, however, required lead-lag blade freedoms to be accounted for while the airframe motion was generally rolling in a rigid-body mode. These phenomena then are opposite extremes in a spectrum of interaction of rotary-wing and fixed-wing dynamic behavior.

Subsequent developments in V/STOL and helicopter design have led to nearly every possible degree of interactive relationship. In tilt-wing transport aircraft detailed account must be taken of the airframe dynamic properties, but the prop/rotor blades may only need to be represented by a fundamental bending mode since they are relatively stiff, but not sufficiently so to be considered rigid. Tilt-rotor V/STOL designs generally feature large-diameter rotors and relatively low blade frequencies so that accurate representation of the rotor blade structural modes as well as the airframe is required. Hence, in tilt-rotor configurations, the analyst is concerned with preventing the occurrence of helicopter-type phenomena

3

such as ground and air resonance, airplane-type phenomena
such as whirl flutter involving blades and wings, classical
flutter of the airframe and individual blades, and a variety
of instabilities caused by adverse coupling between the flap,
lag, and pitch freedoms of the blades. Limit-cycle instabili-
ties of a nonlinear nature must also be avoided.

It is evident that the conventional treatment of blade insta-
bility, wing stability, ground resonance, etc., as separate
phenomena is not valid in such cases and that a comprehensive
methodology is required. While most of the instability
mechanisms are well understood when viewed as general physical
phenomena, it is not uncommon in specific cases for an air-
craft to be in serious trouble because of one or more of them.
More than a general qualitative understanding is required
when margins of safety are to be established. Precise quan-
titative methods of analysis are required.

It is the purpose of this review to assess the problems which
are known to exist and the methods available for their predic-
tion. The limitations of the methodology in relation to known
behavior will be defined.

CLASSIFICATION OF UNDESIRABLE AEROELASTIC EFFECTS

We may group the phenomena under discussion into several
distinct categories.

Mechanical Instability (Ground and Air Resonance)

Mechanical instability is a phenomenon in which the inertial
coupling between blade lagging motion and hub motion in the
plane of the rotor produces a growing oscillation (see
Figure 1). This may occur on the ground or in flight. The
introduction of rotor aerodynamic effects may modify the
severity and parametric boundaries of this type of phenomenon
but the essential nature of these instabilities remains the
same. Early studies (1) showed that this type of instability
can occur only when the blade lead-lag frequency is below 1P
and when the mounting frequency equalled $\Omega - \omega$ blade.

Aeromechanical Instability

When aerodynamic forces are present, an instability involving
mechanical coupling has been experienced which involves a
lead-lag mode above 1 per rev (2) (see Figure 2). This showed
a similar coalescence of hub frequency as in ground resonance,
but in this instance the instability occurred when the hub
frequency was equal to $\Omega + \omega$ blade.
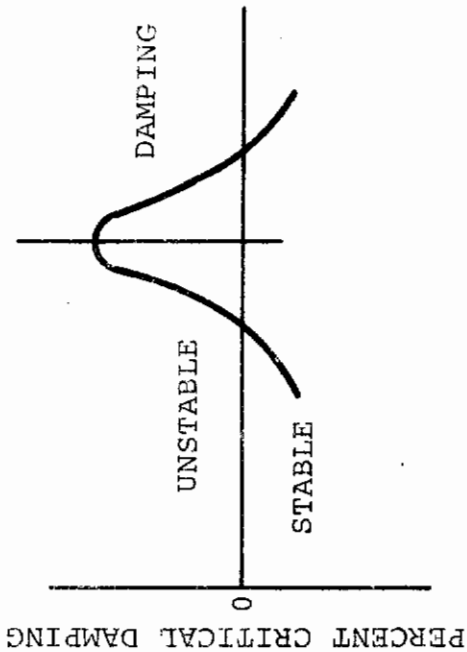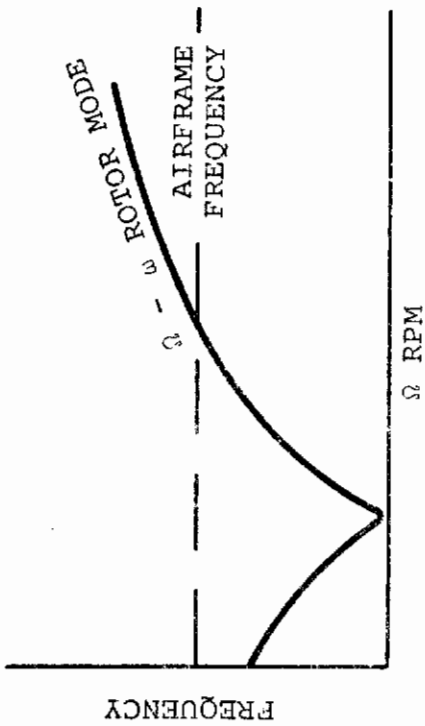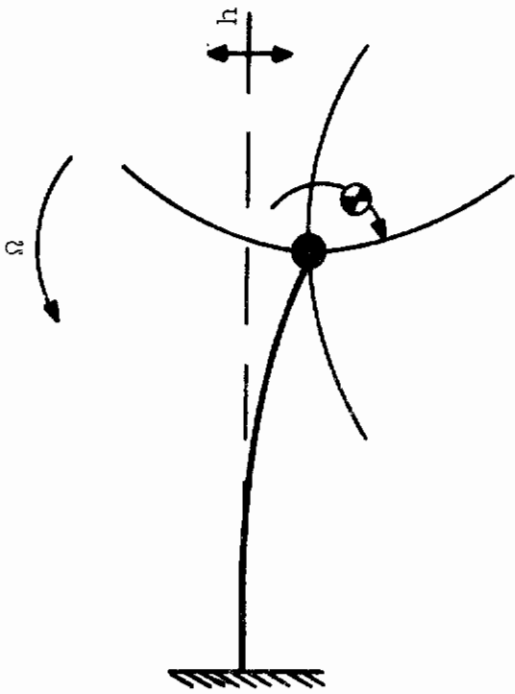
4

Figure 1. Characteristic Features of Mechanical Instability
(Air and Ground Resonance)

5

- BLADE FREQUENCY GREATER THAN Ω
- HIGHER ROTOR MODE INVOLVED
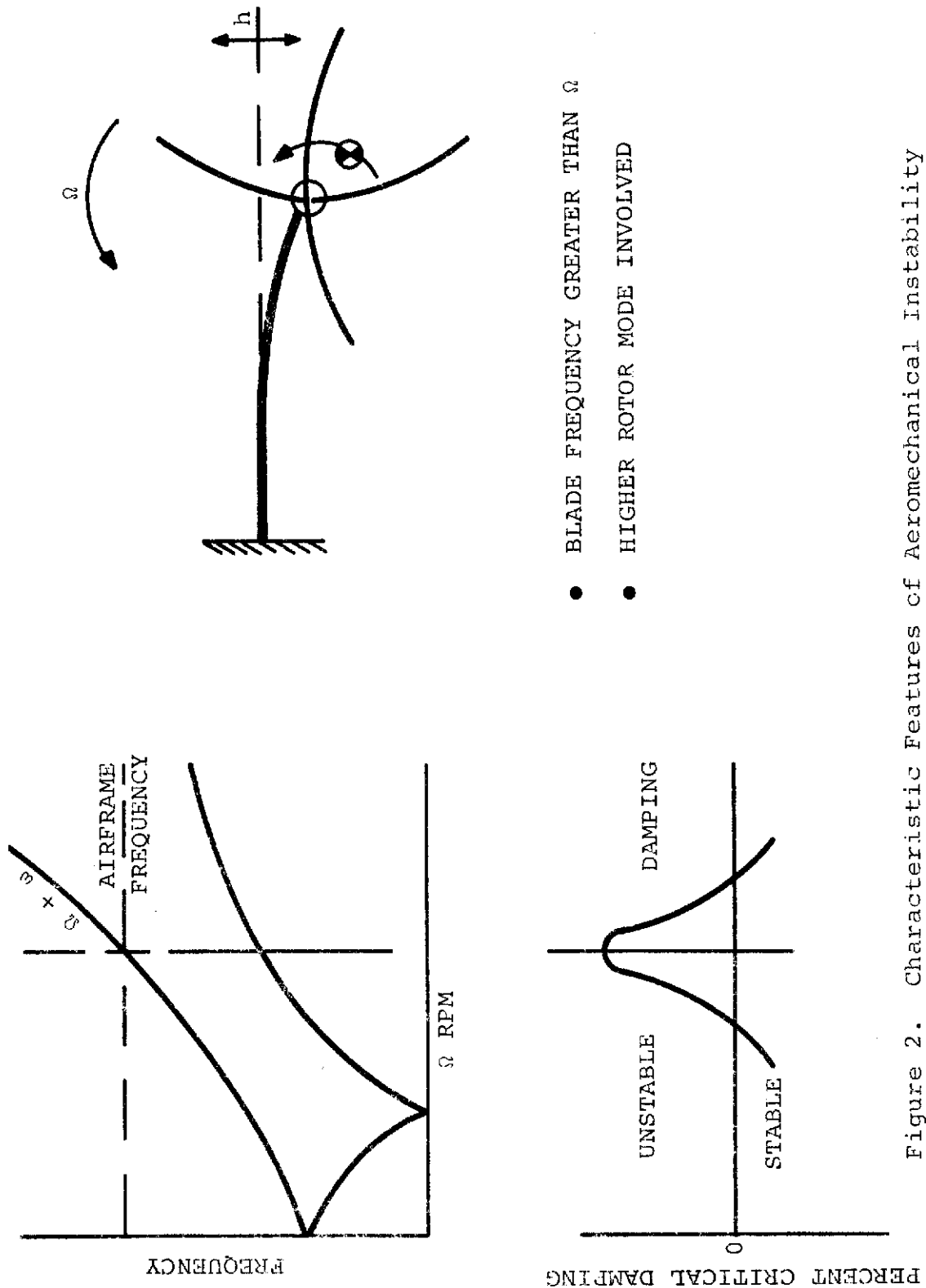
Figure 2. Characteristic Features of Aeromechanical Instability

Static Divergence

At the high advance ratios associated with cruise flight in
tilt-rotor V/STOL aircraft, the aerodynamic forces acting on
the rotor when its axis is inclined to the freestream provide
a large component of lift which is significantly destabilizing
in the static aeroelastic sense. Prediction of divergence
involves an analysis taking account of wing and blade struc-
tural properties and the aerodynamic effects of the net flow
through the rotor. Prop/rotors generate side forces and yaw-
ing moments as well as normal forces and pitching moments when
inclined to the freestream, so that yawing as well as tor-
sional flexibility must be considered in a conservative
analysis as indicated in Figure 3. Prediction capability for
divergence is in a reasonably satisfactory state as indicated
by Figure 3, showing predictions accurate within $\pm$ 6 percent
for the Boeing-Vertol Model 213 1/9-scale stowed-rotor con-
version model, shown in Figure 4.

Whirl Flutter

The term whirl flutter was originally used to describe the un-
stable whirling motion of propeller assemblies which occurs if
inadequate stiffness and damping are present in the mounting
system. The tendency toward instabilities in anti-vibration
mountings of engine-propeller packages was pointed out by Taylor
and Brown in 1938 (see Reference 3). The pitching and yawing
motion of the engine and propeller occurred in a manner that was
not significantly coupled with the rest of the airframe. While
anti-vibration mountings had the advantage of reducing vibration
levels, it meant that the effective inertias and stiffness of the
engine-propeller were approximately the same in pitch and yaw.
Since the principal coupling between pitch and yaw was gyroscopic
due to propeller rotation, a disturbance in either degree of
freedom would result in a whirling motion of the hub which was
nearly circular. Two modes existed, one retrograde in which the
direction of whirl was in the opposite direction to the shaft
rotation and the other posigrade with the direction of whirl in

the same direction as the shaft rotation. As forward speed
increases from zero, the total damping in the whirl modes
changes. Initially damping in the retrograde mode increases
with speed but eventually begins to reduce until finally the
system becomes unstable. A definitive discussion of the classi-
cal whirl flutter phenomenon is given in Reference 3: the onset
of such a flutter may be accurately predicted by analysis and
has been avoided by the provision of adequate stiffness, damp-
ing, and failsafe characteristics.

In the context of large prop/rotors, the term whirl flutter
has come to be habitually applied to instabilities involving
blade flapping and significant amounts of airframe motion.

FOR STATIC EQUILIBRIUM
INCREMENTAL DEFLECTIONS ARE GIVEN BY

$$\begin{bmatrix} \text{STIFFNESS MATRIX STRUCTURE AND CENTRIFUGAL} \end{bmatrix} \begin{Bmatrix} \Delta P \\ \Delta Y \\ \Delta \theta C \\ \Delta \theta S \end{Bmatrix} = q \begin{bmatrix} \text{AERODYNAMIC DERIVATIVE MATRIX} \end{bmatrix} \begin{Bmatrix} P_0 \\ Y_0 \\ \theta C_0 \\ \theta S_0 \end{Bmatrix} + \begin{Bmatrix} \Delta P \\ \Delta Y \\ \Delta \theta C \\ \Delta \theta S \end{Bmatrix}$$

$$\begin{Bmatrix} \Delta P \\ \Delta Y \\ \Delta \theta C \\ \Delta \theta S \end{Bmatrix} = \left[\left(\text{STIFFNESS MATRIX} \right) - q \left(\text{AERODYNAMIC DERIVATIVE MATRIX} \right) \right]^{-1} \times q \left(\text{AERODYNAMIC DERIVATIVE MATRIX} \right) \begin{Bmatrix} P_0 \\ Y_0 \\ \theta C_0 \\ \theta S_0 \end{Bmatrix}$$
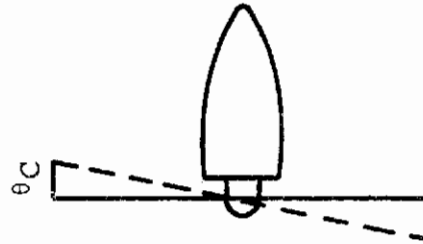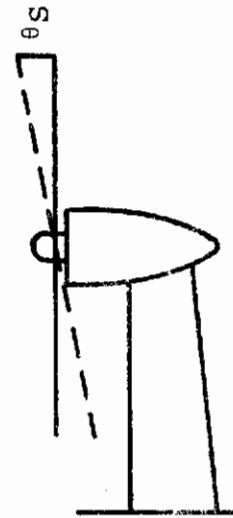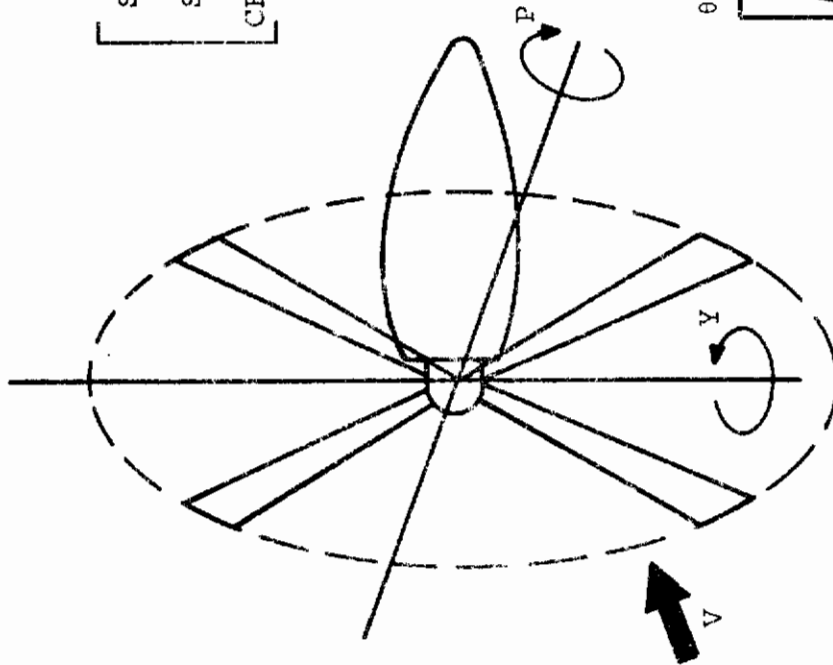
- WING AERODYNAMIC CONTRIBUTION NOT SHOWN
- P = AMOUNT OF WING AND NACELLE TWIST SENSED AT ROTOR
- Y = AMOUNT OF HORIZONTAL BENDING SLOPE SENSED AT ROTOR

Figure 3. Mechanism of Static Divergence for Wing with Flexible Rotor

- AT 1,000 RPM DIVERGENCE PREDICTED AT 170 FT/SEC
- DIVERGENCE OCCURRED AT 160 FT/SEC
- ACCOUNTING FOR WING-INDUCED FLOW REDUCED THEORETICAL VALUE TO 150 FT/SEC
- PREDICTED VALUES CORRECT WITHIN ± 6 PERCENT
- BLADE FREQUENCIES

  0.76 PER REV
  1.26 PER REV
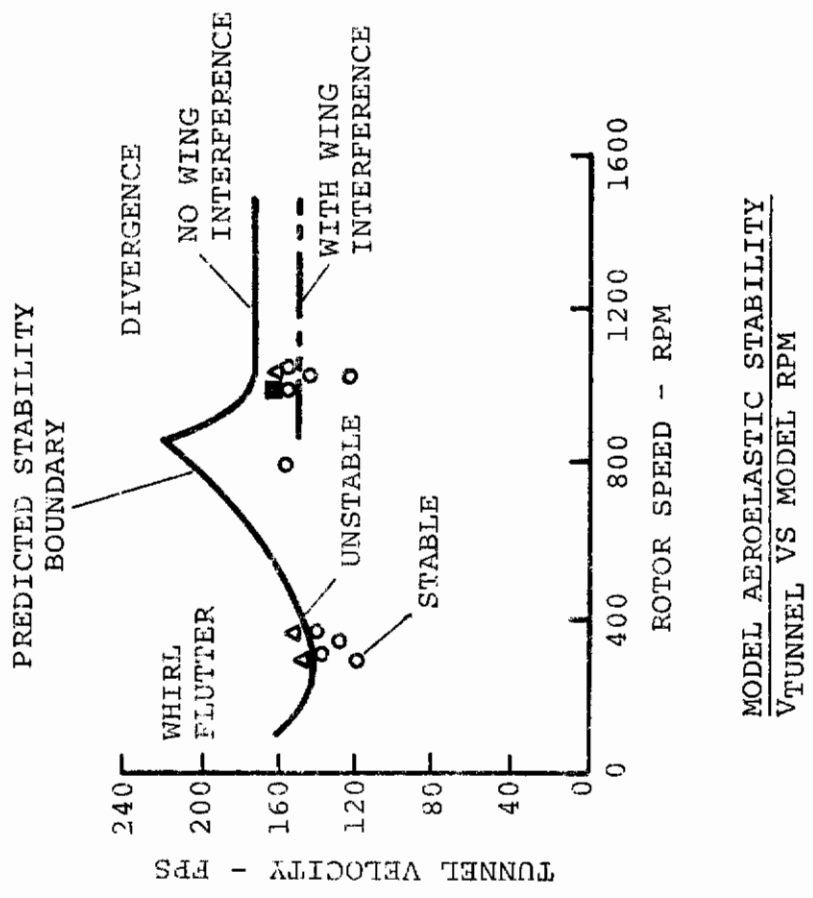
TEST POINTS

○ STABLE
△ FLUTTER
■ DIVERGENCE

PREDICTED STABILITY BOUNDARY

DIVERGENCE

NO WING INTERFERENCE

WITH WING INTERFERENCE

WHIRL FLUTTER

UNSTABLE

STABLE

ROTOR SPEED – RPM

TUNNEL VELOCITY – FPS

MODEL AEROELASTIC STABILITY
V_{TUNNEL} VS MODEL RPM

Figure 4. Prediction of Static Divergence of M213 1/9-Scale Conversion Model with Reduced-Stiffness Wing Spar by C-40 and C-41 Computer Programs

The degrees of freedom involved may be such that no significant whirling motion of the hub is observed. Degrees of freedom participating in such a case may be wing vertical bending and torsion and blade flapping. However, the flapping behavior of the blades will be patterned such that the tip path plane is pitching and yawing and therefore, in a certain sense, whirling. Many cases correctly classified as whirl flutter may exhibit significant amounts of lead-lag blade motion; this occurs when the blades are highly twisted and the modes have strong components of both flap and lag. Lead-lag motion will also be present as a forced response when there is significant in-plane hub motion present in the airframe contribution to the whirl mode.

Distinguishing Features of Whirl Flutter, Mechanical Instability, and Aeromechanical Instability

It is useful to distinguish between the various instabilities on the basis of the following frequency and modal participation criteria.

Whirl flutter involves predominantly flapping blade modes: these will most often have frequencies above 1 per rev since the centrifugal stiffening will automatically ensure this unless special features such as negative δ_3 are present in the blade. Frequency coalescence of rotor natural modes with airframe modes is not a requirement since whirl flutter may occur even with rigid blades. Individual blade motion in the flutter mode will be complex but may generally be resolved into the two frequency components $\Omega \pm \omega_F$ which are expected when a rotating system is excited at a fixed system frequency ω_F.

In contrast, mechanical instability and aeromechanical instability will generally exhibit a clear coalescence of modal frequency in the rotor and in the fixed system. The presence of hub motion in the plane of the rotor and of lead-lag blade motion is a requirement. In twisted blades noticeable amounts of blade flapping may also be present.

Air and ground resonances involve blade lead-lag freedoms below 1 per rev; aeromechanical instability involves lead-lag freedoms above 1 per rev. In the first case an airframe frequency ω is coalescent with the lower rotor frequency $\Omega - \omega_b$ and in the aeromechanical case the coalescence occurs in the upper rotor frequency $\Omega + \omega_b$.

These frequency relationships in the unstable mode along with the predominant blade motion will give a clear indication, in almost all cases, of the mechanism of the instability. These characteristics are summarized in Table I.

10

TABLE I

INSTABILITIES ENCOUNTERED IN PROP/ROTOR VEHICLES

Instability	Principal Freedoms	Frequency Characteristics	Comments
Whirl Flutter	Pitch, yaw of prop, blade flapping, hub linear and angular motion	$\omega_B > \Omega$ $\omega_I = \omega_{AIRFRAME}$ $\omega_{BF} = \Omega \pm \omega_{AIRFRAME}$	ω_B = blade natural frequency ω_{BF} = frequencies of blade oscillation in the flutter mode
Ground Resonance	Blade lead-lag linear hub motion in plane of rotor	$\omega_B < \Omega$ $\omega_I = \omega_{AIRFRAME} = (\Omega - \omega_B)$	
Air Resonance	Blade lead-lag linear hub motion in plane of rotor	$\omega_B < \Omega$ $\omega_I = \omega_{AIRFRAME} = (\Omega - \omega_B)$	Essentially same as ground resonance. Aerodynamic damping may be stabilizing.
Aeromechanical Instability	Blade lead-lag linear hub motion in plane of rotor	$\omega_B > \Omega$ $\omega_I = \omega_{AIRFRAME} = (\Omega + \omega_B)$	Essentially same as air resonance, although blade frequency above 1/rev.
Limit-Cycle Instabilities	Blade flapping, pitching, and lead-lag plus linear and angular hub motion	$\omega_I = \omega_{AIRFRAME} = (\Omega \pm \omega_B)$	Blade deflections due to flight conditions provide flap-lag-pitch coupling.

Blade Instabilities

Instabilities of the rotating blade are a category which
involve detailed treatment of the blade internal properties
such as chordwise center of gravity location relative to the
elastic axis and blade deflections under load. The influence
of centrifugal and coriolis forces and interactions of flap,
lag, and pitch or torsion when the blade is deflected are
further effects which must be considered. This means that the
analysis of blade instabilities is inherently more difficult
than the phenomena discussed in the preceding paragraphs.

In addition to blade classical pitch-flap flutter, pitch-lag,
pitch-flap, and pitch-lag-flap mechanisms may be present due
to blade deflections, actual or effective δ_3 and α_2, steady
thrust and torque, and coriolis coupling between flap and lag.
Hub motion due to airframe vibratory freedoms will generally
couple with the blades if there is an instability due to any
of these mechanisms, so that the oscillatory motion of the
blades will assume a pronounced overall rotor pattern with
superficial similarity to ground or air resonance or whirl
flutter.

The detailed discussion of blade instabilities is presented
after the discussion on classical rotor airframe problems.
It is concluded that a comprehensive capability requires the
inclusion of blade effects normally ignored in the analysis of
whirl flutter and mechanical instabilities. These effects,
such as blade finite deflections, seem to provide the neces-
sary mechanisms to explain the occurrence of limit-cycle
behavior and other phenomena not falling into the traditional
classifications.

Stall Flutter

The aerodynamic nonlinearity associated with stall provides
the mechanism for a single-degree-of-freedom instability in
blade pitch or torsion. This may become a serious source of
blade and pitch link loads if the blade is operating with a
significant proportion of its span in stall. This occurs most
frequently in high-speed helicopter flight where the retreat-
ing blade experiences large excursions of angle of attack.
The destabilizing effect of stall and its effect on blade and
pitch link loads is discussed in full detail in Part II and
will not be pursued further in this section.

TECHNICAL ASPECTS OF CLASSICAL ROTOR/AIRFRAME INSTABILITIES

MECHANICAL INSTABILITY OF ROTOR/AIRFRAME SYSTEMS

Ground resonance has been the most frequently encountered form of mechanical instability experienced in helicopters, and for many years has been predicted with sufficient accuracy that preventive measures have generally been successful. The phenomenon most often involves a coupled horizontal and rolling motion of the blades in which the overall center of gravity of the rotor disc precesses about the rotor shaft in the opposite direction to shaft rotation, as indicated schematically in Figure 1. The precession of the disc center of mass creates periodic inertia forces which are reacted at the hub. This produces a forced response in the pylon and airframe. A potentially unstable situation exists if the precession frequency is near that of a normal mode of the rest of the system. However, the occurrence of an instability depends on a number of parametric conditions. These include, but are not limited to, the amount of linear motion at the rotor hub normal to the shaft, the relative magnitude of blade and airframe masses, and damping in the blade and aircraft degrees of freedom.

The frequency at which the retrograde motion of the blade center of gravity occurs is $\Omega - \omega_b$, where Ω is the angular velocity of the rotor shaft and ω_b is the natural frequency of an individual blade. Since the regression mode frequency is directly related to Ω, a number of potentially unstable resonances may occur within the operating rpm range. In conventional helicopters the frequencies of the aircraft on the ground are those most likely to provide coalescence with the rotor frequencies. This type of instability, known as ground resonance, has been successfully prevented in conventional helicopter configurations by the use of blade lag dampers and careful choice of landing gear parameters. A definitive analytical treatment of this problem is given in Reference 1 by R. P. Coleman. This basic approach continues to be used successfully in conventional helicopter work.

A single-rotor helicopter on its landing gear has four sources of hub displacement in the plane of the rotor; these are the two coupled lateral-roll oscillations of the fuselage and the two coupled longitudinal-pitch characteristics. In a tandem helicopter, fuselage yaw introduces an additional source of lateral hub motion which needs to be considered in ground stability analyses. The possibilities of mechanical instability might be expected to increase in tilt-rotor configurations where the rotor is mounted at the tip of the wing, since the number of potentially unstable situations expands by the number of wing modes within reasonable proximity of foreseeable rotor speeds. However, Figure 5 illustrates a typical

13

AIRCRAFT COUPLED FREQUENCY - HZ

ROTOR

HIGHER MODE

$\Omega + \omega_R$

ROTOR

LOWER MODE $\Omega - \omega_R$

l
k
j
i
h
g
f
e
d
c
b
a

CRUISE   HOVER

ROTOR SPEED, Ω - RPM
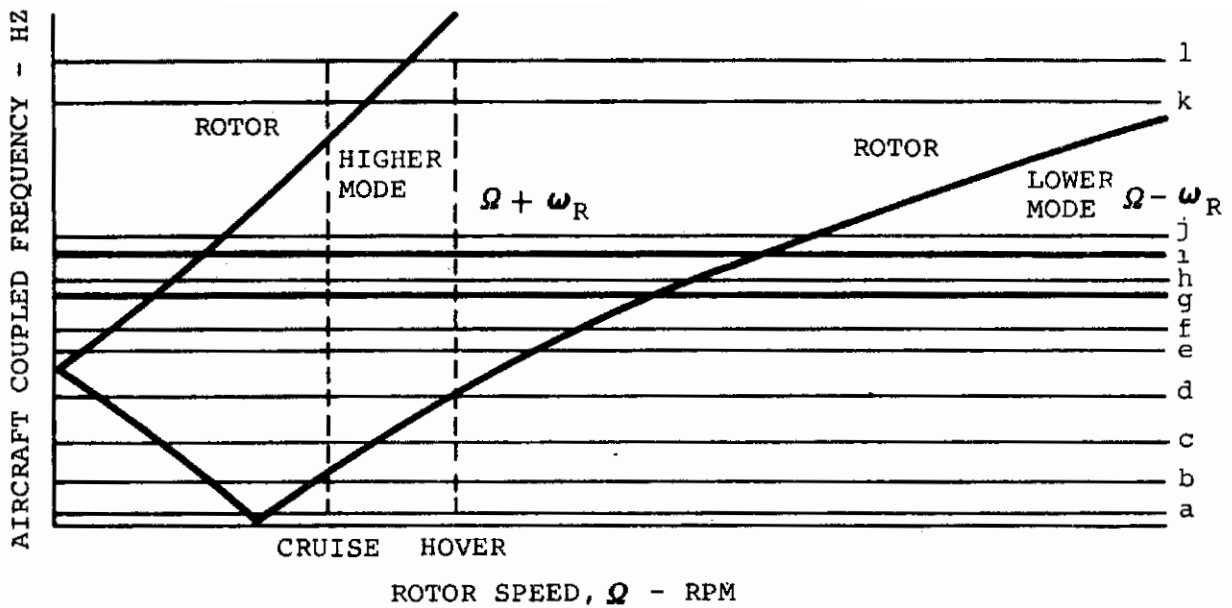
LEGEND:
a. A/C ROLL
b. A/C YAW
c. A/C PITCH
d. A/C VERTICAL
e. A/C LATERAL
f. WING SYM VERT BEND
g. WING SYM FWD BEND
h. WING ANTI-SYM VERT BEND
i. WING ANTI-SYM FWD BEND
j. A/C FORE AND AFT
k. WING SYM TORSION
l. WING ANTI-SYM TORSION

AIRCRAFT FREQUENCY SPECTRUM ON GROUND WITH QUASI-NORMAL BLADE LAG MODES

CRITICAL DAMPING ASSUMED
0.5% IN BLADES
1.0% IN FLEXIBLE AIRFRAME MODES
3.0% IN RIGID BODY MODES

PERCENT CRITICAL DAMPING

NEGATIVE

UNSTABLE

STABLE

WING SYM BENDING

WING A/S BENDING

A/C LATERAL

ROTOR SPEED, Ω - RPM

DAMPING IN MARGINAL AND UNSTABLE MODES
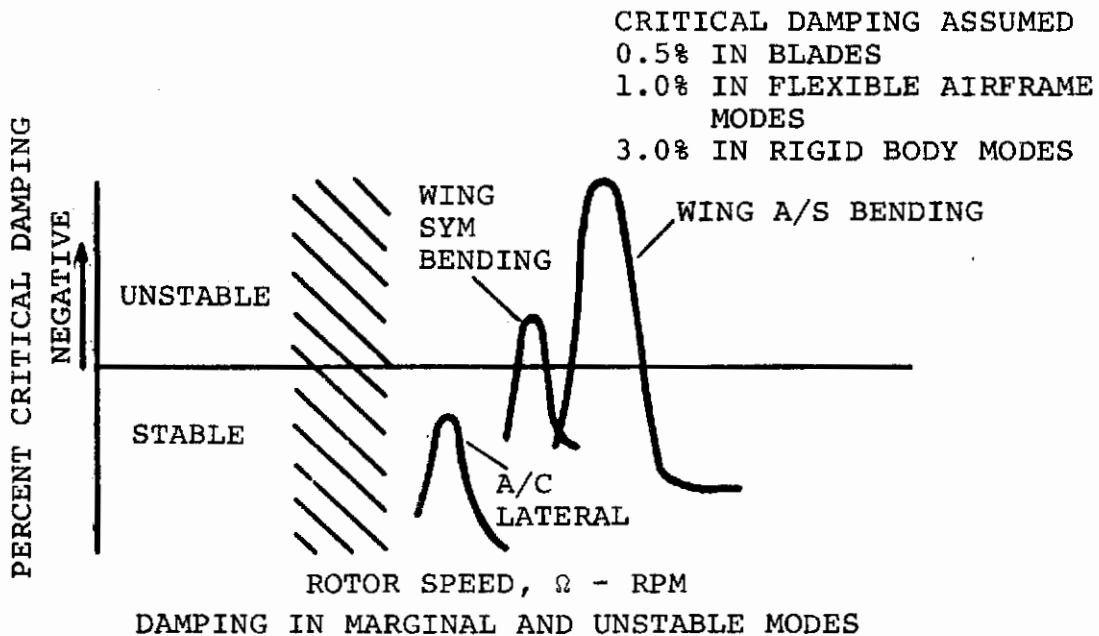
Figure 5.   Summary Chart of Potential and Predicted Mechanical Instabilities on a Tilt-Rotor Design

14

situation existing in one tilt-rotor design. The operational rpm range is stable and the aircraft lateral mode, which is troublesome in most helicopters, occurs at a frequency beyond maximum hover rpm and is stable for small nominal amounts of blade structural damping (i.e., heavy lag dampers required in most helicopter applications). The two instabilities predicted occur at frequencies well beyond the design rpm range and involve wing horizontal bending in the symmetric and anti-symmetric modes.

When the aircraft is in flight, the rigid-body degrees of freedom may usually be disregarded because their frequencies from a structural stability standpoint become approximately zero. However, the airframe frequencies persist with little change in magnitude or mode shape into the flight regime and instabilities of a mechanical nature occurring in flight are referred to as air resonance. The potential for instability due to frequency coalescence continues into the cruise regime of tilt-rotor aircraft and a changing spectrum of frequencies needs to be considered as the rotor and nacelle tilt from the vertical hover mode to the cruise mode. Blade damping increases rapidly with collective pitch and inflow velocity to the extent that conventional air resonance in the cruise mode is generally not a problem.

The predictive capability for helicopter ground resonance has been acceptable for many years. Good predictive capability has also been established in tilt-rotor work as shown by Figure 6. In this test of a 1/9-scale Boeing Folding Tilt-Rotor model (4), mechanical instability was predicted at 1,050 rpm and 1,070 rpm with wind velocities of 140 feet per second and 104 feet per second respectively. A mild air resonance condition was experienced in test at 1,050 rpm and 104 feet per second. The unstable region is associated with coalescence of the wing vertical bending frequency and the lower $(\Omega-\omega_L)$ rotor frequency and extends to either side of the point of intersection of the frequency curves.

AEROMECHANICAL INSTABILITY

The mechanical instabilities discussed in the preceding paragraph are associated with the lower $(\Omega-\omega_L)$ lead-lag mode of rotors having blade natural frequencies below 1 per rev. Reference 2 described an instability which involves mechanical coupling between the rotor upper lag frequency $(\Omega+\omega_L)$ and linear motion of the hub. The interesting feature of this case is the fact that the blade lead-lag frequency involved is significantly above 1 per rev. Predictive capability appears to be excellent as shown in Figure 7.

15
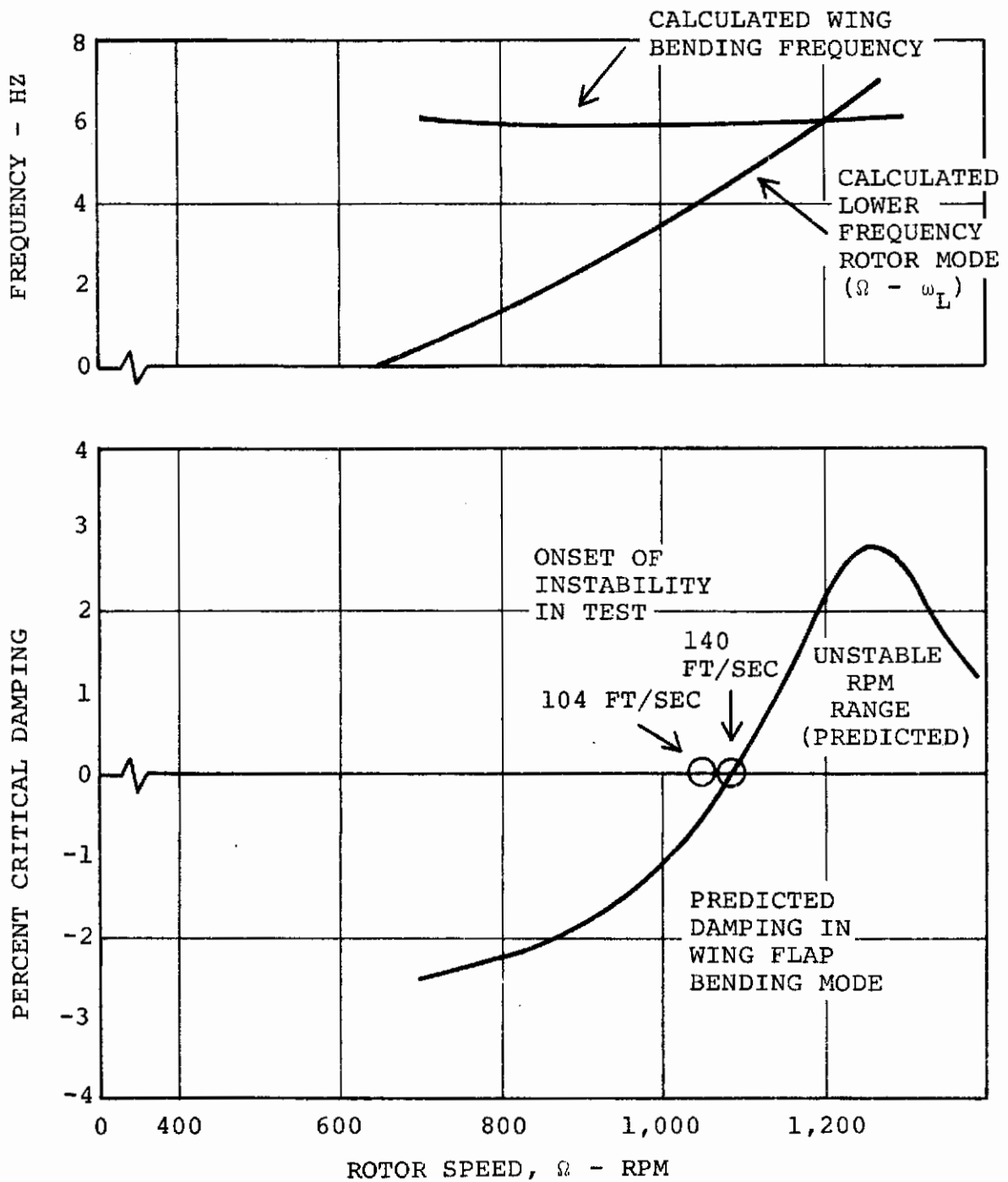
Figure 6. Correlation of Test Air Resonance
Instability with Analysis

16

- FOCAL MAST SYSTEM PROVIDES BLADE PITCH CONTROL FEEDBACK

- MAST STIFFNESS SELECTED SO THAT MAST PITCHES IN OPPOSITE SENSE TO WING AT WING FUNDAMENTAL FREQUENCY

- AT THIS FREQUENCY SWASHPLATE AND ROTOR HAVE NO ANGULAR MOTION IN SPACE AND NO PRECESSIONAL AIRLOADS GENERATED. HOWEVER, IN-PLANE MOTION IS STILL PRESENT

- AEROMECHANICAL INSTABILITY OCCURS WHEN FOCAL MAST FREQUENCY AND BLADE LEAD-LAG FREQUENCIES COALESCE, I.E., AIR RESONANCE

- AEROMECHANICAL INSTABILITY OCCURS FOR BLADE IN-PLANE FREQUENCIES GREATER THAN 1/REV
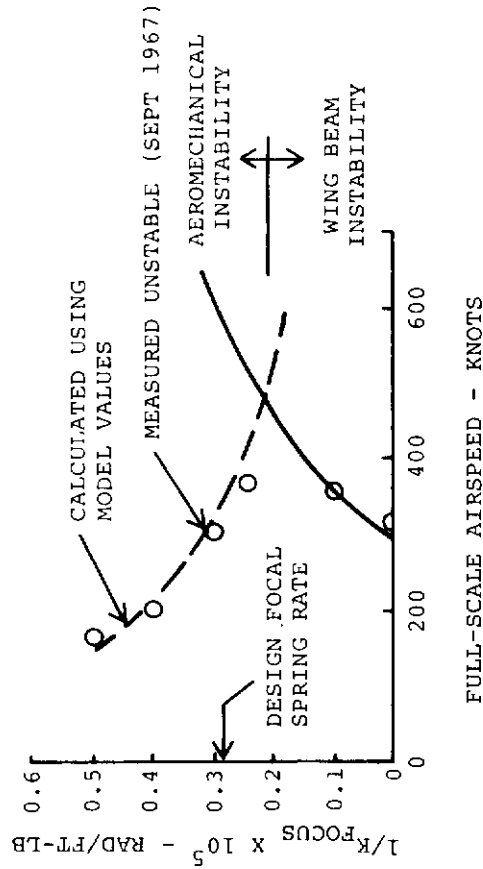
Figure 7. Comparison of Theory and Test of Effect of Focal Mast Stiffness on Stability for Bell Model 266

WING/ROTOR DIVERGENCE

When a wing supports large propellers or rotors, a number of
factors are present which make the accurate prediction of
divergence conditions more difficult than is the case with a
clean wing configuration. These include the following.

Local Flexibilities

The net compliance of the rotor in pitch is the sum of wing
pitch, tilt actuator, and bearing flexibilities. This net
value may be significantly less than that due to the wing
alone.

Location of Prop/Rotor

The aerodynamic forces on the prop/rotor act well forward of
the wing torsional axis and, in the case of tilt-rotors, near
the outer wingtip. This generally means that the static aero-
elastic behavior is dominated by the rotor hub force and
moment derivatives and that these must be accurately estimated
if reliable divergence speeds are to be calculated.

Technical Discussion of Factors Influencing Divergence
Behavior

Elements which determine the behavior of rotor derivatives are
aeroelastic as well as aerodynamic. Blade flapping natural
frequency has been seen to significantly influence all hub
force derivatives (see Figure 8). Lock number and advance
ratio also influence the derivatives significantly.

The effect of Lock number variation is shown in Figure 9 for
constant blade flap natural frequency and very high lag and
torsion frequencies. These results show that the rotor deriv-
atives are highly sensitive to blade frequencies and mass-
inertia properties so that particular accuracy must be
observed in these parameters in divergence prediction and
correlation studies. Preliminary studies of blade lag fre-
quency also indicate a strong influence on the rotor normal
force derivative $C_{N\alpha}$, which is directly related to divergence
properties as shown by Figure 10.

Elementary Mathematical Formulation

The mechanism of static divergence will be illustrated by the
following discussion of the behavior of a prop/rotor mounted
on a wing (Figure 11). The wing and rotor are tilted to the
airstream by an angle α_0. The aerodynamic loading at the
rotor tends to twist the wing and produce further aerodynamic
force increments. These in turn produce more twist and so on.
If the wing is stiff enough, the process will be a finite

18
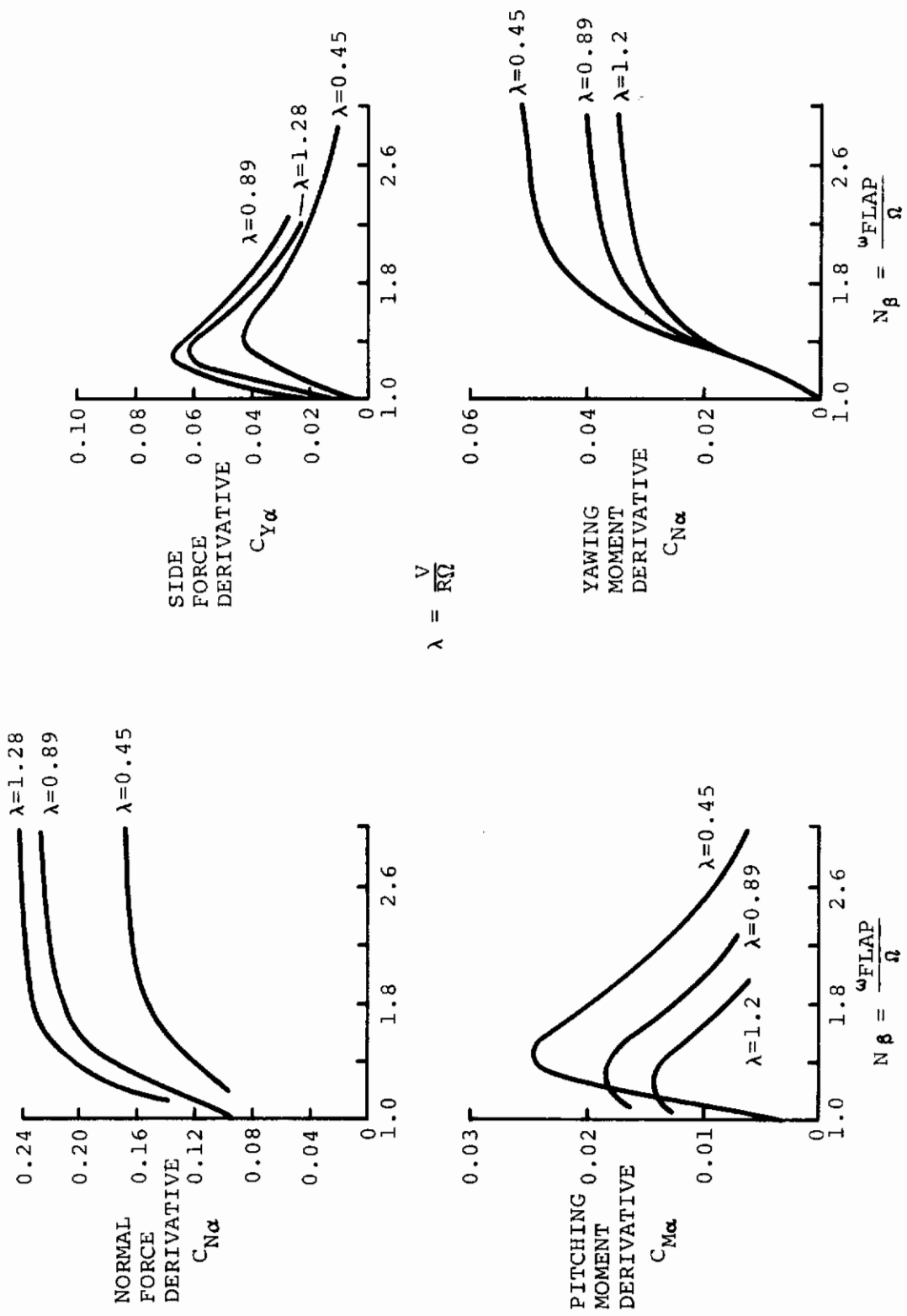
Figure 8. Variation of Rotor Derivatives With Flap Frequency and Lag Frequency High

19
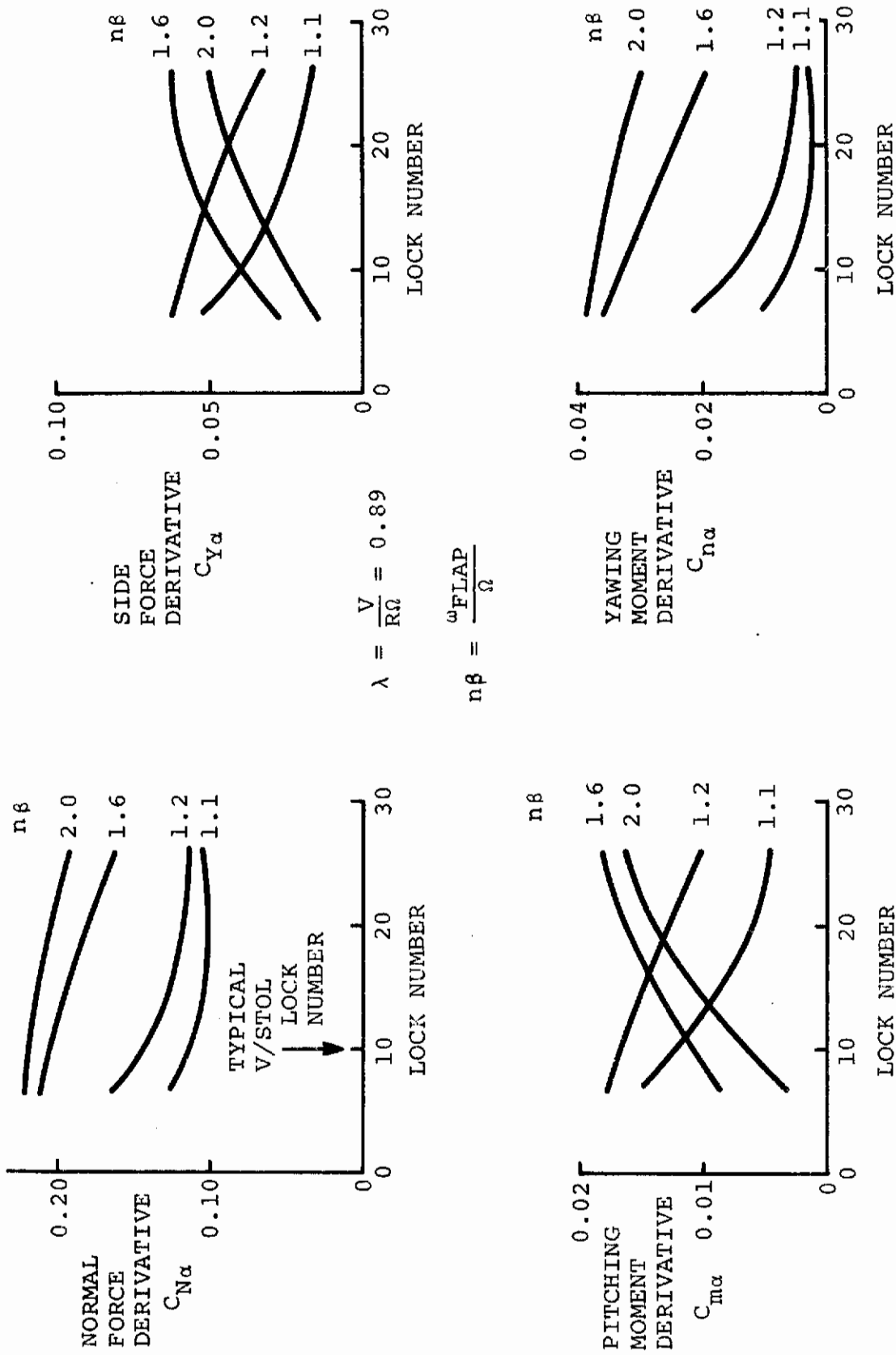
Figure 9. Effect of Lock Number on Rotor Derivatives for Flap Frequency Ratios $n\beta = 1.1$, 1.2, 1.6, and 2.0

$$\lambda = \frac{V}{R\Omega} = 0.89$$

$$n\beta = \frac{\omega_{FLAP}}{\Omega}$$

NORMAL FORCE DERIVATIVE $C_{N\alpha}$

SIDE FORCE DERIVATIVE $C_{Y\alpha}$

PITCHING MOMENT DERIVATIVE $C_{m\alpha}$

YAWING MOMENT DERIVATIVE $C_{n\alpha}$
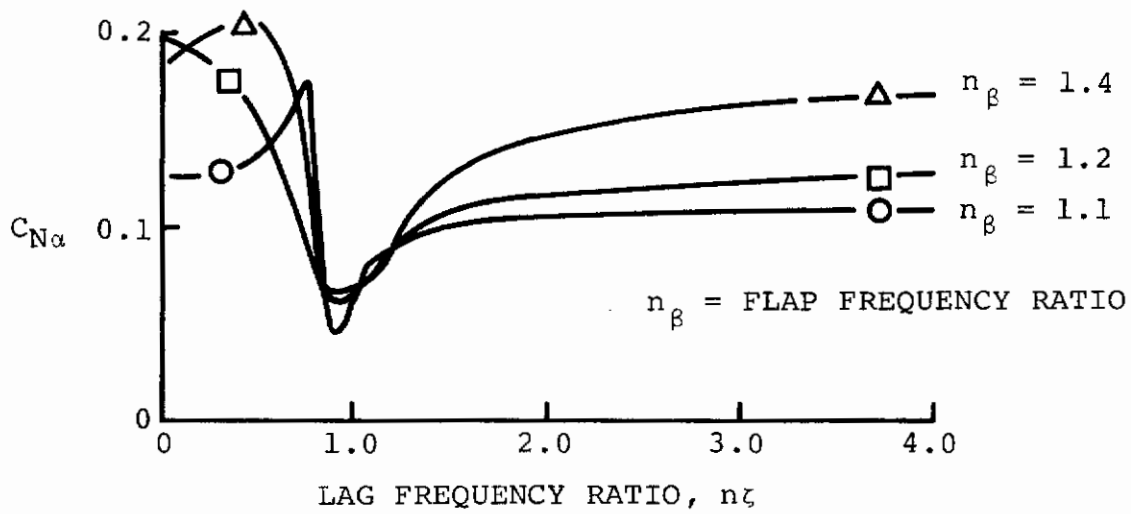
Figure 10. Variation of Normal Force With Lag Frequency Ratio
Calculated With Boeing-Vertol C-41 Derivative Program
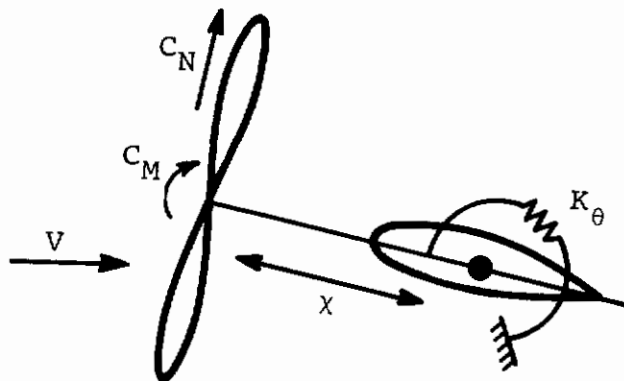
Figure 11. Simplified Mathematical Model for
Prop/Rotor Divergence

amount. Ignoring for the moment the effects of wing aero-dynamic force, we may express the behavior mathematically as follows: Let the initial unloaded wing and rotor setting be α_0. Assume that the only aerodynamic loads present are those on the rotor and that, as a consequence of the rotor aerody-namic effects, the wing twists through an angle α. Then, if the system reaches an equilibrium twist angle, we may state that

$$K_\theta \alpha = \text{Aerodynamic Moment About the Torsion Axis}$$

$$= 1/2 \rho V^2 (\alpha_0 + \alpha) S \{x C_{N\alpha} + D C_{m\alpha}\} \tag{1}$$

where K_θ = torsional stiffness of the wing at the
 rotor location
$1/2 \rho V^2$ = dynamic pressure
 α = elastic twist of the wing
 α_0 = initial incidence of the wing
 C_N = normal force derivative
 C_m = hub pitching moment derivative
 S = rotor disc area
 D = rotor disc diameter
 x = moment arm from the rotor hub to the
 torsional axis

From Equation 1 we may solve for the elastic twist

$$\alpha = \{K_\theta - 1/2 \rho V^2 S (x C_{N\alpha} + D C_{m\alpha})\}^{-1} \cdot 1/2 \rho V^2 S \alpha_0 \{x C_{N\alpha} + D C_{m\alpha}\}$$

So long as $\{K_\theta - 1/2 \rho V^2 S (x C_{N\alpha} + D C_{m\alpha}\}$ remains positive, a finite solution for α exists. However, when $K_\theta \leq 1/2 \rho V^2 S (x C_{N\alpha} + D C_{m\alpha})$, the net stiffness is zero or negative and the system is divergent. We define the divergence speed to be

$$V_{DIV} = \left(\frac{K_\theta}{1/2 \rho S (x C_{N\alpha} + D C_{m\alpha})} \right)^{1/2} \tag{2}$$

Induced In-Flow Effects

The magnitude of rotor hub derivatives is also strongly influ-enced by the in-flow induced by the wing and the rotor itself. Flight experience, e.g., XC-142 experience (Figure 12) and wind tunnel test work have shown that the presence of a lift-ing wing behind the prop/rotor can bring about large increases in the rotor aerodynamic derivatives compared with those of an isolated rotor (Figure 13). The mechanism may be explained by reference to potential flow theory in the 2-dimensional case where the prop/rotor is ahead of a wing of high aspect ratio.

22

- PROPELLER RADIUS SMALL RELATIVE TO WING CHORD

- MEASURED SLOPE OF C_N CURVE APPROXIMATELY TWICE THEORETICAL

- DIFFERENCE ACCOUNTED FOR BY WING CIRCULATION

- DISCREPANCY SUFFICIENTLY LARGE TO AFFECT FLYING QUALITIES

B-67 PROGRAM ―――――

TND3217 { OUTER PROP △
          INNER PROP ○

$C_T/\sigma = 0.02$

THEORETICAL ISOLATED PROP

SHAFT TILT - DEGREES

$$C_N = \frac{N_p}{qS}$$

COMPARISON OF THEORETICAL ISOLATED PROPELLER NORMAL FORCE AND MEASURED VALUES
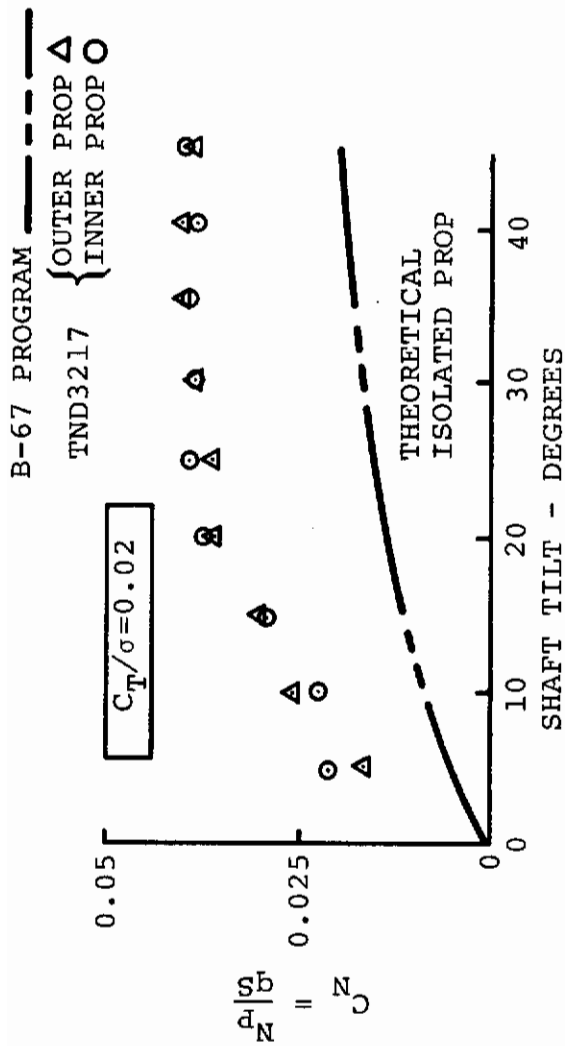
Figure 12. Effect of Wing-Induced Flow From Comparison of Theoretical and Measured Hub Normal Force on the XC-142 Aircraft

23
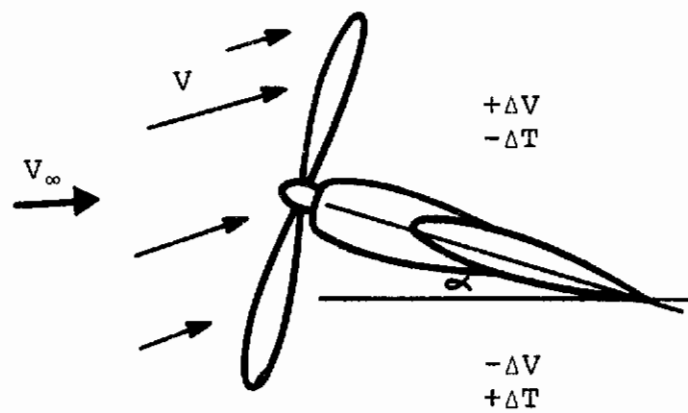
Figure 13.   Incremental Velocity and
            Thrust Effects Due to Presence
            of Wing

Intuitively we recognize that the upwash produced by the wing increases the angle of attack of the rotor. This may be interpreted as an increase in the rotor derivatives, in particular that of normal force, $C_{N\alpha}$.

The wing lift also induces incremental velocities normal to the disc with the tendency that the flow through the upper half disc is increased and flow through the lower section is decreased. This produces an azimuthal blade angle of attack variation which is experienced as a nose-up pitching moment. Since this is proportional to the wing angle of attack, the effect may be accounted for by a change in the rotor derivative. Both of these effects, $\Delta C_{N\alpha}$ and $\Delta C_{m\alpha}$, are destabilizing for normal configurations.

Estimates of Magnitude of Induced-Flow Velocity Component

We may usefully discuss these effects further in an elementary but quantitative manner by considering a prop/rotor in front of a wing of infinite aspect ratio.

For such a wing with uniform lift L per unit span, the circulation function is given by $L = \rho \Gamma V_\infty$.

Also, $L = 1/2 \rho V_\infty^2 C \cdot C_L$.

Hence, $\Gamma = V_\infty C/2 \cdot C_L$.

Hence the potential at a radial distance r from the quarter-chord point is

$$\omega = \frac{\Gamma}{2\pi} \log_e r$$

giving
$$V_\theta \equiv \frac{\partial \omega}{\partial r} = \frac{\Gamma}{2\pi r}$$

$$= \frac{V_\infty}{2\pi} \cdot \frac{1}{\gamma} \{C_{Lo} + \alpha \frac{dC_L}{d\alpha}\}$$

where γ is radial distance expressed in half chords and assuming $\frac{dC_L}{d\alpha} \simeq 2\pi$, $\frac{V_\theta}{V_\infty} = \frac{1}{\gamma} \{\alpha_0 + \alpha\}$.

V_θ may be resolved into components parallel and normal to the rotor disc and the effect integrated over the rotor disc to produce a set of modified derivatives.

The magnitude of the effect may be estimated by considering a point directly ahead of the wing. Assuming as in Figure 14 that the rotor is located one chord length ahead of the leading edge, we have:

25
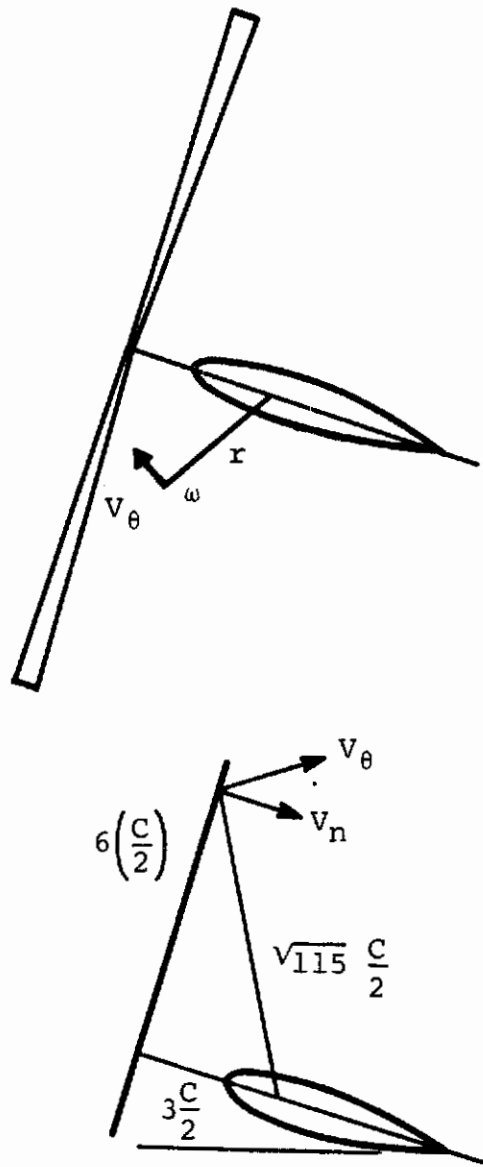
Figure 14. Induced Velocity Components
           Caused by Circulation
           (2-Dimensional Approximation)

26

$$\alpha_{ROTOR} = \alpha_{WING} + \frac{V_\theta}{V_\infty} = \alpha_\omega + 1/3 \{\alpha_0 + \alpha_\omega\}$$

or the change $\Delta\alpha R$ in effective rotor shaft angle produced by a change $\Delta\alpha$ in wing angle is

$$\Delta\alpha_{ROTOR} = (1 + 1/3)\ \Delta\alpha_{WING}$$

This is equivalent to an increase in the rotor derivatives relative to those of an isolated rotor and the effect is clearly significant.

The incremental induced flow normal to the rotor will be estimated at the 3/4R station of the blade. If the blade radius is of the order of 8 semichords and the hub is 3 semichords from the center of pressure, the radial distance is 45 semichords. The induced flow normal to the disc is

$$V_n = V_\theta \ \text{Cos}\ \theta = \frac{V_\infty}{\gamma^1}\ \{\alpha_0 + \alpha\}\ \text{Cos}\ \theta$$

$$= \frac{V_\infty}{\sqrt{45}}\ \{\alpha_0 + \alpha\}\ \frac{3}{\sqrt{45}}$$

i.e.,
$$V_n = \frac{V_\infty}{15}\ \{\alpha_0 + \alpha\}$$

and this may be expressed as an equivalent rate of pitch about the rotor hub

$$\dot{\rho} = \frac{V_n}{6\left(\frac{c}{2}\right)} = \frac{V_\infty}{90\left(\frac{c}{2}\right)}\ (\alpha_0 + \alpha)$$

Hence, a unit incremental change in wing angle of attack produces an induced-flow effect at the rotor of an order equivalent to pitching about the hub with angular velocity $\frac{V_\infty}{90\left(\frac{c}{2}\right)}$ rad/sec.

Hence, at a forward speed of 360 feet per second, we have an effect equivalent to $\frac{8}{C}$ rad/sec pitch velocity, for each radian of incremental wing angle of attack.

That is, we have additional induced $C_{m\alpha}^1$ which may be estimated by

$$1/2 \ V^2 S \ DC_{m\alpha}^{1} = 1/2 \ V^2 SDC_m \ \{V/90\left(\tfrac{C}{2}\right)\}$$

or
$$C_{m\alpha}^{1} = V_\infty/90 \ C_{mQ} \times (2/C) = V/90 (C/2) \cdot C_{mq}$$

Since C_{mq} tends to vary inversely with J or λ, this effect will tend to remain constant over the speed range.

In actual practice the situation is more complicated since large prop/rotors are generally located at the wingtip and two-dimensional assumptions are involved. Additional effects due to the wingtip vortex, fuselage proximity, the nacelle and spinner, and thrust-induced effects are all present to a greater or lesser degree.

Recommendations

The conclusions that may be drawn from the preceding discussion on divergence are that a satisfactory state of the art exists. Caution must be exercised, however, in the assessment of V/STOL vehicles for which the rotor hub force derivatives may dominate the behavior. These have been seen to depend critically on blade elastic and inertial properties as well as the purely aerodynamic characteristics of the rotor blade. Also, in certain cases, the effect of wing-induced inflow components may be very significant. However, if care and good judgement are used in quantifying these effects, accurate predictions of static divergence are possible.

It is also noted that divergence is a static aeroelastic phenomenon, in which the wing twists under the influence of nonvibratory loads. It is therefore important to evaluate and use the mode of twist appropriate to such loads, rather than the mode of twist associated with the fundamental vibration mode.

This implies a divergence calculation in which the basic static aeroelastic properties, rather than the vibratory modes, are used to represent the wing. Thus, if the divergence speed is sought using a flutter-oriented program, particular care must be taken to ensure that the inputs will permit the structure to adopt the nonvibratory torsional wing mode shape associated with divergence.

WHIRL FLUTTER AND OSCILLATORY BEHAVIOR
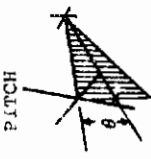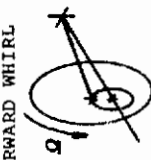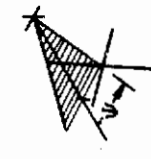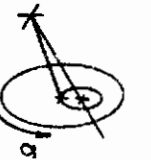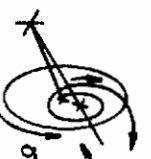
The oscillatory stability of a tilt-rotor configuration is considerably influenced by the presence of large, flexible rotors. In addition to providing gyroscopic coupling (as is the case with rigid propellers), the blade flexibility adds additional degrees of freedom whose effects must be accounted for in assessing stability. An acceptable measure of success

has been achieved in predicting the oscillatory behavior of propeller systems and certain types of flexible blade systems. Reference 3 reports that good correlation with test is achieved for propellers which are stiff enough to be considered rigid. Better correlation was reported using empirically measured propeller derivatives, but conservative results were obtained with calculated values. The principal conclusions of Reference 3 in relation to the whirl behavior of rigid propellers are presented in Figures 15 and 16.

The conclusion was that the technology for analysis of the phenomenon for rigid propellers was in a satisfactory condition. In the development of an articulated propeller system, a small model tested by Grumman exhibited instability in which blade flapping played a critical part (Reference 3). This test was of limited value because of the small scale of the model and the isotropic inertial properties of the nacelle. A carefully engineered model test conducted in 1968 (Reference 5) produced a significant amount of whirl flutter data. This model featured an articulated flapping rotor mounted at the tip of a wing spar which was scaled to be representative of the full-scale modes and frequencies of a tilt-rotor aircraft in vertical and horizontal bending and torsion (see Figure 17). The nacelle inertias and degrees of freedom were representative of full scale. Windmilling tests of this model provided many flutter data points. The testing procedure was to select a blade collective pitch setting and increase tunnel speed gradually until an unstable condition was reached or the rpm stress limits were attained. The procedure was repeated for a wide range of collective pitch settings and a flutter boundary defined. This was done for a set of parametric variations of wing spar stiffness, blade hinge offset, and blade inertia. The analytical correlation was good in that the mode of flutter was correctly predicted, although in places the prediction was overly conservative (Figure 18). Typical flutter traces from this test are shown in Figure 19. These results are in broad agreement with results reported by Bell (Reference 2) for a similar system, Figure 20. The lack of agreement noted in the flutter speeds of Figure 18 may have resulted from approximations in the mathematical model then current (C-26). This assumed a zero hinge offset with the blade frequency controlled by a restraining spring. The correlation was observed to be better with the smaller (5 percent) hinge offset than in the case of the 12-1/2 percent offset, indicating that the discrepancy in mode shape introduced by the mathematical model was important. Later programs include a general mode shape capability.

An interesting feature of the Bell results is the phenomenon described as aeromechanical instability. This is described as involving the lead-lag cyclic rotor mode and the focal mount stiffness. When the angular frequency of the rotor Ω plus the

29

NATURAL VIBRATION MODES OF SYSTEM
WITH RIGID PROPELLER

RESUME OF PROPELLER WHIRL
TREND STUDIES

Figure 15. Whirl Behavior of Rigid Propellers

RIGID WING

WING BENDING MODE

WING BENDING TORSION MODE
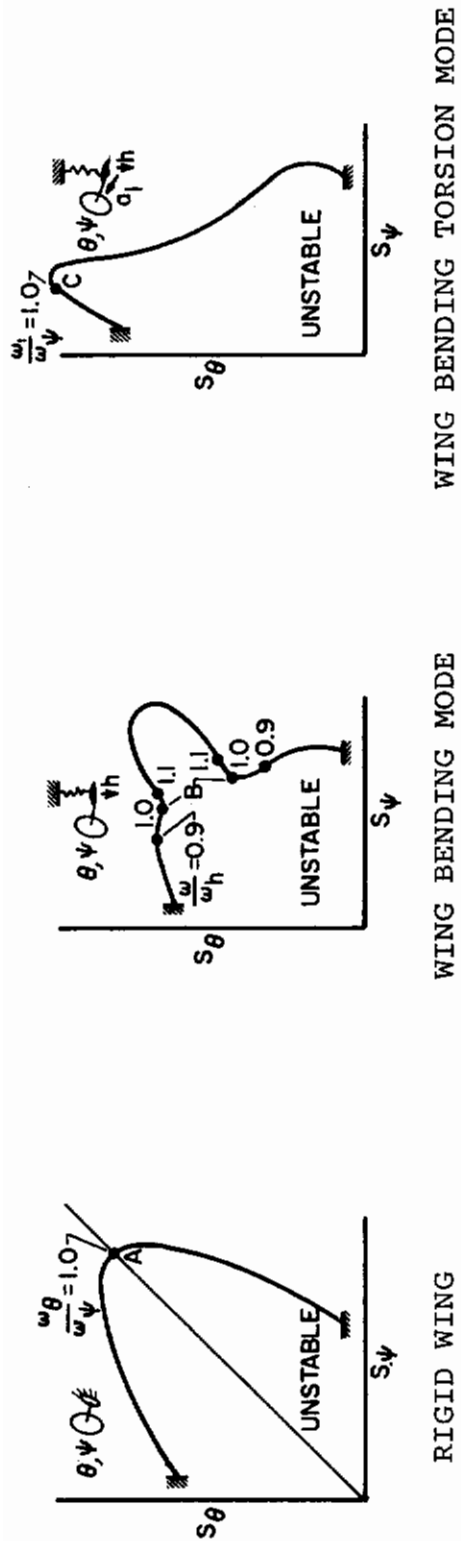
Figure 16. Influence of Wing Flexibility on Whirl Flutter

31
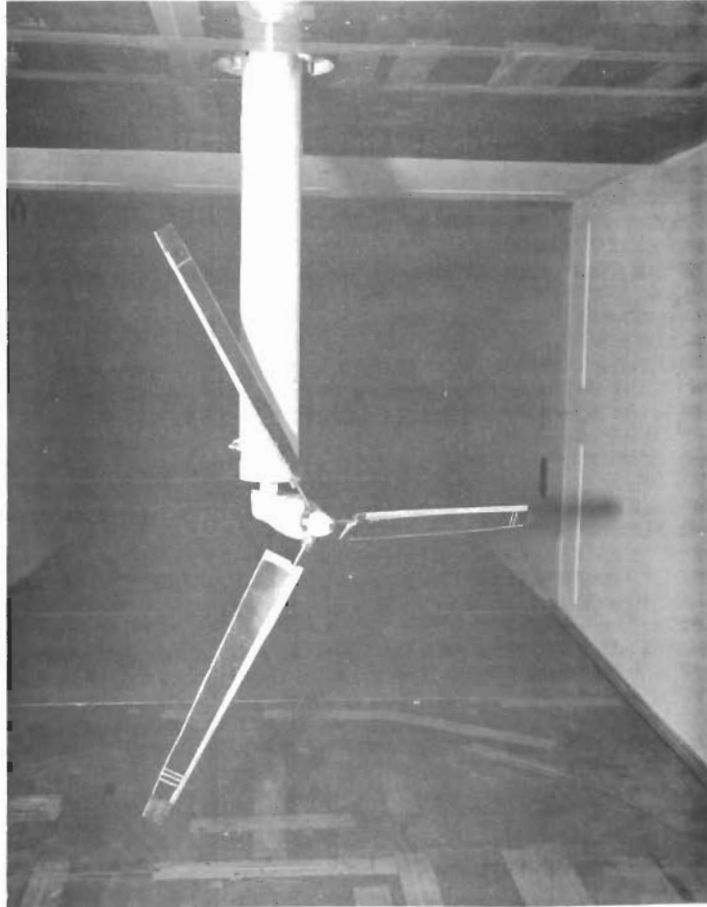
1/22-SCALE MODEL FEATURES

o BLADES ARTICULATED IN FLAP

o OFFSET VARIABLE

o BLADE INERTIA VARIABLE

o WING SPAR STIFFNESS VARIABLE

o WING SPAR FAIRED BY NON-
   STRUCTURAL AIRFOIL

o TILT RANGE 0 - 90 DEGREES

Figure 17. Vertol M160 Dynamically Similar 1/22-Scale
            Windmilling Model

32

WING SPAR NO. 7

FLUTTER
(PREDICTED)

COLLECTIVE PITCH - DEGREES

WING SPAR NO. 4

FLUTTER
(PREDICTED)

STABLE
(PREDICTED)

COLLECTIVE PITCH - DEGREES

WING SPAR NO. 3

FLUTTER
(PREDICTED)

STABLE
(PREDICTED)

COLLECTIVE PITCH - DEGREES

VELOCITY - FEET PER SECOND

TEST POINTS

⊙ STABLE
● FLUTTER

UNCOUPLED FREQUENCIES (HZ)			
WING SPAR NO.	3.	4.	7.
WING VERTICAL BENDING:	6.0	2.44	3.73
WING HORIZONTAL BENDING:	9.7	11.6	11.1
WING TORSION:	9.93	8.8	6.41

Figure 18. Correlation of C-26 Program Analysis With Flutter Test Points
for Vertol MI60 1/22-Scale Dynamically Similar Model

33

- FREQUENCY IN FIXED SYSTEM 0.45 PER REV

- BLADE FLAPPING FREQUENCY 0.55 AND 1.45 PER REV

- BLADE FREQUENCIES ARE $\Omega \pm \omega$ WING

BLADE FLAPPING PEAKS 1.45/REV MEAN LINE 0.55/REV

FLUTTER FREQUENCY 0.45/REV

WING VERTICAL BENDING

WING CHORDWISE BENDING

WING TORSION

1 PER REV

TIP DEFLECTION - INCHES

INCHES

INCHES

DEGREES

Figure 19. Typical Flutter Traces From Test of Vertol M160 1/22-Scale Dynamically Similar Model

34
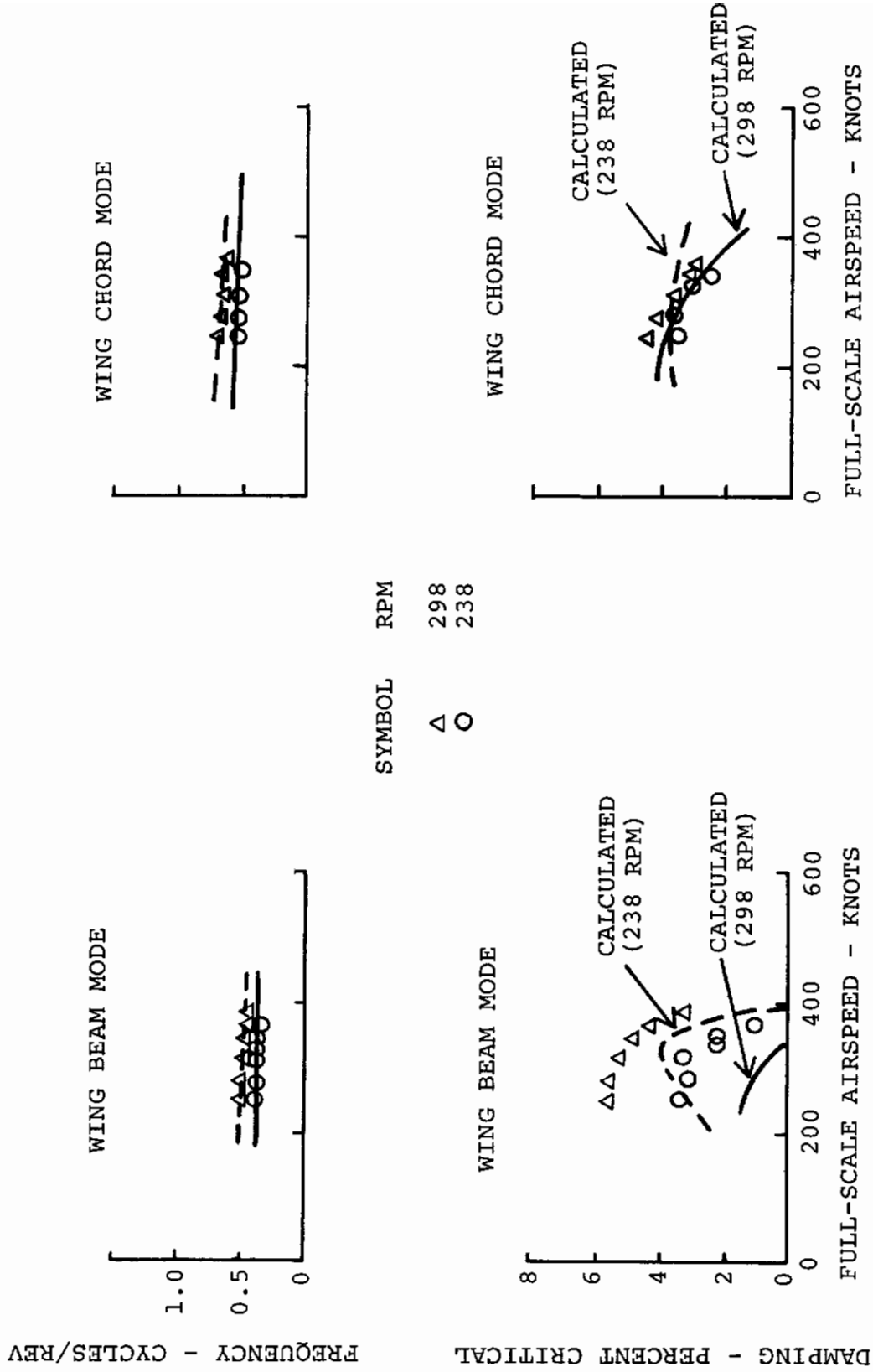
Figure 20. Whirl Flutter Stability of Bell Model 266 With Focused Rotor Locked Out

35

blade second mode frequency (approximately 3/rev) coalesced with the focal mount frequency, an instability occurred. The airspeed at which this occurred is proportional to the focal mast spring stiffness as shown in Figure 7 and good correlation between analysis and test is reported. This is of considerable interest because it demonstrates that mechanically coupled instabilities are not confined to blade modes with frequencies below one per rev. It also demonstrates the need for care in the application of feedback to suppress instabilities. This point is also made in Reference 6, where it is shown that rotor blade pitch feedback introduced to improve handling results in loss of damping in an air resonance mode.

CHARACTERISTICS OF STATE-OF-THE-ART THEORY

A number of assumptions have traditionally been made in analysis addressing propeller whirl and other airframe-rotor interactive modes of behavior. The features of a typical group of such analyses are listed in Table II. Most of these assumptions have been made around technical grounds, although simplicity and minimization of analytical derivation have also been factors. All the analyses listed are for the cruise configuration, i.e., axial flow only, on the basis that tilt and transition occur at very much lower airspeeds than maximum design dive speed and that this would therefore be the most critical case. A less plausible assumption has been that the effects of blade deflections under load could be ignored. Blade torsion has also been ignored on the assumption that blade torsional frequencies would be so high compared with the other frequencies of the system that this degree of freedom would not participate in low-frequency whirl flutter.

This assumption is frequently tenable provided the blade remains undeflected in flap and lag. However, when the blade is deflected, finite steady amounts of perturbation in either flap or lag will generate an associated twisting motion which has the same effect as δ_3 or α_2. These effects may be important even if the torsional natural frequency is high relative to the flap and lag frequencies.

TABLE II

BOEING-VERTOL STATE-OF-THE-ART V/STOL STABILITY PROGRAMS

Program Number	Degrees of Freedom	Blade Description	Aerodynamic Assumptions	Comments
C-26	6: Wing uncoupled bending, yawing, and torsion. Tip path collective pitch and yaw.	Articulated rigid blade. Out-of-plane flap only.	Axial-flow lifting line. No wing aerodynamics.	(A) Correlation good for small offset. (B) Variable gearing between blade pitch and wing torsion.
C-27	9: Wing uncoupled bending, yawing, and torsion. 2 coupled flap-lag modes per blade. Perturbations about undeflected condition.	Hingeless rotor with coupled elastic deflections in and out of rotor plane.	Axial-flow lifting line. No wing aerodynamics.	(A) Correlation good for whirl flutter and mechanical instability. (B) Correlation not good when blades are deflected in steady state.
C-40	Up to 4 rotor blades representation as in C-27. Airframe representation generalized to coupled vibration modes plus 6 rigid-body modes. Landing gear added.	As C-27	Wing and empennage aerodynamics added. Two-dimensional incompressible oscillatory aerodynamics.	(A) Correlation good for classical and whirl flutter and mechanical instability. (B) Not good for deflected blades.
C-41	Blade representation as in C-27.	As C-27	Axial-flow lifting line.	Solves for blade response and hub force and moment derivatives when rotor shaft is given small pitch rate. Correlation good.

OSCILLATORY BEHAVIOR NOT READILY PREDICTED BY CURRENT STATE-OF-THE-ART TECHNOLOGY

It is noted from the foregoing discussion that the prediction and correlation of static and oscillatory aeroelastic behavior have been reasonably successful in a number of important applications. These applications are those where the classical assumptions of small deflections and near-axial flow were valid. See Table II for description of Boeing-Vertol state-of-the-art analyses.

A number of cases which depart from these assumptions and in which correlation is not so good are now presented.

EFFECT OF TILT

Model test results in the cruise configuration indicate a quite good predictive capability for whirl flutter in the cruise configuration. Behavior during transition does not show the same good correlation. The few published data on this topic relate to rigid-rotor behavior. Figure 21 shows data from the Boeing 1/22-scale model which indicates significant behavior variation with tilt. The blades on this model were articulated and designed to have freedom only in flap out of the plane of rotation. It is seen that, with one wing stiffness, flutter occurs with 4-1/2 degrees of tilt at much lower speeds than when the rotor shaft is untilted. With a different wing stiffness condition, the onset of flutter is increasingly delayed as the shaft is tilted.

This behavior has not been successfully correlated with existing analyses. Features present in the test which were not accounted for in the available analyses are the effects of nonaxial flow and the initial steady-state cyclic flapping of the blades.

LIMIT-CYCLE PHENOMENA

The model test data discussed above are for a rotor whose blades have freedom only to flap or whose lead-lag frequencies are high. A later test conducted by Boeing was on a hingeless rotor model, Figure 22, whose blades had flexure mode frequencies of 0.84 and 1.2 per rev at the operating rpm and collectives. This model did not exhibit the clear-cut divergent oscillations encountered on the earlier model, but rather limit-cycle oscillations which were clearly self-sustaining. These occurred only at a combination of negative thrust and rpm conditions such that the blades were coned back significantly from the precone angle, Figure 23. The freedoms involved in these instabilities included fundamental vertical flexure torsion mode of the wing and blade flap, lag, and torsion. This type of instability appears to have something

38
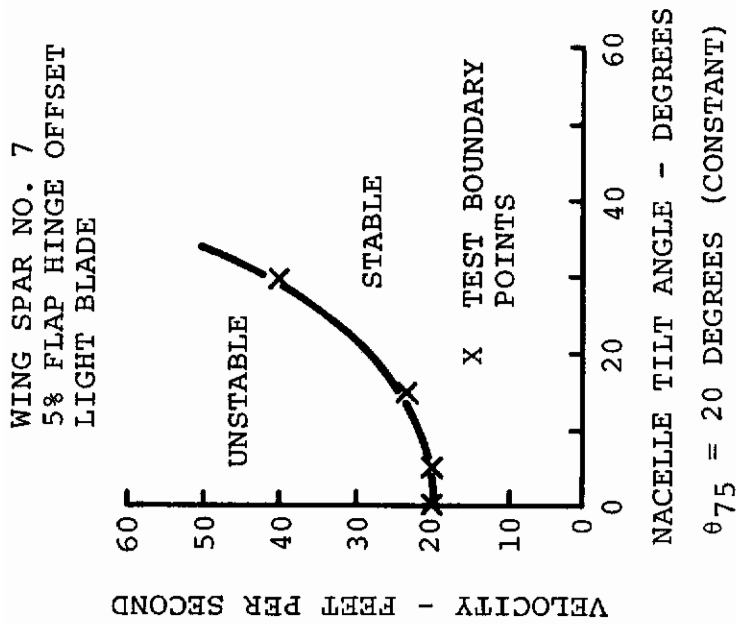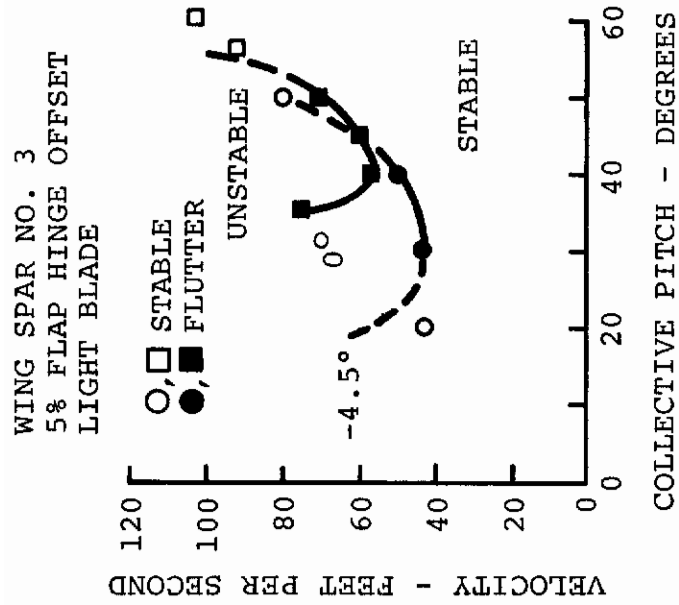
Figure 21. Effect of Nacelle Tilt on Flutter Speed

Figure 22.   1/10-Scale M160 Dynamic Model

Figure 23. Data Points and Flutter Regions for Basic Cruise Configurations of Vertol M160 1/10-Scale Dynamically Similar Model

NOTE: ALL
- O POINTS 825 RPM
- X FLUTTER (825 RPM) POWERED
- ⊠ FLUTTER (WINDMILLING)
- ⊗ STABLE (WINDMILLING)
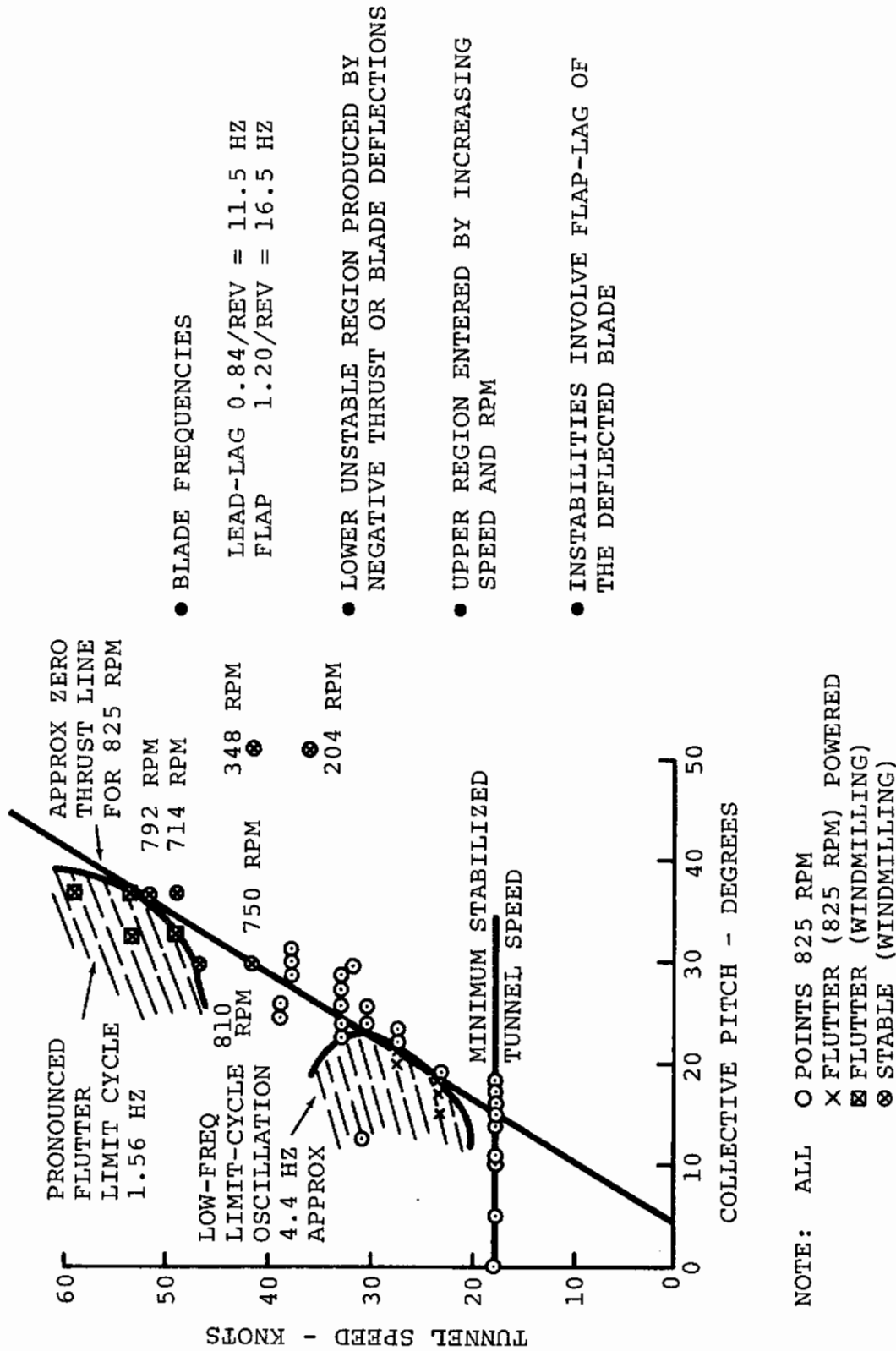
- BLADE FREQUENCIES

  LEAD-LAG 0.84/REV = 11.5 HZ
  FLAP   1.20/REV = 16.5 HZ

- LOWER UNSTABLE REGION PRODUCED BY NEGATIVE THRUST OR BLADE DEFLECTIONS

- UPPER REGION ENTERED BY INCREASING SPEED AND RPM

- INSTABILITIES INVOLVE FLAP-LAG OF THE DEFLECTED BLADE

41

in common with the behavior predicted in Reference 7. However, the analysis of Reference 7 is not by itself adequate to predict the behavior noted since it does not include the hub degrees of freedom, which appear to be an important component of motion in the unstable mode.

BLADE MOTION - AH-56 1P-2P INSTABILITY

Experience with the AH-56 (8) indicates that the flap-lag coriolis-type instability is a threat in any situation where the lag impedance to in-plane forces induced by flapping is small. An unstable region was observed to exist when the blade cyclic flapping exceeded a certain limit which approached a minimum when the blade lag frequency was at 2P, Figure 24. The mechanism of this instability seems to be similar to that discussed in Reference 7 where collective flap deflection of the blade produces in-plane forces to drive the lag mode when its frequency is near 1P. In Reference 8, the mechanism involves large cyclic initial conditions of blade flapping which produce in-plane coriolis 2P loads. This creates the conditions necessary for a flap-lag instability. When the lag frequency is exactly 2P the instability becomes a slow rotor tilt divergence.

AIRFRAME AND ROTOR INSTABILITY IN FORWARD FLIGHT

Also reported in Reference 8 is an effect described as a 1/2-per-rev hop. This seems to be similar to effects described by Hohenemser, References 7 and 9. The phenomenon is described as occurring in high-speed forward flight and can be predicted conservatively by an analysis whose critical parameters are collective pitch stiffness, blade lag frequency, and flap-pitch coupling or δ_3. In Figure 25, sensitivity studies conducted by Lockheed indicate that a 13-degree-of-freedom analysis predicts the behavior with a conservative margin of approximately 10 percent. An increase of 10 percent in the critical speed required a 20-percent increase in collective stiffness. The sensitivity to lag frequency depended on the rpm.

At 3 percent above operating rpm, there was no change in the critical speed for a range of in-plane frequency from 1.46 to 1.52 per rev. At 3 percent below operating rpm, the same change in lag frequency produced a shift in critical speed from 150 knots to 160 knots, i.e., to produce a 6-percent increase in speed we require a 4-percent increase in lag frequency. A 50-percent increase in lag damping was calculated to increase the critical speed by less than 2 percent.

Overall, the underestimated speed was conservative by about 10 percent.

42

Figure 24. Relation of Unstable Regions to Lag Frequency 2P Coalescence in AH-56A Instability
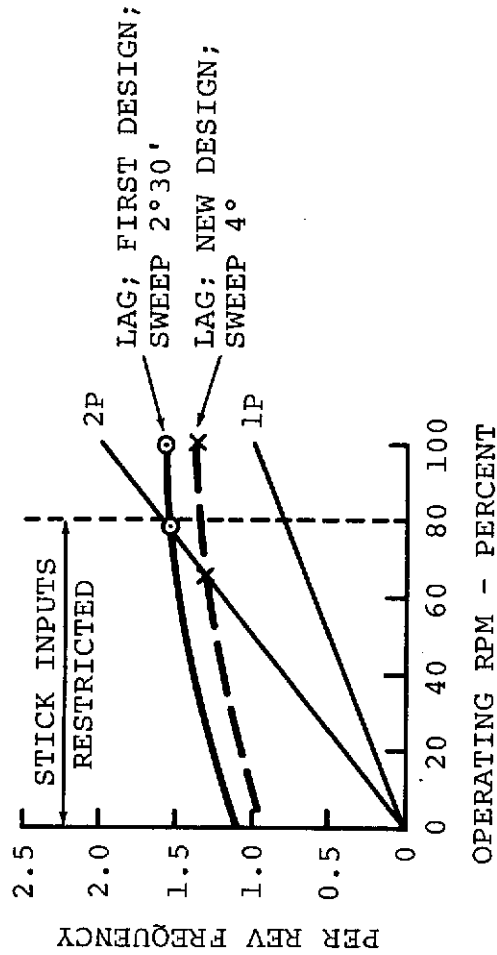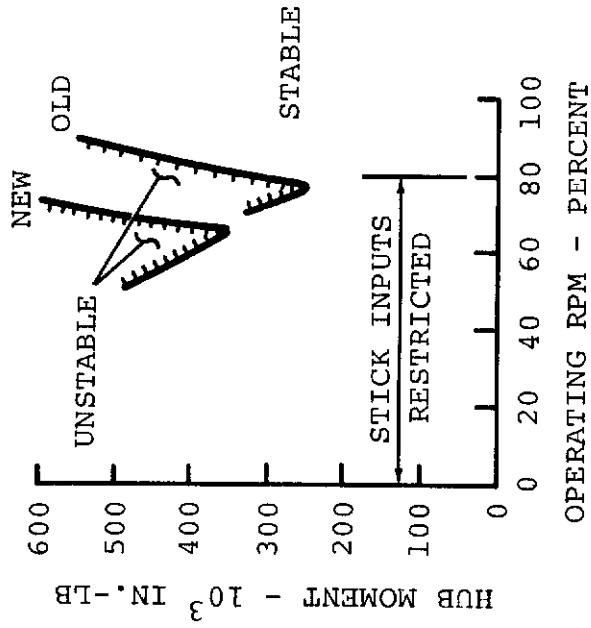
ORIGINAL DESIGN: IN-PLANE FREQUENCY = 1.6P; SWEEP 2°30'
θ IV DESIGN: IN-PLANE FREQUENCY = 1.4P; SWEEP 4°0'

43

EFFECT OF IN-PLANE FREQUENCY
ON STABILITY BOUNDARIES

$\omega/\Omega = 1.46$

EFFECT OF IN-PLANE DAMPING
ON STABILITY BOUNDARIES

1,350 FT-LB/RAD/SEC

EFFECT OF COLLECTIVE STIFFNESS
ON STABILITY BOUNDARIES

$K\theta = 50 \quad 55 \quad 60 \times 10^3$ FT-LB/RAD

$\omega/\Omega = 1.46$ — — —
$\quad\quad\quad 1.50$ —··—··—
$\quad\quad\quad 1.52$ ————
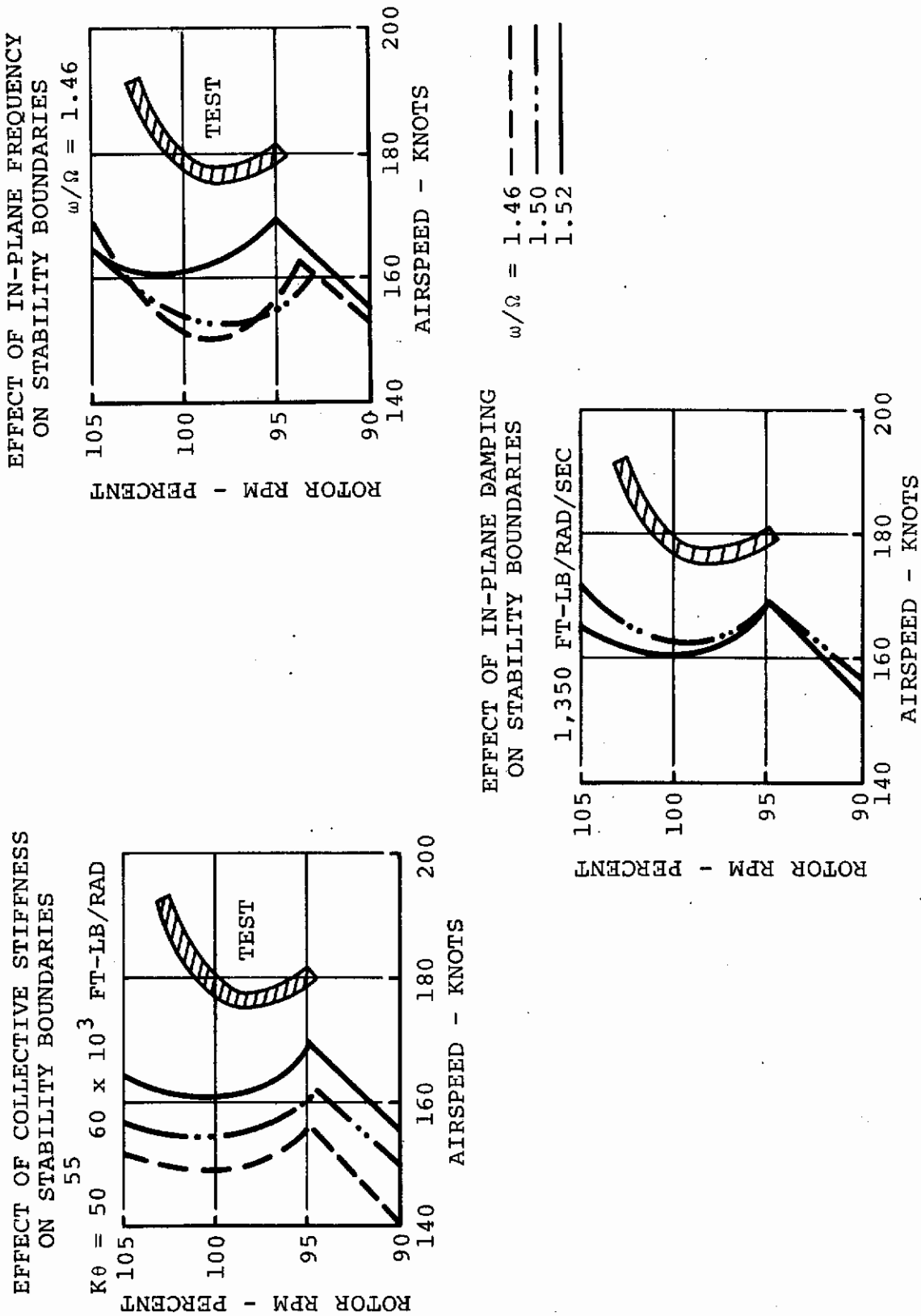
Figure 25. Correlation of Analysis and Test for AH-56A Subharmonic Hop

44

SUMMARY OF ROTOR/AIRFRAME STABILITY PREDICTION CAPABILITY

At this point several things have become clear:

1. Typical analyses used to predict divergence, whirl flutter, and aeromechanical and mechanical instability are successful enough when the inherent assumptions are valid. Such assumptions have included: (a) small perturbations about zero deflection equilibrium conditions, (b) axial flow through the rotors.

2. Incidents in which the existing theory has not proved successful have involved finite blade deflections and nonaxial flow.

It is concluded that these effects must be considered if the range of correlated phenomena is to be extended. Since a considerable body of literature exists on the behavior of individual blades, this will be examined to provide guidelines as to what effects are important in the context of the overall aircraft. This study will indicate which effects must be included in an upgraded capability.

BLADE INSTABILITY MECHANISMS

Since one of the departures of state-of-the-art analyses from
reality relates to the blade idealizations used, and since a
considerable body of literature exists concerning the stabil-
ity of individual blades, a survey of the main mechanisms
identified for individual blades will now be undertaken. This
will indicate additional features to be included in an up-
graded technology if correlation with a wider range of phe-
nomena is to be attempted.

The principal mechanisms and types of instability in individ-
ual blades are listed in Table III and discussed in detail in
the following paragraphs.

BLADE CLASSICAL FLUTTER

A blade possesses all the potential for undesirable aeroelas-
tic behavior familiar from fixed-wing experience, but even the
classical problems tend to be more severe when encountered in
the rotating environment. The flexure torsion flutter prob-
lem, for example, becomes more sensitive to chordwise center-
of-gravity location because of the additional coupling
produced by the centrifugal force field.

For hover or vertical flight, as in the propulsion mode for
tilt rotors, the equations take the same form as those for
classical fixed-wing flutter:

$$\begin{bmatrix} 1 & Ca \\ \overline{Ca} & 1 \end{bmatrix} \begin{Bmatrix} \ddot{\theta} \\ \ddot{\beta} \end{Bmatrix} + \begin{bmatrix} M_{\dot{\theta}} & C_v \\ \overline{C_v} & M_{\dot{\beta}} \end{bmatrix} \begin{Bmatrix} \dot{\theta} \\ \dot{\beta} \end{Bmatrix} + \begin{bmatrix} M_\theta & C_d \\ \overline{C_d} & M_\beta \end{bmatrix} \begin{Bmatrix} \theta \\ \beta \end{Bmatrix} = 0$$

The equations have been divided through by the pitching and
flapping mass moments of inertia I_θ and I_β respectively. In
the first equation, the θ coefficient arises from aerodynamic
pitch damping.

The θ coefficient consists of three components:

1. The aerodynamic moment resulting from the center of
    pressure not being at the pitch axis.

2. The centrifugal restoring moment or tennis racquet
    effect.

3. The elastic restoring moment due to the pitch spring,
    i.e., control stiffness.

46

TABLE III

INSTABILITIES ENCOUNTERED IN PROP/ROTORS

Instability	Principal Freedoms	Frequency Characteristics	Comments
Classical Flutter	Flap-pitch or torsion. CG offset from torsion axis.	ω Flap $< \omega_I < \omega$ torsion aerodynamic forces tend to produce coalescence.	Flutter mode may involve overtone bending.
Flap-Lag-Pitch α_2, δ_3 coupling	Two or more of flap, lag, pitch with α_2 or δ_3 present.	ω_I = frequency coalescence of participating modes due to rpm, velocity effects.	Mechanism essentially classical.
Flap-Lag-Pitch Deflected Blades	As above. Effective δ_3 results from flap oscillation when blade has steady lag. α_2 results from lead-lag oscillation when blade has steady flap deflection.	ω_I = frequency coalescence of participating mode.	Mechanism essentially same as above. Limit cycle.
Flap-Lag Coriolis Hover	Flap-lag perturbations about deflected equilibrium position.	$\omega_I = \omega_{LAG}$	Flap perturbation produces lead-lag coriolis force. Lead-lag response produces additional lift and flap response. Limit cycle.
Flap-Coriolis $\mu \neq 0$	Flap-lag about deflected equilibrium positions.	$\omega_I = \omega_{LAG}$	Azimuthal variation of lift on blade gives coupling additional to coriolis forces.

The pitching moment arising from flapping (i.e., the coefficient of ƒ in the first equation) may be similarly identified. The $\ddot{f}$ term arises from the product of inertia about the pitch-flap axes, the $\dot{f}$ term because the lift does not in general act at the pitch axis, and the ƒ term due to centrifugal forces acting on the masses which may be off both flapping and pitching axes. In the second equation, the $\dot{f}$ term is strictly aerodynamic flap-damping, and if there is no flap-spring, the ƒ term is just due to centrifugal restoring moments. The $\dot{\theta}$ term is due to product of inertia, and the $\dot{\theta}$ term is the aerodynamic flapping moment arising from blade pitch. Finally, the θ coefficient C_d has two parts: (a) a centrifugal flapping moment arising from product of inertia and (b) an aerodynamic part which exists because lift causes a flapping moment. For a rigid uniform blade, with zero δ_3, and neglecting all wake aerodynamic effects, aerodynamic contributions to effective mass, and structural damping, the coefficients are:

$$M_{\dot\theta} = \frac{\gamma}{8} \frac{I}{I_\theta} \frac{\Omega}{R^2} \left[\frac{c}{2} - a \right] \left[\frac{c}{2} - 2a \right] \quad ; \quad M_{\dot f} = \frac{\gamma}{8} \Omega$$

$$M_\theta = \omega_\theta^2 - \frac{\gamma}{8} \frac{I}{I_\theta} \frac{\Omega^2}{R} \cdot a \quad ; \quad M_f = \omega_f^2$$

$$Ca = \frac{I_R}{I_\theta} \quad ; \quad \bar{C}a = \frac{I_R}{I}$$

$$C_v = \frac{\gamma}{8} \frac{I}{I_\theta} \frac{\Omega}{R} \cdot a \quad ; \quad \bar{C}_v = - \frac{\gamma}{6} \frac{\Omega}{R} \left(\frac{3}{4}c - a \right)$$

$$C_d = \Omega^2 \frac{I_r}{I_\theta} \quad ; \quad \bar{C}_d = \Omega^2 \left(\frac{I_r}{I} - \frac{\gamma}{8} \right)$$

where γ = Lock Number = $2\pi\rho CR^4/I$
  ω_f = uncoupled, rotating flap natural frequency
  ω_θ = uncoupled, rotating pitch natural frequency
  I_r = product of inertia about pitch-flap axes
  I_θ = moment of inertia about pitch axis
  I = moment of inertia about flap axis

The literature dealing with this problem for cases which involve the rigid-body flapping and pitching motions of hinged blades, with and without various amounts of elastic bending and twisting motion, is reasonably complete (see References 10, 11, 12, and 13). The principal parameter of influence in these cases is, as it is for fixed wings, the distance between

the section center of gravity and the section aerodynamic center*, although this is not obvious in the coefficients listed above since the chordwise position of the center of gravity is integrated into the product of inertia, I_r.

Further, the critical flutter speed will tend to be a minimum where a flap-bending degree of freedom and a pitch-torsional degree of freedom are close together, for any given value of pitch frequency. When these effects are considered, the critical flutter speed will tend to be directly proportional to the pitch-torsional frequency. When flexible modes and nonuniform blade properties with span are considered, the coefficients involve integrals over the span which must be evaluated numerically. The coefficients listed above are the values of such integrals for the special case of a linear flap mode and a twist mode in which all the rotation occurs at the root (i.e., pitch).

Quasi-static aerodynamics usually are satisfactory for predicting the critical speeds, although fixed-wing type unsteady, potential flow results are often used (Reference 13, for example). The relationship is such that quasi-static aerodynamics remain if F and G are assumed to be 1 and 0, respectively, and aerodynamic effective mass terms (i.e., those which are coefficients of accelerations) are dropped. An exception to this rule is that some analysts drop the $\dot{\alpha}$, or effective camber terms when making the quasi-static assumption. Where the total downwash velocities through the rotor are low enough that the wake shed and trailed from oscillating blades remains close to the rotor disk, then neither fixed-wing unsteady nor quasi-static aerodynamics are adequate to the task of predicting rotor flutter. Such so-called wake flutter cases are examined, for example, in Reference 12, using the results of Reference 14. Figure 26 taken from the former paper shows that several additional branches of what appears to be flutter of a classical type can exist when a rotor blade operates close to its own wake or that of a preceding blade.

Reference 14 also shows that, at low values of inflow, single-degree-of-freedom pitch flutter can occur if the pitch axis is forward of the quarter chord. These effects apparently become negligible when the axial distance between shed vorticity in chord lengths, $\frac{2\pi u}{n\Omega c}$, is greater than about 3. Under these circumstances, the major differences between these rotor

---

*This term really implies the center of pressure for changes in lift, as distinct from center of pressure including steady-moment terms which are of no consequence to classical flutter.

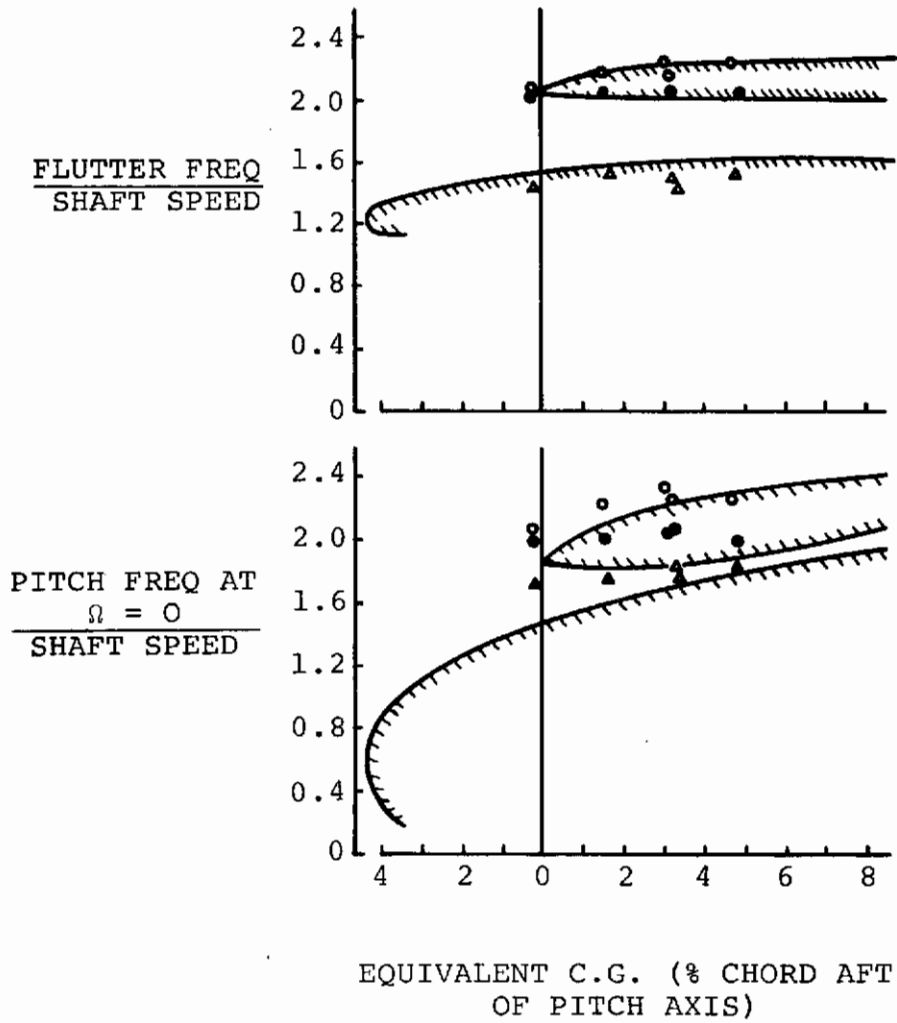PITCH-FLAP RATIO = 2, VIRTUAL δ_3 = 63.4°

Figure 26. Pitch-Flap Flutter of a Blade
Operating in Wake Effects

flutter cases and wing flutter are in the dynamic effects associated with rotation.

FLAP-PITCH FLUTTER (δ_3)

The kinematic coupling between flapping and pitching, tan δ_3, is shown in Reference 11 to be destabilizing for bending modes where the root bending slope is in the same direction as the tip deflection. This, of course, is an effect with no direct counterpart in the case of fixed-wing aircraft; furthermore, it is not likely to have been predicted intuitively since positive δ_3 is stabilizing from many considerations. When the root slope direction is opposite from the tip bending deflection, tan δ_3 tends to be stabilizing.

FINITE DEFLECTIONS, PITCH-LAG COUPLING

Large, steady bending deflections, mentioned earlier in connection with drag forces and static divergence, have potential importance for helicopter rotor blade flutter as well, as was pointed out in Reference 10. In cases where a blade section is above the extension of the pitch axis at the same radial station (as in Figure 27), then there are important additional coriolis moments introduced about the inboard pitch axis. To illustrate this effect, consider a blade with a pitch axis and flapping axis in the plane of rotation and at the centerline of the rotor. Suppose this blade was preconed to a value β_0. In this case not only would the feathering moments of inertia about the pitch axis change as compared to a blade where $\beta_0 = 0$, Figure 28, but the coupling term C_V would change by the amount $-2\dfrac{I}{I_\theta} \Omega \sin^2 \beta_0$. Further, Reference 10 points out that, in such cases, the steady lift at an outboard section vertically displaced will be laterally displaced an amount $\theta \chi \sin \beta_0$ by rotation, θ, about the inboard pitch axis. This component of pitching moment plus that caused by variations in in-plane aerodynamic force acting through the vertical offset moment arm about the pitch axis will change the terms C_V and M_θ by the amounts

$$\Omega \frac{\gamma}{2} \frac{I}{I_\theta} \beta_0 \left(\frac{\theta_0}{4} - \frac{2}{3} \lambda \right) \text{ and } \Omega^2 \frac{\gamma}{2} \frac{I}{I_\theta} \beta_0 \left(\frac{\theta_0}{4} - \frac{2}{3} \lambda \right)$$

respectively. Similar steady bending effects in the plane of rotation can also introduce additional pitching moments as a result of lift variations. Since the center of gravity also moves aft, however, and it is center of gravity-aerodynamic center relationship that matters, rather than reference to the pitch axis, these steady in-plane bending effects are less likely to be important. Where concentrated masses are added, however, the effective center of gravity can move more rapidly

51
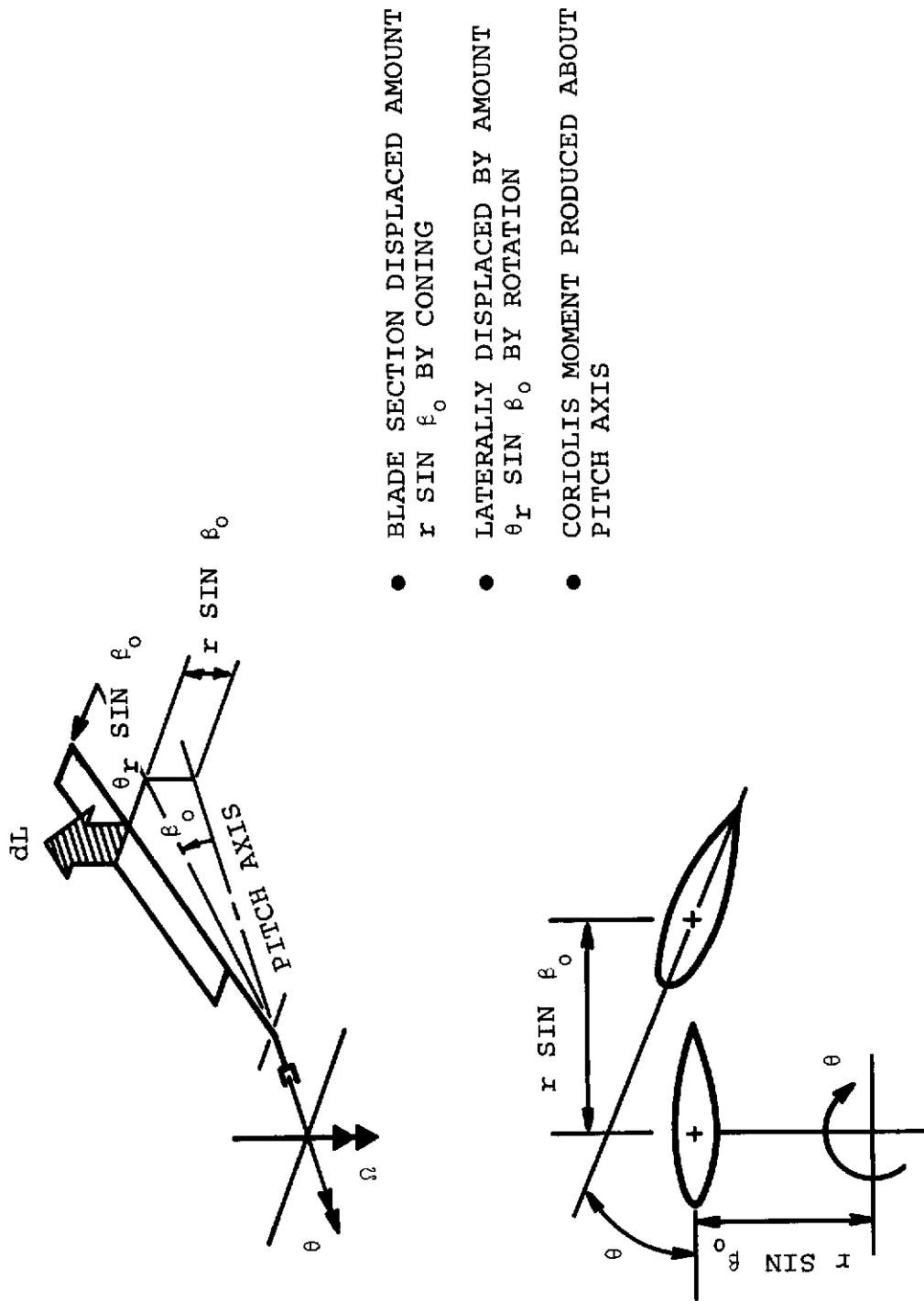
- BLADE SECTION DISPLACED AMOUNT r SIN β_o BY CONING

- LATERALLY DISPLACED BY AMOUNT θr SIN β_o BY ROTATION

- CORIOLIS MOMENT PRODUCED ABOUT PITCH AXIS

Figure 27.   Mechanism of Pitch-Lag Coupling
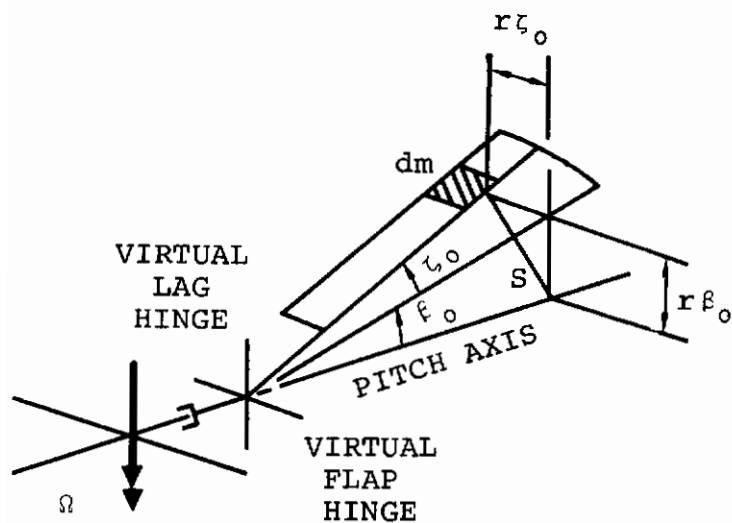
$$I_\theta \ (\text{PITCH INERTIA})$$

$$= I_\theta^1 + \int S^2 dm$$

$$= I_\theta^1 + \int \left[(r\beta_o)^2 + (r\zeta_o)^2 \right] dm$$

$$= I_\theta^1 + \beta_o^2 I_\beta + \zeta_o^2 I\zeta$$

Figure 28. Finite Deflection Effect on Blade Pitch Inertia

than the aerodynamic center, so that in such cases the effect
of steady lag-bending deflections should not be neglected in
stability analyses.

PITCH-LAG AND FLAP-LAG INSTABILITIES

In the preceding section, steady in-plane deflections were
mentioned as a potentially important part of the configuration
when flap-pitch instabilities are considered. When lag hinges
and/or substantial flexibility in chordwise bending are incor-
porated, such deflections must often be considered as addi-
tional degrees of freedom (Figure 29). There is under these
circumstances an increase in the number of dynamic instabil-
ities possible. An early theoretical analysis showing the
possibility of a classical type instability involving lag
motion appeared in Reference 15, and the first analysis of a
case where such instabilities were actually encountered was
given in Reference 16. The degrees of freedom involved are
lagging and flapping. The most critical parameter, however,
is a kinematic coupling, $\tan \alpha_2$, causing a pitch angle change
to occur as a result of blade lag deflections (Figure 30).
For this reason, the phenomenon has been called a pitch-lag
instability. The equations of motion for a rotor with δ_3 but
no flap hinge offset and zero twist are:

$$
\begin{bmatrix} 1 & \\ & 1 \end{bmatrix} \begin{Bmatrix} \ddot{\beta} \\ \ddot{\xi} \end{Bmatrix} + \begin{bmatrix} M_{\dot{\beta}}, & C_v \\ \overline{C_v}, & M_{\dot{\xi}} \end{bmatrix} \begin{Bmatrix} \dot{\beta} \\ \dot{\xi} \end{Bmatrix} + \begin{bmatrix} M_{\beta} & C_a \\ \overline{C_a} & M_{\xi} \end{bmatrix} \begin{Bmatrix} \beta \\ \xi \end{Bmatrix} = 0
$$

where $C_v = \Omega \, \gamma \left[\dfrac{\theta_o}{4} - \dfrac{\theta_o}{3} \, e_\xi \right]$

$$
C_a = - \frac{\gamma}{8} \, \Omega^2 \tan \alpha_2
$$

$$
\overline{C}_v = \frac{2 \beta_o}{\Omega} \left(\omega_\xi^2 + \Omega^2 \right) - \frac{\gamma I}{I_\xi} \frac{\Omega}{2} \left[\theta_o \left(\frac{1}{4} - \frac{2}{3} e_\xi + \frac{e_\xi^2}{2} \right) + \lambda \left(1/3 - \frac{e_\xi}{2} \right) \right]
$$

$$
\overline{C}_a = \frac{\gamma I}{I_\xi} \frac{\Omega^2}{2} \tan \delta_3 \left(\frac{1}{3} - \frac{e_\xi}{2} \right) \lambda
$$

$$
M_{\dot{\xi}} = \frac{C_\xi}{I_\xi} + \frac{\gamma I}{I_\xi} \Omega^2 \left\{ \tan \delta_3 \left(\frac{1}{4} - 2/3 \, e_\xi + \frac{e_\xi^2}{2} \right) \right.
$$
$$
\left. - \frac{\theta_o \lambda}{2} \left(\frac{1}{3} - e_\xi + e_\xi^2 \right) \right\}
$$

$$
M_\xi = \omega_\xi^2 + \frac{\gamma I}{I_\xi} \frac{\Omega^2}{2} \tan \alpha_2 \left(\frac{1}{3} - \frac{e_\xi}{2} \right) \lambda
$$

Here $M_{\dot{\beta}}$ and M_{β} are as defined earlier but the latter has the
quantity $\dfrac{\gamma \Omega^2}{8} \tan \delta_3$ subtracted from it to account for the ef-
fect of δ_3.
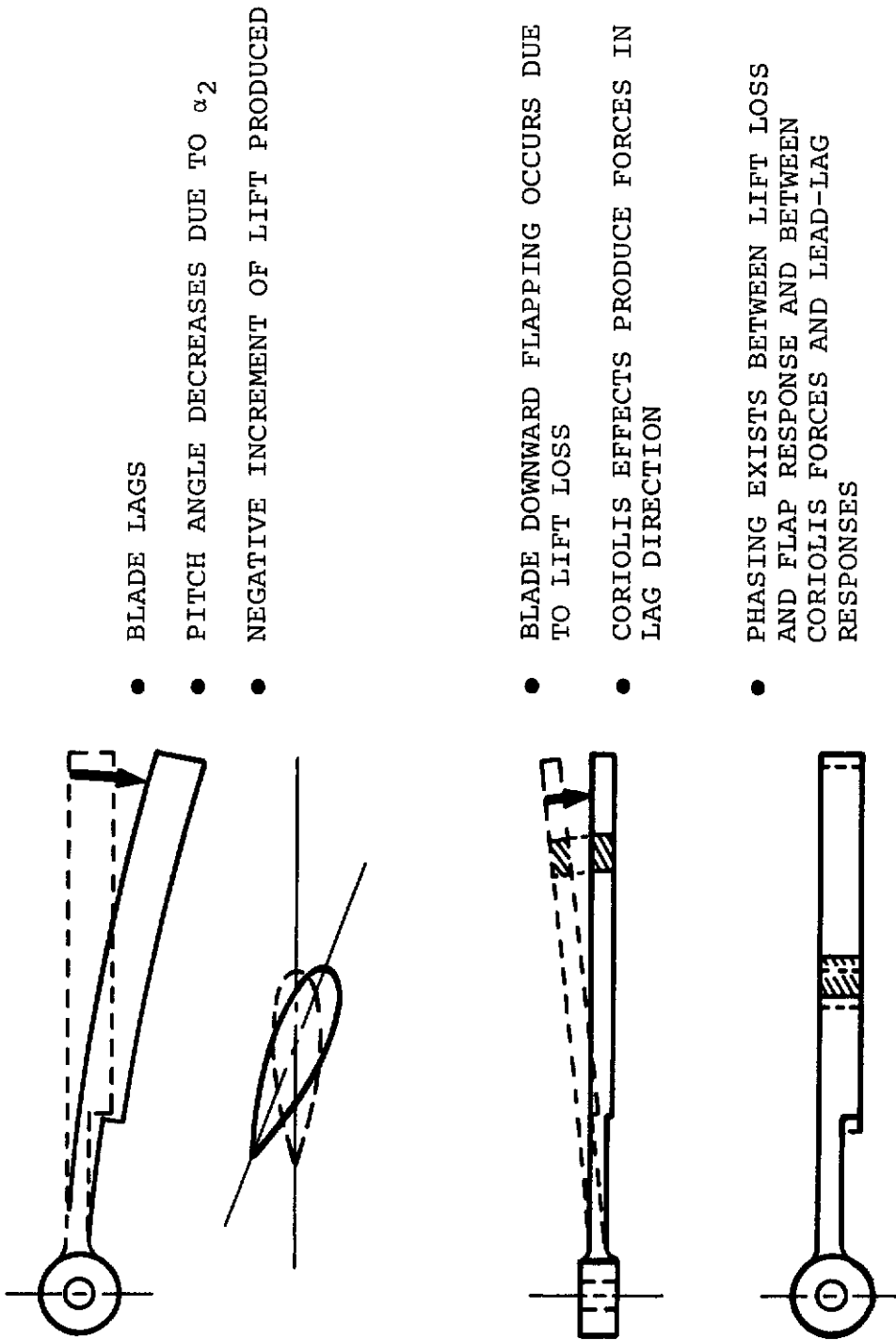
- BLADE LAGS

- PITCH ANGLE DECREASES DUE TO α_2

- NEGATIVE INCREMENT OF LIFT PRODUCED

- BLADE DOWNWARD FLAPPING OCCURS DUE TO LIFT LOSS

- CORIOLIS EFFECTS PRODUCE FORCES IN LAG DIRECTION

- PHASING EXISTS BETWEEN LIFT LOSS AND FLAP RESPONSE AND BETWEEN CORIOLIS FORCES AND LEAD-LAG RESPONSES

- WITH ADVERSE SET OF FREQUENCY RE-LATIONS SYSTEM MAY BE UNSTABLE

Figure 29. A Mechanism of Pitch-Lag Flap Instability With Coriolis and α_2 Coupling
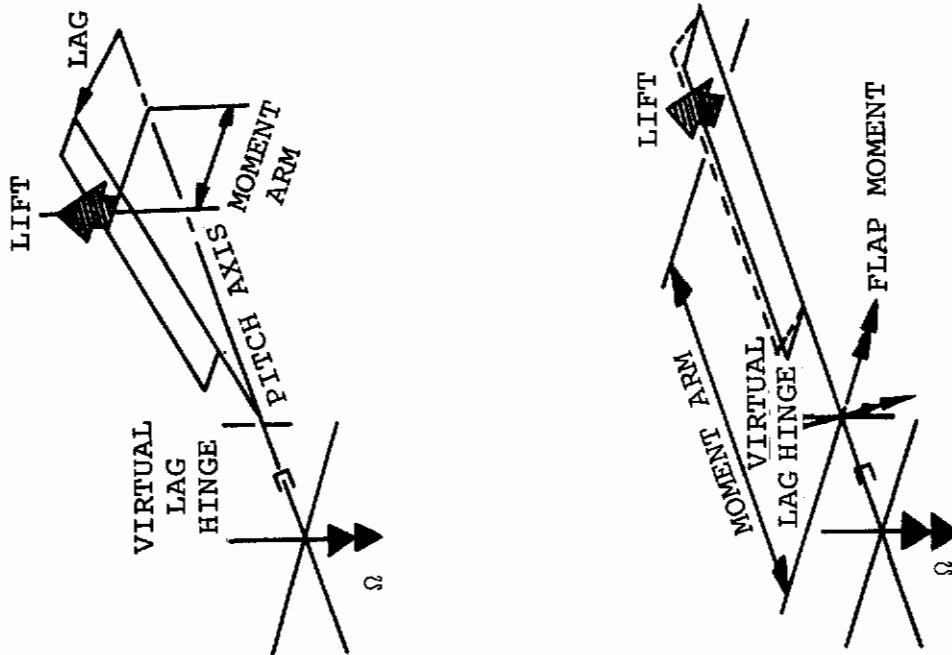
- BLADE LIFT MOVES WITH BLADE LAG DEFLECTION

- A NOSE-DOWN MOMENT ABOUT PITCH AXIS IS PRODUCED

- PITCH MOMENT PRODUCES ROTATION OF VIRTUAL LAG HINGE

- FLAP MOMENT THEN HAS COMPONENT IN LEAD DIRECTION

- PITCH-LAG INSTABILITY MAY OCCUR

- COUPLINGS DO NOT EXIST IF PITCH AXIS IS OUTBOARD OF LAG HINGE

Figure 30. Pitch-Lag Coupling in Rotor Blade

56

Pitch-lag kinematic coupling can arise from inclination of the lag hinge with respect to the blade axis and/or the adverse positioning of control links with respect to such axes when all the other blade angles such as lag, flap, and pitch are accounted for as initial deflections (Figure 31). If this kinematic coupling is such that the blade pitch angle increases as the blade lags forward (negative, in the convention of the above equations) and the lagging frequency, ω_ξ, is below the flap frequency, ω_β, (which also implies $\omega_\xi < \Omega$), Reference 16 shows clearly that an instability can result and presents the following simple stability criterion,

$$C_\xi + \frac{\tan \alpha_2}{1 - \frac{\beta_o}{\theta_o} \tan \delta_3} \quad 2 \Omega I_\xi \frac{\beta_o^2}{\theta_o} > 0$$

The value of lag damping is particularly critical where the principal motion is in lagging or chordwise bending and the frequency of the unstable motion is close to the uncoupled lagging frequency. Reference 17, in further studies of this phenomenon, shows that the aerodynamic damping due to lag motion and proper accounting for blade hinge offsets must be included to be assured of a conservative analysis.

SPECIAL ASPECTS OF PROP/ROTORS

The coupled flap-lag analyses of References 15 through 17 are all intended for the helicopter state, in which the total inflow is relatively small compared to the rotor tipspeed. When a V/STOL prop-rotor operates in high-speed airplane flight regimes, the inflow ratio, J, is no longer negligible compared to unity, and this gives rise to additional aerodynamic couplings between motions in the plane of rotation and out of the plane of rotation. In fact, flap-lag instabilities can occur, as discussed in Reference 18, for rotors with natural rotating lag-bending and flap-bending frequencies close to and higher than rotor speed. As pointed out in this reference, the need for high geometric pitch angles at high values of J rotates the low beamwise bending stiffness of the prop-rotor blades so that substantial beamwise motion (i.e., perpendicular to the local chord plane) contributes to in-plane motion, thus lowering the frequency of the first in-plane mode. Similarly, this rotation orients the chord-bending stiffness so as to have a larger component out of plane, and consequently, the first flap-bending mode tends to be raised. As expected, δ_3 has a substantial influence on this kind of instability. Reference 17 calls attention to the fact that the modes of highly twisted prop/rotor blades at high advance ratios are coupled and that a mode identified as being predominantly in-plane will have substantial out-of-plane flap bending slopes. Thus

57

- BLADE LEAD VELOCITY INCREASES LOCAL WIND VELOCITY AND ADDITIONAL LIFT AND FLAP MOMENT

- LEAD VELOCITY ALSO PRODUCES ADDITIONAL CENTRIFUGAL FORCE STIFFENING IN FLAP MODE

- WHEN THESE INCREMENTS ARE NOT EQUAL FLAPPING OCCURS

- FLAPPING VELOCITY PRODUCES ADDITIONAL CORIOLIS LEAD-LAG FORCES

- THE MECHANISM MAY BE UNSTABLE FOR SUFFICIENTLY LARGE VALUES OF INITIAL FLAP DEFLECTION AND APPROPRIATE FREQUENCY RATIOS OF FLAP AND LAG MODES

ADDITIONAL LIFT

SECTION LIFT

ANGLE OF ATTACK

DUE TO ROTOR SPEED

RESULTANT LOCAL WIND VELOCITY

INFLOW

DUE TO BLADE LEAD VELOCITY

ADDITIONAL LIFT DUE TO BLADE LEAD VELOCITY

INCREMENTAL CENTRIFUGAL FORCE

r SIN β_o

VIRTUAL FLAP HINGE

β_o

Ω

INCREMENTAL CENTRIFUGAL FORCE DUE TO BLADE LEAD VELOCITY
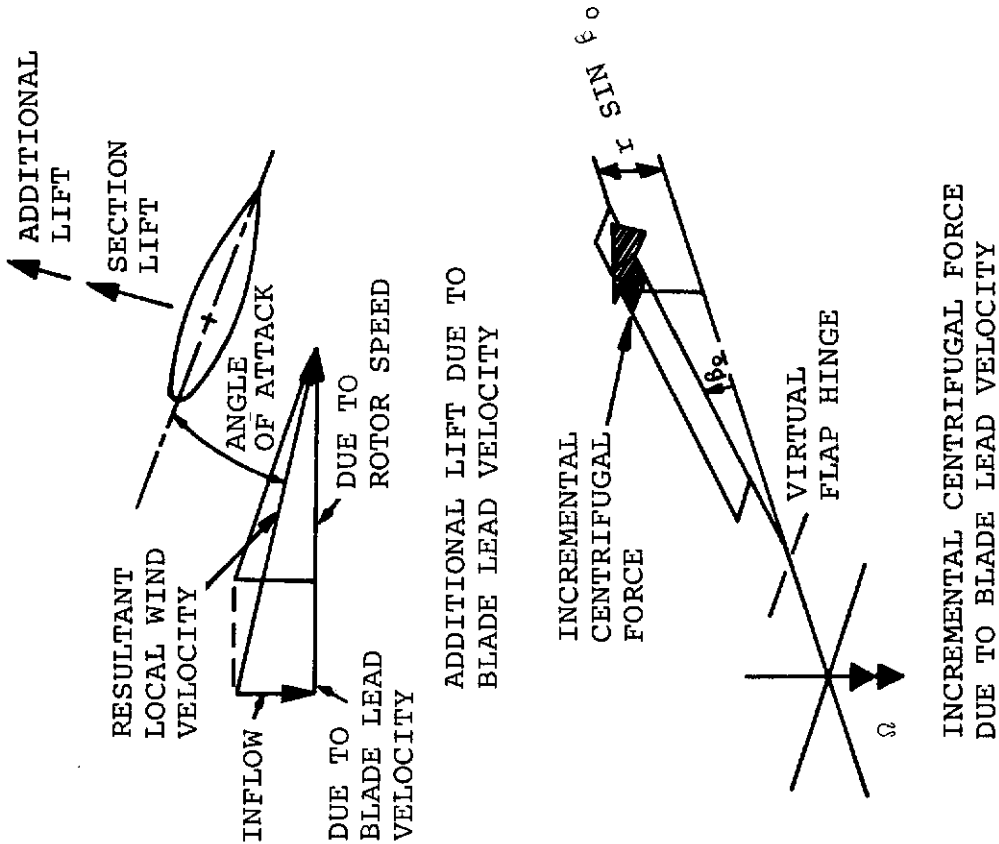
Figure 31. Mechanism of Flap-Lag Instability (Hover Case)

58

Approved for Public Release

the presence of δ_3 provides kinematic pitch coupling for a predominantly in-plane mode, i.e., in such a situation δ_3 can provide effective pitch-lag coupling α_2.

COUPLED FLAP-PITCH-LAG FLUTTER

It is not unusual to have natural frequencies in flap, pitch, and lag reasonably close to one another and rotor blades may be shown to be susceptible to flutter in situations where out-of-plane bending or flapping motions and in-plane bending are coupled, both to each other and to torsional or pitching motions.

An example of such an analysis is found, for example, in Reference 9. Although the hub configuration considered is unusual, many important characteristics of rotor flutter are discussed in this paper. The steady inflow, for example, was found to be important, even though the rotor is in the helicopter state; further, these studies showed the coupling between lag-bending and pitch to be one of the most important parameters. The importance of inflow in flap-lag instabilities was also noted in Reference 18 for the prop/rotor case.

The lag bending pitch coupling is associated with the effect shown in References 15 through 17 to be critical for pitch-lag instabilities. However, these references demonstrate a destabilizing effect produced by increasing angle of attack as the blade leads forward while Reference 9 indicates it to be stabilizing. The difference appears to be due to the fact that, in References 16 and 17, the lag frequency is considerably lower than rotational speed, while in Reference 9 it is not. The simplified criterion given in Reference 16 is obtained by neglecting terms associated with the lag frequency ratio on the assumption of their being small compared with other terms in the equation, particularly some multiplied by the lag damping constant. In Reference 17, this approximation was not made but the frequency ratios were of the same size so that the results of Reference 17 essentially confirmed Chou's approximation.

For blades without lag hinges, the lag frequency is higher and the damping is much lower.

Equation 21 of Reference 16 shows that, if $\tan \alpha_2$ is positive and $\frac{\omega_\xi}{\Omega}$ is not small compared to 1.0, then a second amplified pitch-lag stability criterion emerges; namely for stability

$$\tan \alpha_2 < \frac{\theta_o}{2\beta_o^2}\left[1 - \left(1 - \frac{C_\xi}{I_\xi \Omega}\right)\left(\frac{\omega_\xi}{\Omega}\right)^2 + \frac{C_\xi}{I_\xi \Omega}\left(1 + \frac{C_\xi}{I_\xi \Omega}\right) - \frac{\beta_o}{\theta_o} \tan \delta_3 \right]$$

59

Note that, here if $C_\xi \rightarrow o$ and $\omega_\xi \rightarrow \Omega$, virtually any amount of positive tan α_2 will be unstable.

It is important to note that the results of Reference 9 emphasize the importance of lag-bending frequency ratio in arriving at stability criteria. The effects of steady bending deflections discussed in Reference 10 are also borne out by the results of Reference 9 where increases in blade tip weight increased the flutter stability, principally by reducing the amount of steady flap-bending and hence, the contribution to lag-pitch coupling.

FLAP-LAG CORIOLIS INSTABILITY

All of the instabilities discussed so far are variations on the classical flutter theme in which blade twist or pitch is replaced as an independent degree of freedom by flap or lag, with pitch appearing as a geared effect due to the presence of δ_3 or α_2. Thus, while the phenomena are of great practical importance, they do not present anything unexpected in terms of classical theory.

However, References 7 and 19 identify a quite different type of instability. This is limit cycle in nature and requires only the presence of flexural degrees of freedom in flap and lead-lag, and can occur with blade pitching or twisting totally absent. The essential coupling consists of coriolis forces between flap and lead-lag perturbations which are present when the blade is deflected due to thrust. The strength of the coupling depends on the amplitude of the initial deflection and the frequency of the flapping mode. The mechanism is self-limiting since the strength of the coupling is reduced as the amplitude of oscillation grows. Reference 7 also shows that the effect of forward flight (μ) is destabilizing in this mode of behavior.

The phenomenon is of less significance for articulated rotors since the balance of aerodynamic load and blade steady flap which exists tends to eliminate the coupling mechanism. In hingeless rotors, however, this type of instability may be quite troublesome, although not catastrophic. Reference 7 shows that blade equations in flap and lag in the hover case may be written in the form:

$$\begin{bmatrix} 1 & o \\ o & 1 \end{bmatrix} \begin{Bmatrix} \ddot{\beta} \\ \ddot{\xi} \end{Bmatrix} + \begin{bmatrix} \gamma/8 & -2\beta_o n_\xi^2 \\ -2\beta_o & 2n_\xi \eta \end{bmatrix} \begin{Bmatrix} \dot{\beta} \\ \dot{\xi} \end{Bmatrix} + \begin{bmatrix} 1 + n_\beta^2 & o \\ o & n_\xi^2 \end{bmatrix} \begin{Bmatrix} \beta \\ \xi \end{Bmatrix} = 0$$

where n_β is the flap nonrotating natural frequency
n_ξ is the lead-lag natural frequency

It is observed that, if there is no elastic restraint in flap, i.e., if $n_\beta = 0$, the two equations are effectively decoupled. The physical explanation of this is that when the blade has an effective mean positive angle of attack, a rate of lead motion produces an incremental upward aerodynamic moment and an incremental downward centrifugal flapping moment. If β_0 is obtained by the balance of thrust moment and centrifugal moment, these two opposing incremental effects are equal and no flap-lag coupling exists. If β_0 is reduced because of elastic flapping restraint, the incremental aerodynamic flapping moment dominates and a rate of lead motion produces an up-flapping moment which can cause unstable blade behavior.

When a balance of centrifugal and thrust moments is accomplished by the use of precone, the incremental centrifugal moment is restored to the same magnitude as the incremental aerodynamic moment and the motions are decoupled. Thus small perturbations in flap and lag about the preconed position are always stable.

In forward flight, however, additional coupling terms are present and preconing will not guarantee stability. In forward flight the following additional contributions to the coefficient of the damping matrix are present:

$$\left[\begin{array}{cc} \frac{1}{6} \gamma \mu \, \text{Sin} \, \psi \, , & \bar{\alpha} \gamma \mu \, \text{Sin} \, \psi \\ o & , \quad \gamma/3 \, \bar{\alpha}^2 \mu \, \text{Sin} \, \psi \end{array} \right]$$

It is seen that even if $n_\beta = 0$, the term $\bar{\alpha} \gamma \sin \psi$ provides coupling which may destabilize, so that as long as the coning deflection β_0 is non-zero the strength of the coupling between the modes will increase with μ; so we might expect the onset of flap-lag instability as a function of forward speed.

REQUIRED FEATURES OF AN ENGINEERING ANALYTICAL CAPABILITY

THE NEED FOR COMPREHENSIVE ANALYSES

When we define the requirements of an engineering capability for stability analysis, the question may pose itself as to why such an analysis or capability is required. Most of the phenomena discussed are described adequately in the literature. However, it will frequently be found that the mathematical models in published papers are selected to demonstrate the phenomenon rather than to represent a hardware system. The influence of additional members of the system is often ignored, although these may have a cumulative effect which, from a practical point of view, may be just as important as the critical parametric variations on which published material tends to concentrate. Thus, unstable behavior indicated by examination of one system element (say, the rotor blade) in isolation may be significantly improved or impaired when the influence of the rest of the system is taken into account. As an example of potential interaction of this sort, we will discuss flap-lag coriolis instability analyzed in Reference 7. In this type of instability the coriolis forces couple the rotor flapping freedom and the lead-lag freedoms and, under certain conditions of blade natural frequency and steady deflection, an instability occurs at the lead-lag natural frequency. However, we know that blade lead-lag motion will couple with airframe motion in the plane of the rotor (ground resonance or mechanical instability) so that, when the three degrees of freedom are examined together, we should not be surprised if the total system were less stable than either of its component subsets. The opposite might hold true depending on the circumstances of the particular configuration.

It is difficult to envision a heavily damped airframe mode coupling with the blade lead-lag and absorbing sufficient energy to stabilize the flap-lag systems. Speculation of this kind can only be ended by a comprehensive analysis which takes into account all the potentially significant factors. (The same objective can be achieved using a modeling technique but a prior analytical approach is justified.)

Nevertheless, valuable guidance is provided by the academic studies investigating 1- and 2-degree-of-freedom systems so far as they define critical parameters which must be considered in formulating more general analyses and provide rules which may be used effectively in preliminary design.

The other major source of information on parameters which influence stability is experience with dynamically similar models and full-scale hardware.

ANALYTICAL REQUIREMENTS FOR PROP/ROTOR CONFIGURATIONS

An engineering analytical capability must address the problems outlined in the previous sections in a quantitative way. A modal description of blade freedoms is a primary requirement. The use of equivalent hinge offset systems is a generally understood way of demonstrating the existence of the various phenomena and their parametric sensitivity; however, for accuracy in the prediction of point design behavior, and particularly in the case of highly twisted blades, a modal approach is required, since the relationships between flap, lag, and torsion vary along the span and cannot be easily accounted for by constants such as α_2 and δ_3.

We may then outline the principal features necessary for the upgraded technology designed to address the problem areas not covered adequately by current state-of-the-art capabilities (see Table IV).

- Blade Degrees of Freedom

  A minimum blade representation is required which will include analytically the mode which is predominantly:

  (a) Fundamental out-of-plane flap

  (b) Fundamental lead-lag

  (c) Fundamental torsion

  (d) Pitch of the blade about the pitch axis

- The requirement is satisfied by the provision for four general mode shapes with each allowed components in flap-lag-torsion. This then permits representation of (a) through (d) in as general a form as may be required. It also permits consideration of higher modes than the fundamental if this is desired. The analysis must address the stability of perturbations about initially deflected conditions of the blades caused by aerodynamic and inertial loadings.

- Airframe Degrees of Freedom

  The hub to which the blades attach must have degrees of freedom representing the rigid-body motion of the aircraft, the vibratory modes of the airframe, and local freedoms introduced by soft mounting or by gimbaling the rotor.

  The number of such airframe and rigid-body modes required depends on the special circumstance pertaining in any given case.

63

- A minimum capability will include:

  (a) Six rigid-body degrees of freedom

  (b) As many general airframe modes as are required
       to represent:

       (1) Wing fundamental vertical bending and
            torsion

       (2) Wing fundamental horizontal bending

       (3) Fuselage bending and torsion

       (4) Local modes of the nacelle

  (c) Adequate representation of landing gear dynamics
       to permit prediction of ground resonance effects.

- Blade and Hub Geometry

  Control system representation must take account of the
  fact that the pitch axis may occupy a variable posi-
  tion with respect to the blade deflected shapes; the
  amount of pitch, lag-flap coupling is directly influ-
  enced by the spanwise location of the pitch axis.
  Precone, prelead or lag, offset, and sweep are impor-
  tant in various contexts and will be included.

- Aerodynamic Representations

  Aerodynamic sophistication in the blade representation
  is not required for prediction and correlation of the
  phenomena discussed: typical blade chords, fre-
  quencies, and velocities are such that the blade
  frequency parameters, $K = \dfrac{\omega b}{V}$, are small and quasi-
  static assumptions appear to be adequate. Wing-
  induced effects need to be included since they are
  seen to have a potentially powerful effect on the
  rotor derivatives and thus on divergence speeds.
  Wing and empennage properties, however, require that
  account be taken of frequency dependency. The range
  of airframe frequencies present in the airframe might
  lead to errors in stability boundaries if this repre-
  ntation were restricted to be quasi-static.

● Direction and Type of Flow Through Rotor

Small angle assumptions regarding flow are not accept-
able, since the analysis will be used to investigate
flight conditions ranging from the propeller cruise
mode (axial flow) through transition (nonaxial high
angularity) to the helicopter regime (edgewise flow).
In addition, nonuniform effects caused by the wing-
bound circulation must be considered.

● Blade Deflections

One of the more troublesome phenomena in recent years
has been the presence of flap-lag coupling instabil-
ities associated with deflected blades. These have
been limit cycle in nature but would nevertheless be
an unacceptable feature in operation. Prediction
capabilities must therefore include the behavior of
blades deflected under loading arising from steady
centrifugal and aerodynamic forces.

TABLE IV

MINIMUM REQUIREMENTS FOR AN UPGRADED TECHNOLOGY

Airframe Degrees of Freedom	Blade Degrees of Freedom
● Rigid-body modes	● Sufficient to represent fundamental pitch, flap, lag, and torsion
● All vibration modes which are of same order of fre-as $\Omega \pm \omega B$	
	● Model representation must include coupled effects so that effective δ_3, α_2, etc., are included
● These may extend well beyond fundamentals	
	● Dynamic and aerodynamic effects of deflections must be included
● Local nacelle modes	
● Above objectives may be achieved by provision of sufficiently large num-ber of general airframe modes	● Aerodynamics must include effect of μ as well as λ

OUTLINE DESCRIPTION OF THE STABILITY ANALYSIS DEVELOPED UNDER CONTRACT AND DISCUSSED IN VOLUME II

The analytical requirements defined in the preceding paragraphs have substantially been incorporated in the aeroelastic stability analysis computer program described in Volumes II and III.

Airframe Representation

The program permits representation of the six rigid-body degrees of freedom and an additional six elastic modes of the airframe. This is adequate to accommodate the fundamental structural modes and additional selected modes to represent local effects, such as flexibility between the engine-nacelle package and the wing.

Rotor Representation

Two rotors are included in the analysis, each rotor having 3 or more blades. Rotor gimballing freedoms in pitch and yaw are available, and also a shaft rotation mode. Up to four blade modal degrees of freedom may be used, each mode having flap, lag, and torsional components if required. The aeroelastic coupling effects of blade deflections are taken into account in evaluating the coefficients of the differential equation of the system.

Aerodynamic Representation

A two-dimensional strip theory representation has been used for the wings and empennage. The rotor blade aerodynamics account for $\dot{\alpha}$ effects (optional) and for large angles of inflow such as occur in the tilt-rotor transition regime. The program will also account for nonuniform inflow such as induced by the wing, provided that the flow field is specified.

Landing Gear Representation

Although most configurations feature two main gears and a nose gear, the program was written for systems with up to four gears, since a number of helicopters have a four-poster arrangement. An idealized linear spring and damper arrangement is used to represent each set of struts, oleos, and tires.

Application to Articulated Rotors

The program can be used to evaluate articulated rotor systems. Blade flap and lag about a hinge and kinematic effects such as δ_3 or α_2 may be represented by linear mode shapes with the appropriate torsional components.

Part II. Blade Vibratory Loads

P. F. Leone

INTRODUCTION

SOURCE OF AIRLOADS

Velocity Relative to the Airfoil

A prop/rotor blade operating in an environment in which the forward-flight velocity vector has a component in the plane normal to the rotor shaft will experience a 1/rev fluctuation in the total relative wind velocity acting at a blade section. This is the result of the fact that, in the advancing-rotor half cycle, the forward velocity vector adds to the rotational speed vector; whereas, in the retreating-rotor half cycle, the reverse is true (see Figure 32). Since the dynamic pressure acting at an airfoil section is proportional to the square of the total relative wind velocity, it results as a periodic quantity over one rotor cycle containing steady, 1/rev, and 2/rev harmonic components. The introduction of a rotor collective pitch angle is felt as a steady aerodynamic angle of attack by the section which, when multiplied by the dynamic pressure, will give rise to aerodynamic forces which are also periodic in one rotor cycle and contain steady, 1/rev, and 2/rev components. The introduction of a 1/rev cyclic pitch angle to the rotor when multiplied by the dynamic pressure will now introduce an additional vibratory term, being a 3/rev component, as well as its own steady, 1/rev, and 2/rev components (see Figure 33).

Blade Motion and Downwash

Blade flexibility in the flapwise, chordwise, and pitch directions, along with vorticity due to lift variations with time and blade span, generates airloads of all frequencies (see Figure 34). Pitch deflections change the mechanical angle of attack of the airfoil while flapwise and chordwise deflections induce a change in the angle of attack by altering the direction of the wind relative to the blade. Discontinuities in spanwise blade lift generate trailed vortices, with an especially strong vortex trailed at the blade tip. Changes in blade lift with time generate shed vortices from the blade. The distribution of shed and trailed vortices created by the rotor blade itself or by other rotor blades of the same rotor or other rotors operating in the vicinity of the rotor blade in question generates an induced velocity on the blade that further changes the angle of attack and blade lift.

Other Sources of Vibratory Airloads

These periodic aerodynamic forces are those derived from the fundamental expression for a lift force in which the section lift coefficient is a linear function of the aerodynamic angle of attack and the discussion in the preceding paragraphs is
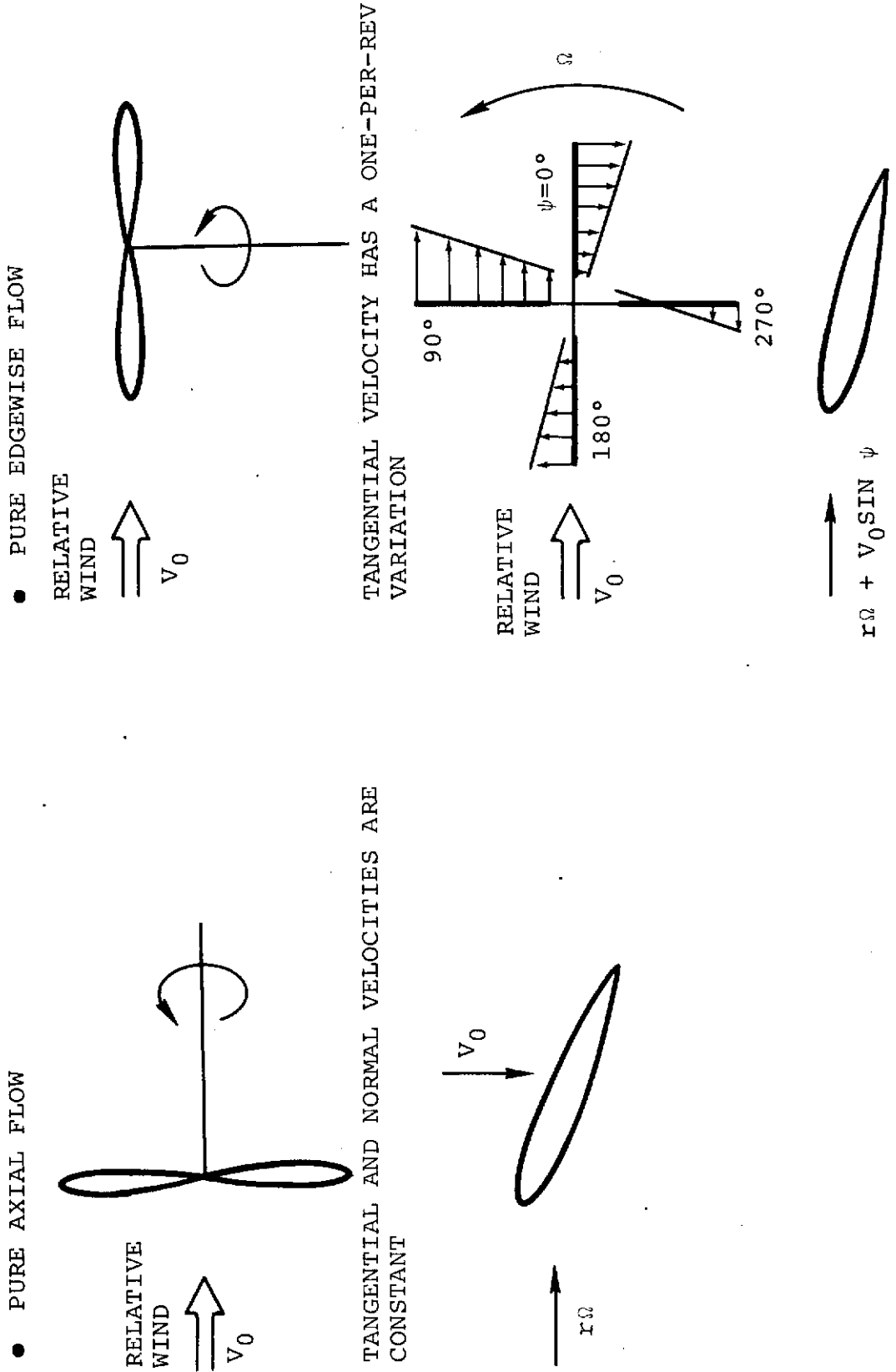
69

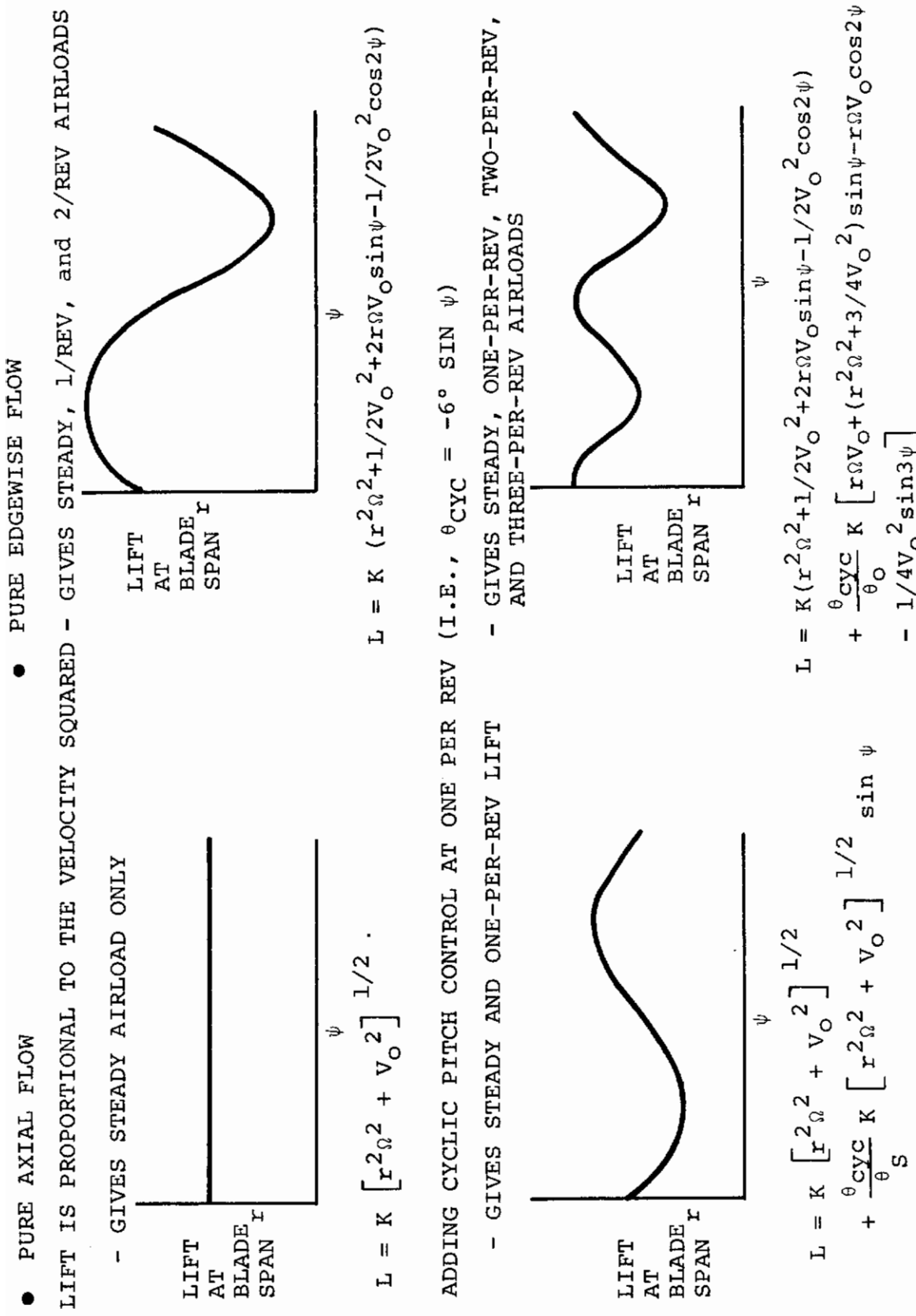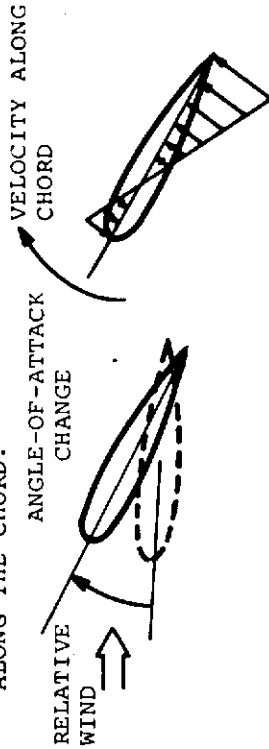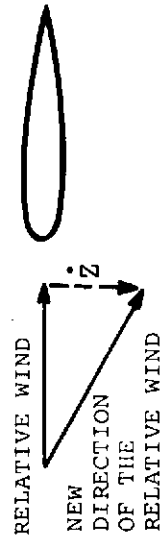Figure 32.   Sources of Prop/Rotor Airloads

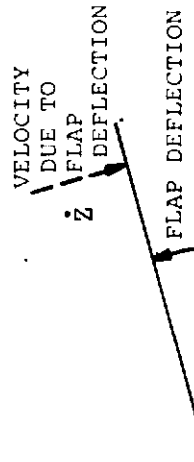- PURE EDGEWISE FLOW

RELATIVE WIND V_0

TANGENTIAL VELOCITY HAS A ONE-PER-REV VARIATION

$\psi = 0°$

90°

180°

270°

Ω

RELATIVE WIND V_0

$r\Omega + V_0 \sin \psi$

- PURE AXIAL FLOW

RELATIVE WIND V_0

TANGENTIAL AND NORMAL VELOCITIES ARE CONSTANT

V_0

$r\Omega$

70

- PURE AXIAL FLOW
- PURE EDGEWISE FLOW

LIFT IS PROPORTIONAL TO THE VELOCITY SQUARED - GIVES STEADY, 1/REV, and 2/REV AIRLOADS

- GIVES STEADY AIRLOAD ONLY

LIFT
AT
BLADE
SPAN

$$L = K \left[r^2\Omega^2 + V_o^2 \right]^{1/2} .$$

$$L = K \left(r^2\Omega^2 + 1/2 V_o^2 + 2r\Omega V_o \sin\psi - 1/2 V_o^2 \cos 2\psi \right)$$

ADDING CYCLIC PITCH CONTROL AT ONE PER REV (I.E., $\theta_{CYC} = -6°$ SIN ψ)

- GIVES STEADY AND ONE-PER-REV LIFT

- GIVES STEADY, ONE-PER-REV, TWO-PER-REV, AND THREE-PER-REV AIRLOADS

LIFT
AT
BLADE
SPAN

$$L = K \left[r^2\Omega^2 + V_o^2 \right]^{1/2} + \frac{\theta_{CYC}}{\theta_S} K \left[r^2\Omega^2 + V_o^2 \right]^{1/2} \sin\psi$$

$$L = K(r^2\Omega^2 + 1/2 V_o^2 + 2r\Omega V_o \sin\psi - 1/2 V_o^2 \cos 2\psi)$$
$$+ \frac{\theta_{CYC}}{\theta_o} K \left[r\Omega V_o + (r^2\Omega^2 + 3/4 V_o^2) \sin\psi - r\Omega V_o \cos 2\psi \right]$$
$$- 1/4 V_o^2 \sin 3\psi \right]$$

Figure 33. Generation of Periodic Airloads

• AIRLOADS OF ALL FREQUENCIES ARE GENERATED BY:

FLAPWISE-CHORDWISE AND PITCH BLADE DEFLECTIONS

VORTEX-INDUCED NONUNIFORM DOWNWASH, WHICH INDUCES CHANGES IN DIRECTION OF THE RELATIVE WIND IN THE SAME MANNER AS $\dot{z}$

$R\Omega$

Ω

TRAILED VORTEX (FUNCTION OF SPANWISE LIFT DISTRIBUTION)

SHED VORTEX (FUNCTION OF TIME VARIATION OF LIFT)

PITCH DEFLECTIONS CHANGE THE MECHANICAL ANGLE OF ATTACK AND INDUCE A VELOCITY ALONG THE CHORD.

VELOCITY ALONG CHORD

ANGLE-OF-ATTACK CHANGE

RELATIVE WIND

FLAP DEFLECTIONS CHANGE THE DIRECTION OF THE RELATIVE WIND

VELOCITY DUE TO FLAP DEFLECTION

$\dot{z}$

FLAP DEFLECTION

RELATIVE WIND

$\dot{z}$

NEW DIRECTION OF THE RELATIVE WIND

Figure 34. Airloads Due to Blade Motions and Trailed and Shed Vortices

valid for aerodynamic angles of attack up to stall. Associated with the lift there are periodic aerodynamic profile and induced-drag forces and quarter-chord moments which are generated by the periodic dynamic pressure acting at an airfoil section and derived from the section drag moment coefficients. Over and above the fundamental periodic aerodynamic section lift, drag, and moment derived from linear incompressible theory, there are additional nonlinear compressible counterparts to these section excitations which contribute to the aeroelastic response of the rotor blade as the local angles of attack vary rapidly. These nonlinear compressible components are of particular importance for those blade sections operating in a stalled environment (see Figure 35).

The Axial-Flow Flight Condition

For a prop/rotor operating in a pure axial-flow environment, the total relative wind velocity acting at a blade section will be a constant (see Figure 32). The introduction of 1/rev cyclic pitch angle to the rotor will now yield a steady and 1/rev lift (see Figure 33). A small component of velocity in the plane normal to the rotor shaft due to the angle of attack of the rotor shaft or cyclic induced lead-lag deflections (see Figure 36) will introduce the multifrequency airloads discussed above.

BLADE LOADS

Components of the Load

The consequence of these periodic aerodynamic forces acting upon the prop/rotor blade is the generation of periodic bending moments which are partially relieved by centrifugal and inertial forces (see Figure 37), the remainder being expended in deforming the blade, thus producing bending strains and their associated bending stresses. These resulting periodic bending stresses are generated throughout the duration of the periodic dynamic pressure in the rotor shaft normal plane; which, as in the case of the helicopter, is the full duration of its forward-flight condition. Consequently, the structural design problem of a prop/rotor blade centers largely upon its ability to withstand these cyclic fatigue stresses for a prescribed period of time.

Effect of Blade Root Constraint

One method for minimizing this basic problem is to employ mechanical hinges at the blade root; this compels the blade bending moments to approach a zero value at the hinges. When mechanical springs and dampers are considered about the hinge axes, nonzero bending moments result that are proportional to the spring and damper rates. A hingeless rotor blade, on the

73

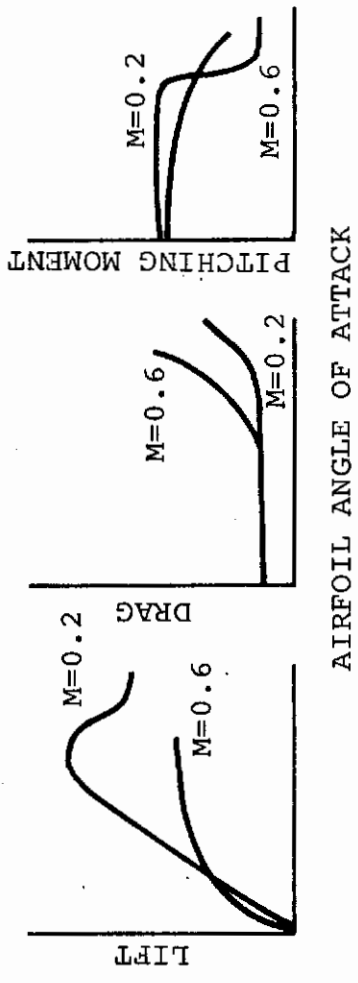- AIRLOADS GENERATE LIFT, DRAG, AND PITCHING MOMENTS ON AN AIRFOIL

RELATIVE WIND

LIFT

DRAG
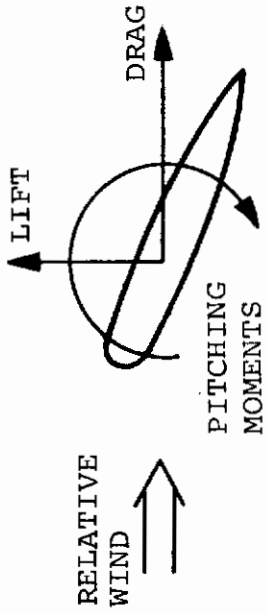
PITCHING MOMENTS

- SIMPLE THEORY ASSUMES THAT LIFT IS A LINEAR FUNCTION OF BLADE ANGLE OF ATTACK, AND THAT DRAG AND PITCHING MOMENT ARE ZERO

LIFT

ANGLE OF ATTACK
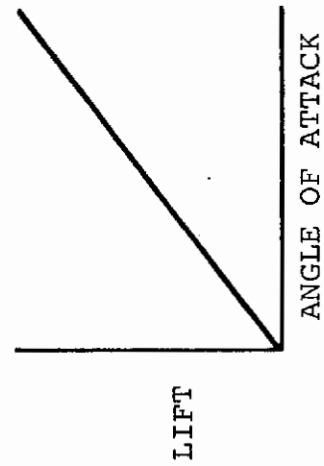
DRAG = PITCHING MOMENT = 0

- THE CONSIDERATION OF DRAG AND PITCHING MOMENTS, AERODYNAMIC NONLINEARITIES (STALL), COMPRESSIBILITY, AND UNSTEADY EFFECTS FURTHER ADDS TO ALL FREQUENCIES OF AIRLOADS

STEADY-STATE, NONLINEAR, COMPRESSIBLE THEORY:

LIFT

M=0.2

M=0.6

DRAG

M=0.6

M=0.2

PITCHING MOMENT

M=0.2

M=0.6

AIRFOIL ANGLE OF ATTACK

UNSTEADY EFFECTS:

LIFT

DRAG

PITCHING MOMENT

AIRFOIL ANGLE OF ATTACK
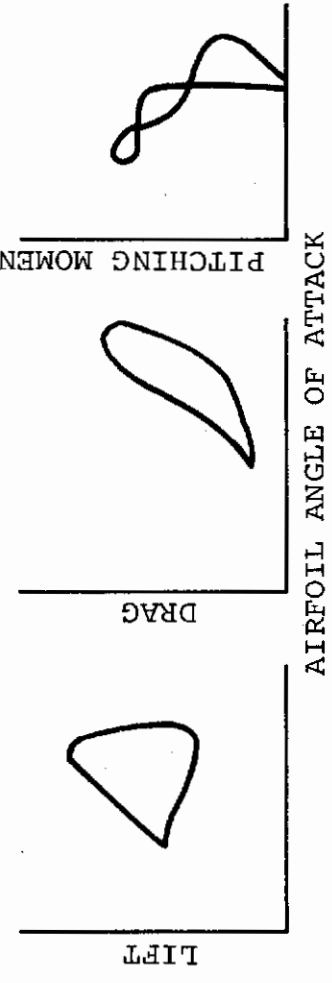
Figure 35. Linear, Unsteady, and Compressibility Effects on Airloads

- FOR A PROP/ROTOR IN AXIAL FLOW A VARYING
  TANGENTIAL COMPONENT OF VELOCITY CAN BE
  OBTAINED BY:

  AN ANGLE OF ATTACK OF THE ROTOR SHAFT
  WITH RESPECT TO THE WIND

- THEREFORE, AIRLOADS OF ALL FREQUENCIES
  CAN BE ACTING IN BOTH HELICOPTER AND
  PROP/ROTOR AIRCRAFT
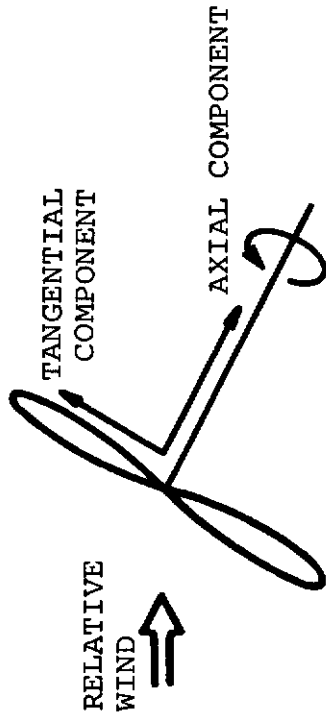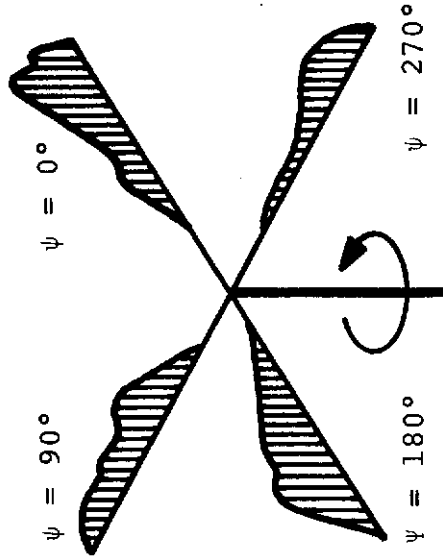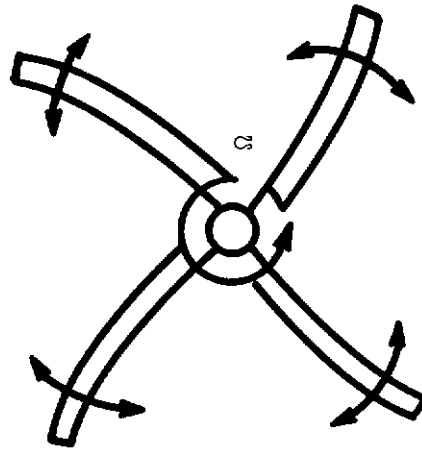
Figure 36. Sources of Alternating Wind
Components in Rotor Disc

75

Figure 37. Blade Loads and Bending Moments

- BLADE LOADS RESULT FROM THE SUM OF AIRLOADS, CENTRIFUGAL FORCES, AND INERTIAL FORCES

- THE BLADE BENDING MOMENT DISTRIBUTION IS A FUNCTION OF THE ROOT RESTRAINT
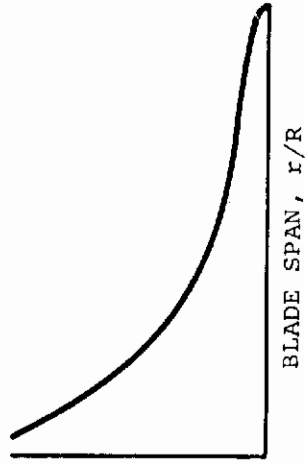
- TO REDUCE BENDING MOMENTS A HINGELESS ROTOR HAS A RELATIVELY SOFT ROOT END TO SIMULATE AN ARTICULATED ROTOR

AIRLOADS
CENTRIFUGAL FORCE
INERTIAL LOADS

RIGID BLADE
ARTICULATED BLADE
BENDING MOMENT
BLADE SPAN, r/R

ARTICULATED
HINGELESS
MECHANICAL FLAP HINGE
EFFECTIVE FLAP HINGE
ROTOR CENTER

other hand, must absorb these root bending moments which rise sharply in this region, the rate being proportional to the bending stiffness at the root (see Figure 37). Consequently, the typical hingeless rotor blade employs a low bending stiffness in the inboard root area to minimize these rapidly rising bending moments. As a result, the typical hingeless rotor blade deforms in its fundamental mode in a manner similar to an articulated rotor blade having a large effective hinge offset from the rotor center in the region of minimum bending stiffness.

Coriolis Loads

Both the articulated rotor blade with mechanical hinges and the hingeless rotor blade featuring effective hinges execute angular motions about the hinge axes which give rise to coriolis inertia forces which must be absorbed by the rotor blade (see Figure 38). These coriolis inertia forces are proportional to twice the product of the rotor angular velocity with a linear velocity of a mass point relative to the rotating frame of reference. Like the aerodynamic forces, these coriolis inertia forces are periodic in nature and contain 1/rev, 2/rev, etc., harmonic components but no steady components.

Blade Dynamics

Because of its elasticity, the prop/rotor blade has natural modes of vibration whose individual natural frequencies vary with the rotor angular velocity (see Figure 39). Since the periodic aeromechanical exciting forces are describable in terms of harmonic components whose frequencies are integral multiples of rotor speed, it is obvious that a resonance can occur in any one natural mode for more than one rotor speed. Fortunately, aerodynamic damping forces are generated by the blade elastic motions which reduce these resonant responses (see Figure 40). However, care must be taken in the design of a prop/rotor blade to avoid such resonances in the normal operating rotor speed band; a determination of the blade natural modes is of primary importance during initial design of the rotor blade. In addition to determining the undamped natural frequencies for each natural mode, it is desirable to include the determination of the associated damped amplification factors for rotor harmonic exciting frequency. These factors are important in assessing the effects of elasticity and mode shape on the aerodynamic damping process generated by the rotor blade in its natural modes of vibration.
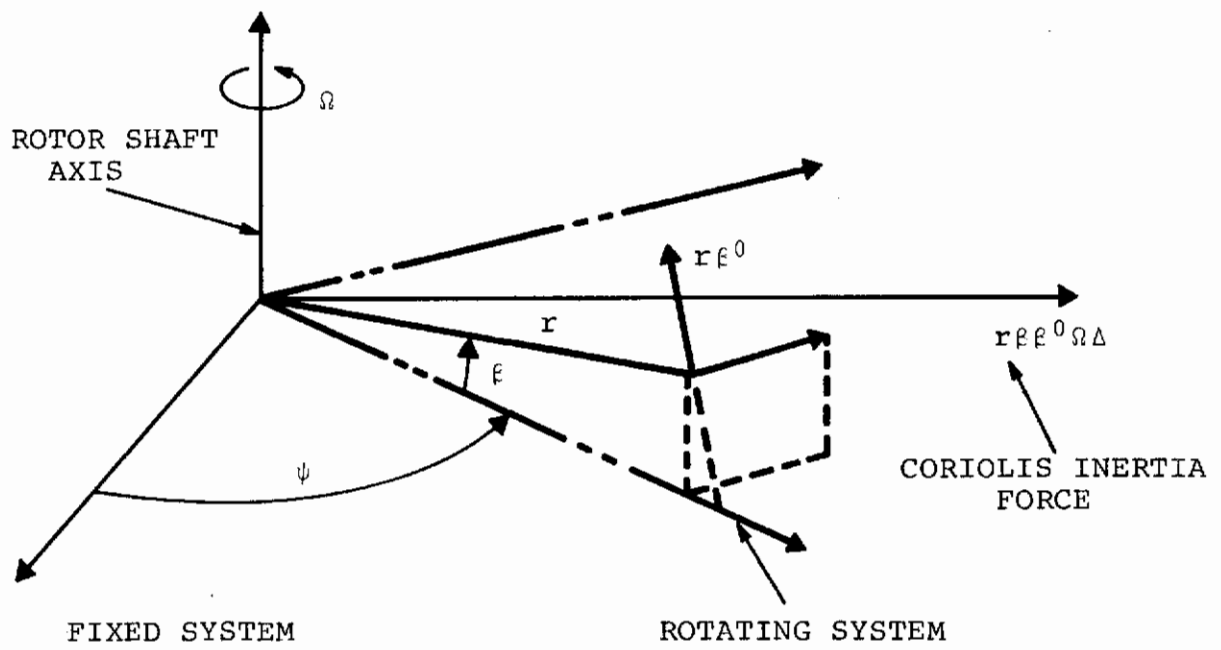
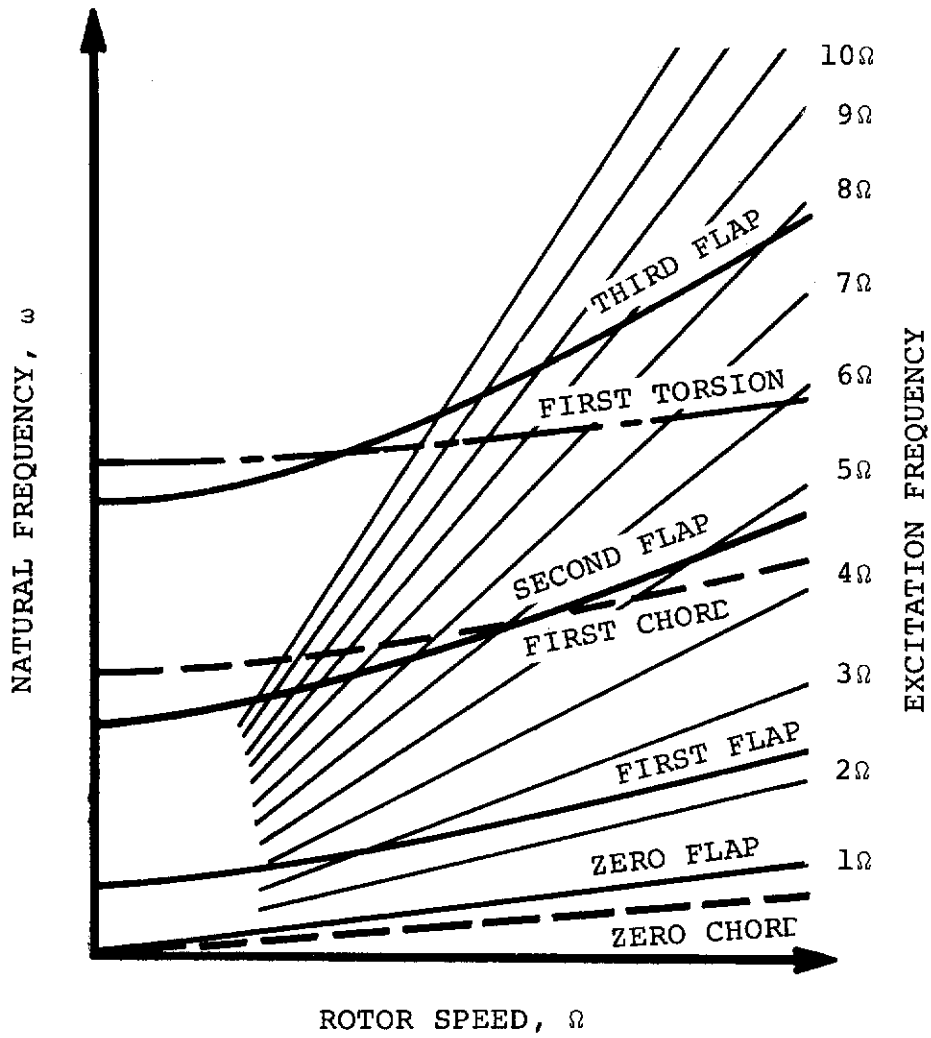Figure 38. Coriolis Inertia Force Due to Flapwise Motion

NATURAL FREQUENCY, ω

EXCITATION FREQUENCY

10Ω

9Ω

8Ω

THIRD FLAP

7Ω

FIRST TORSION

6Ω

5Ω

SECOND FLAP

4Ω

FIRST CHORD

3Ω

FIRST FLAP

2Ω

ZERO FLAP

1Ω

ZERO CHORD

ROTOR SPEED, Ω

Figure 39. Natural Frequency Spectra for
a Prop/Rotor Blade
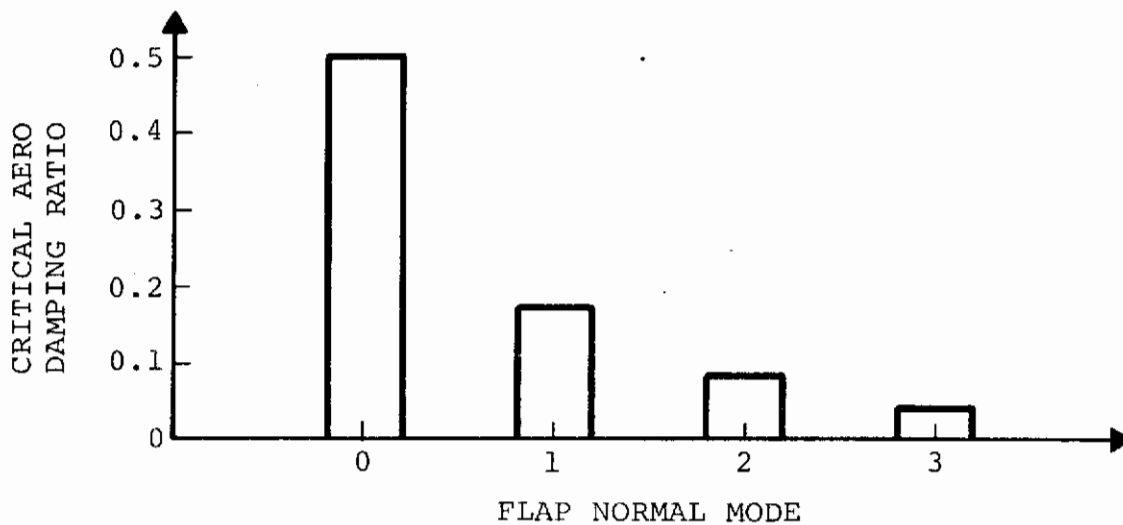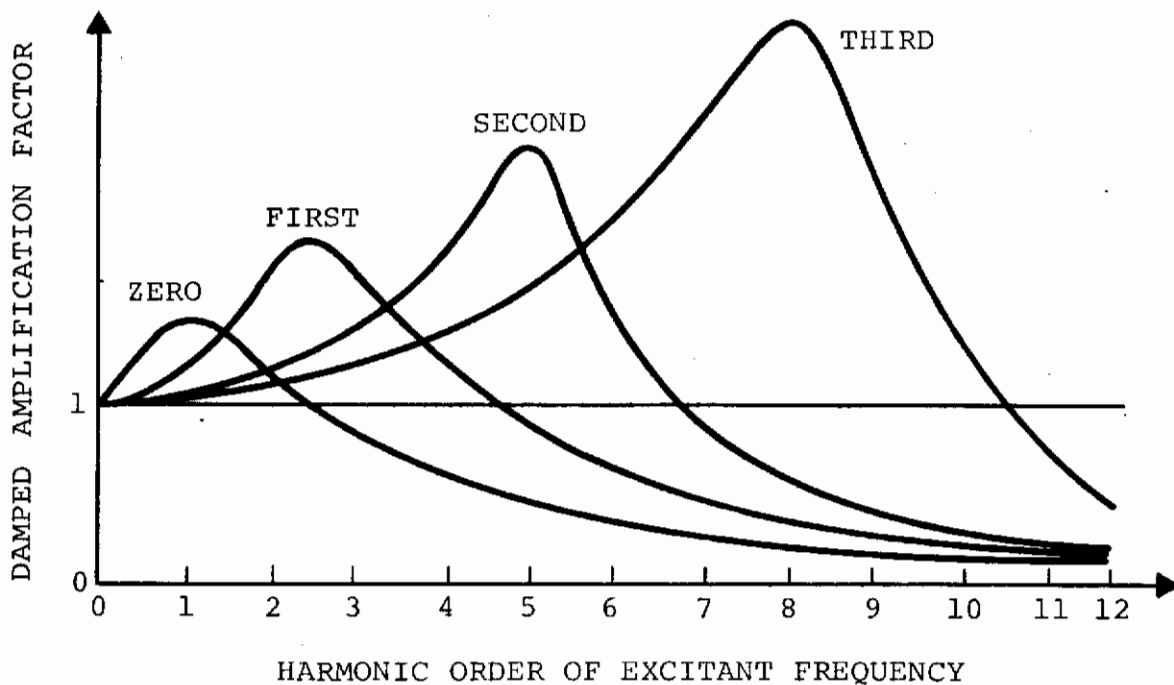
Figure 40. Flap Modes Damped Amplification Factors

80

CURRENT MATHEMATICAL MODEL

ROTOR BLADE REPRESENTATION

The current mathematical model in use by Boeing-Vertol to
predict the aeroelastic response of a prop/rotor blade to
aeromechanical excitations has for its basis the decomposition
of the blade into a finite number of lumped masses intercon-
nected by massless elastic beams (see Figure 41). This basic
technique permits accounting for the nonuniform spanwise dis-
tributions of the blade aerodynamic and structural properties.
Each lumped mass is subjected to its individual aeromechanical
excitation, its resulting response being coupled to its adjac-
ent lumped masses through linear difference equations which
relate the local changes in deflection, slope, moment, shear,
and torque. At the blade root, boundary conditions are satis-
fied which permit the solution for the blade deformation
response at each lumped mass station. The current model
accounts for dynamic and aerodynamic coupling between flap
bending and torsion and uncoupled chord bending and is appli-
cable to a low-twist prop/rotor blade, such as a helicopter
rotor blade. The net result of the analysis is the solution
for the flap bending, chord bending, and torsional aeroelastic
response, including the total solutions for the blade deflec-
tion, slope, moment, shear, and torque, the associated control
system forces, the associated rotor hub loads, and the rotor
performance.

AERODYNAMIC REPRESENTATION

Because of its use of unsteady aerodynamics, nonuniform down-
wash, airfoil section data, shed wake effects, and compressi-
bility effects, the current model has been very successful in
predicting pitch link load waveforms throughout the level-
flight speed range, including, of particular importance, the
stall regime for full-scale helicopter rotors (see Figures 42,
43, and 44). The model has had good success in predicting
flap and chord bending moments and rotor lift distributions
(see Figures 45, 46, and 47) from 110 to 125 knots for the
full-scale H-34 helicopter rotor. In the area of highly
twisted V/STOL wind tunnel model rotors, the mathematical
model has been adequate for predicting flap bending moments
but less successful in predicting the chord bending moments
(see Figures 48 and 49) and pitch link loads. The current
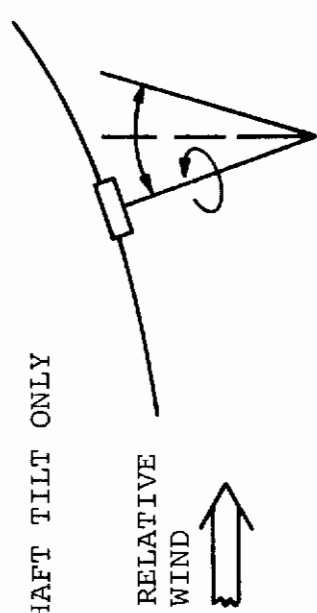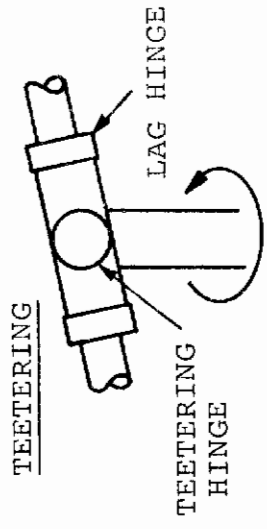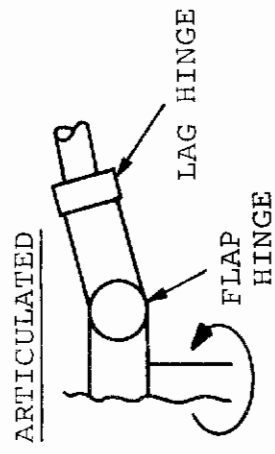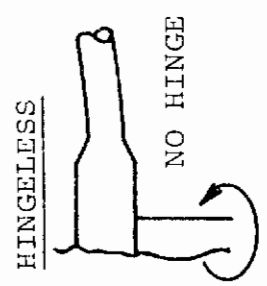aerodynamic capability is reviewed in Figures 50 and 51.

DYNAMIC REPRESENTATION

The poor prediction for the highly twisted model rotor is be-
lieved due largely to the neglect of the large twist angle of
the model and its effects on the resultant elastic and aero-
dynamic coupling. Although the current mathematical model

81
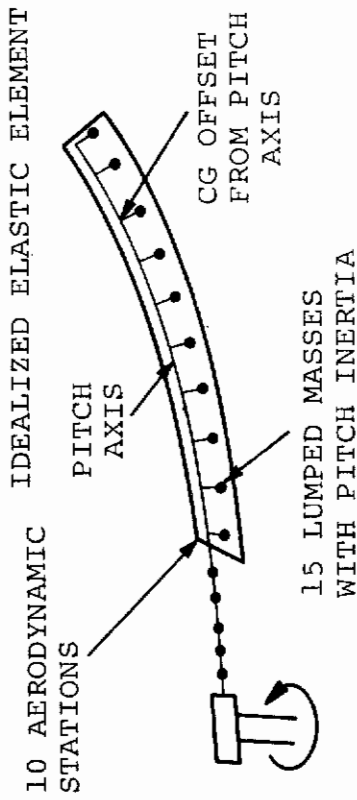
- BLADE IDEALIZATION

  COUPLED FLAP-PITCH AND UNCOUPLED
  LAG
  SMALL BLADE PRETWIST
  VARIABLE CENTER OF GRAVITY
  COINCIDENT SHEAR CENTER, PITCH
  AXIS, AND VERTICAL NEUTRAL AXIS
  FLAP-PITCH DEFLECTIONS ITERATED
  WITH AIRLOADS

10 AERODYNAMIC   IDEALIZED ELASTIC ELEMENT
STATIONS   PITCH
                    AXIS
                    CG OFFSET
                    FROM PITCH
                    AXIS
15 LUMPED MASSES
WITH PITCH INERTIA

- HINGELESS, ARTICULATED, AND TEETERING ROTORS

TEETERING

LAG HINGE

TEETERING
HINGE

ARTICULATED

LAG HINGE

FLAP
HINGE

HINGELESS

NO HINGE

- SMALL ROTOR SHAFT TILT ONLY

RELATIVE
WIND

Figure 41. Current Capability in Dynamics

82
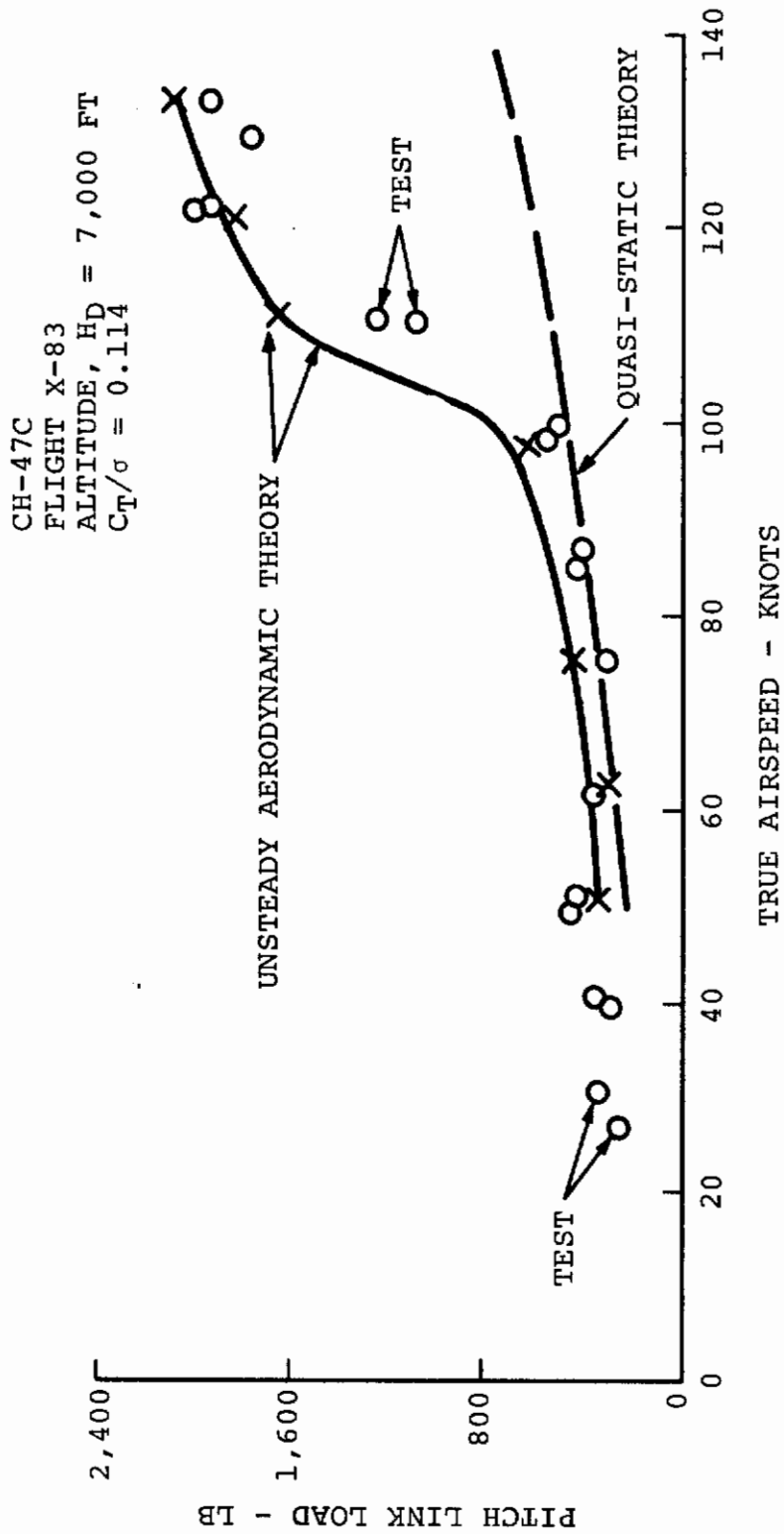
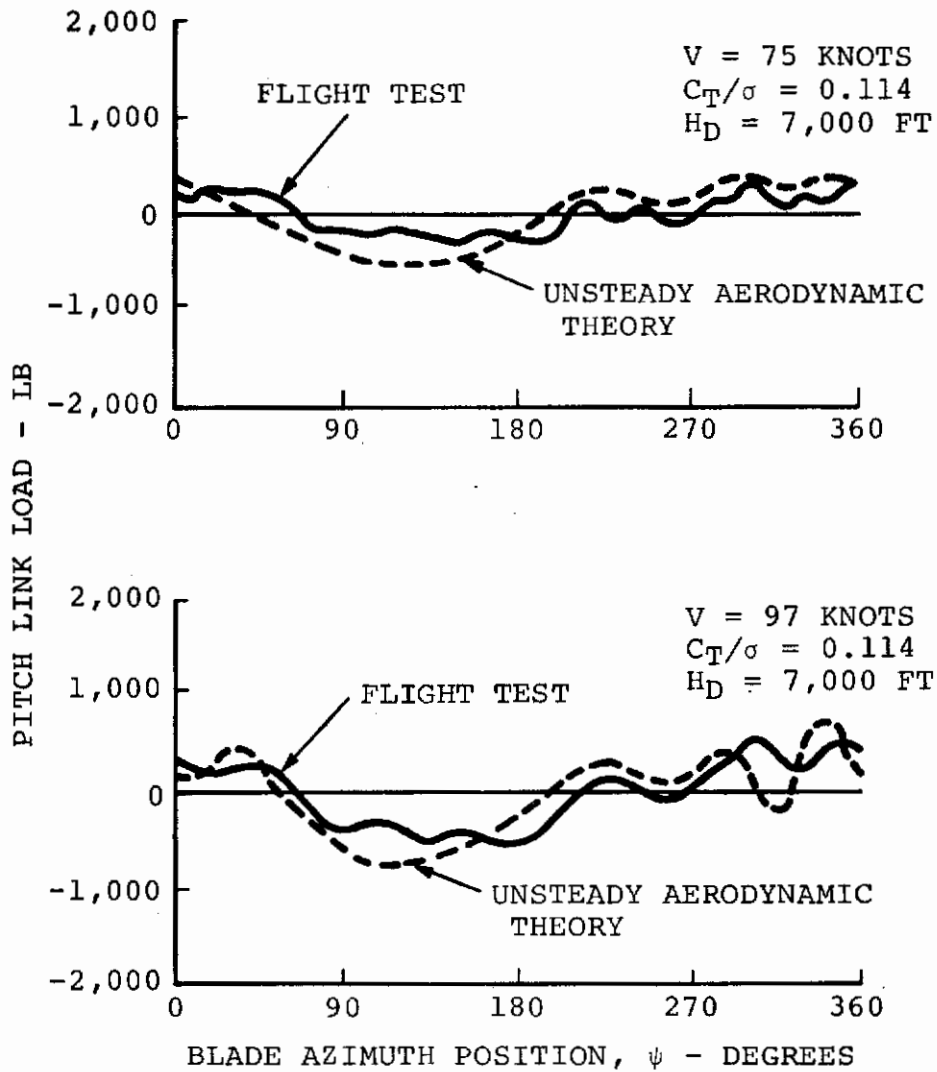Figure 42. Comparison of Test and Analytical Pitch Link Loads for an Airspeed Sweep
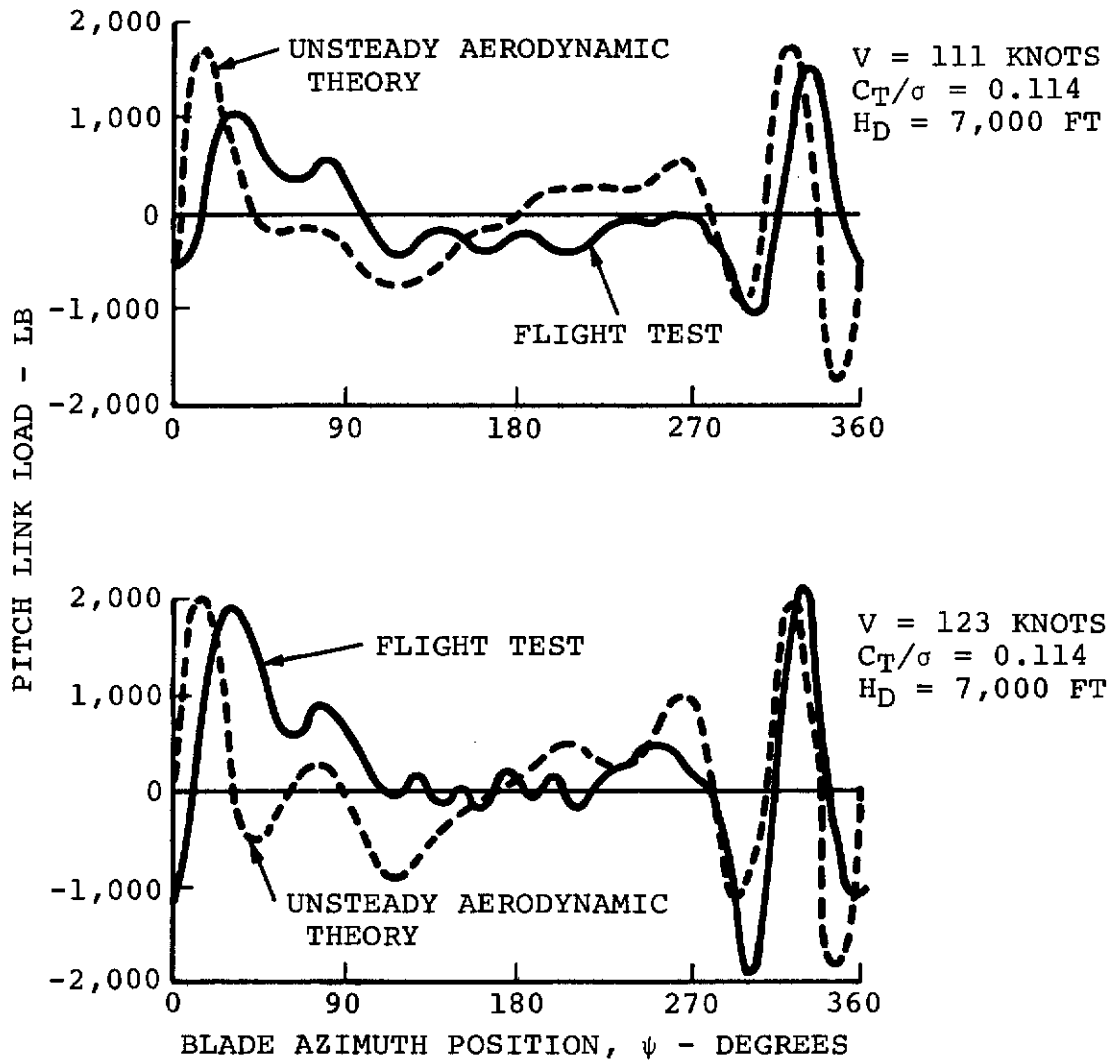
Figure 43. Low-Speed Pitch Link Load Waveforms

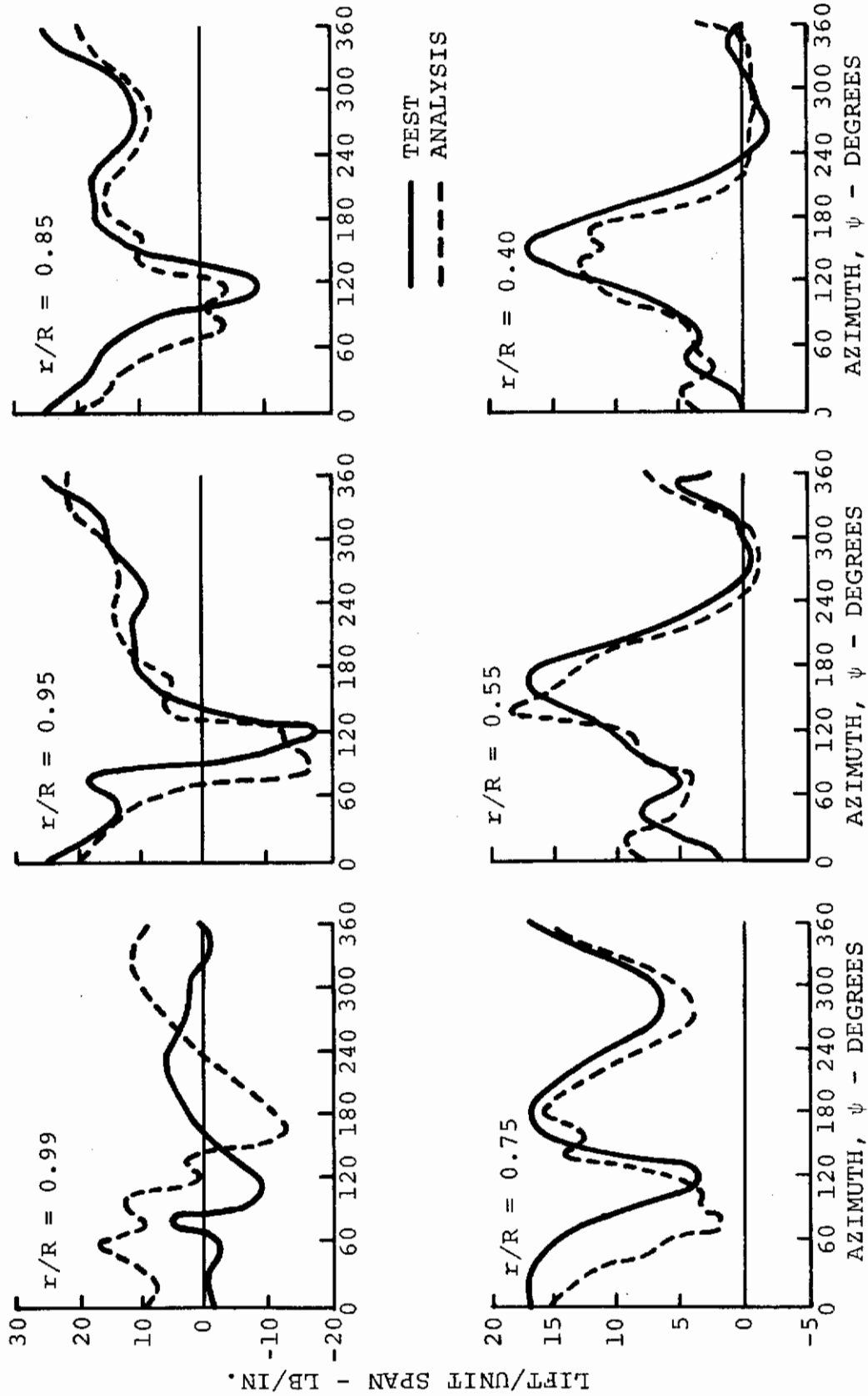Figure 44. High-Speed Pitch Link Load Waveforms

85

Figure 45. Typical Lift Waveform Correlation at All Radial Positions for H-34 Rotor in Ames 40- by 60-Foot Tunnel
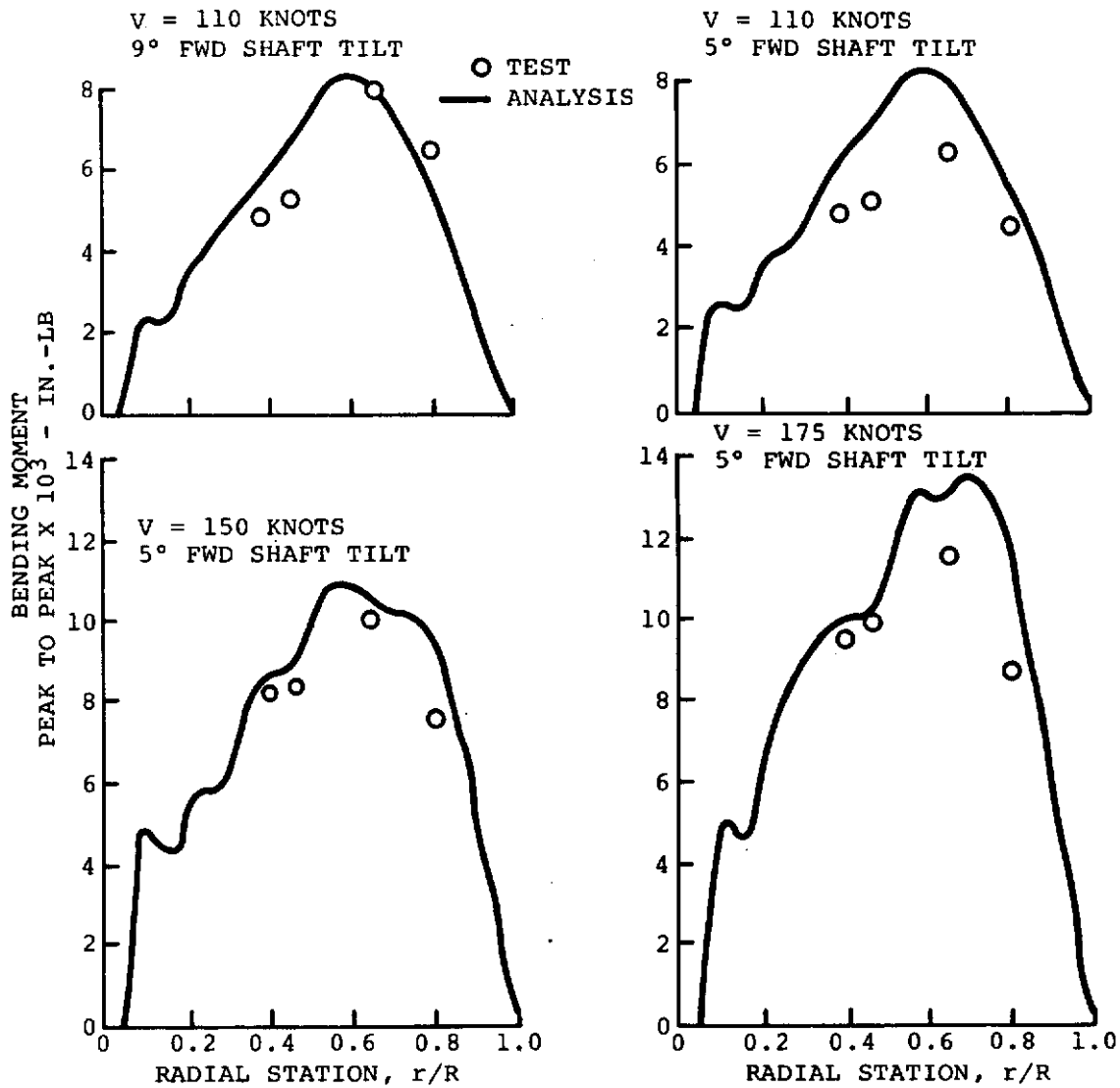
Figure 46. Analytical Flap Bending Moment Peak-to-Peak
Spanwise Envelope Compared With Test for Forward
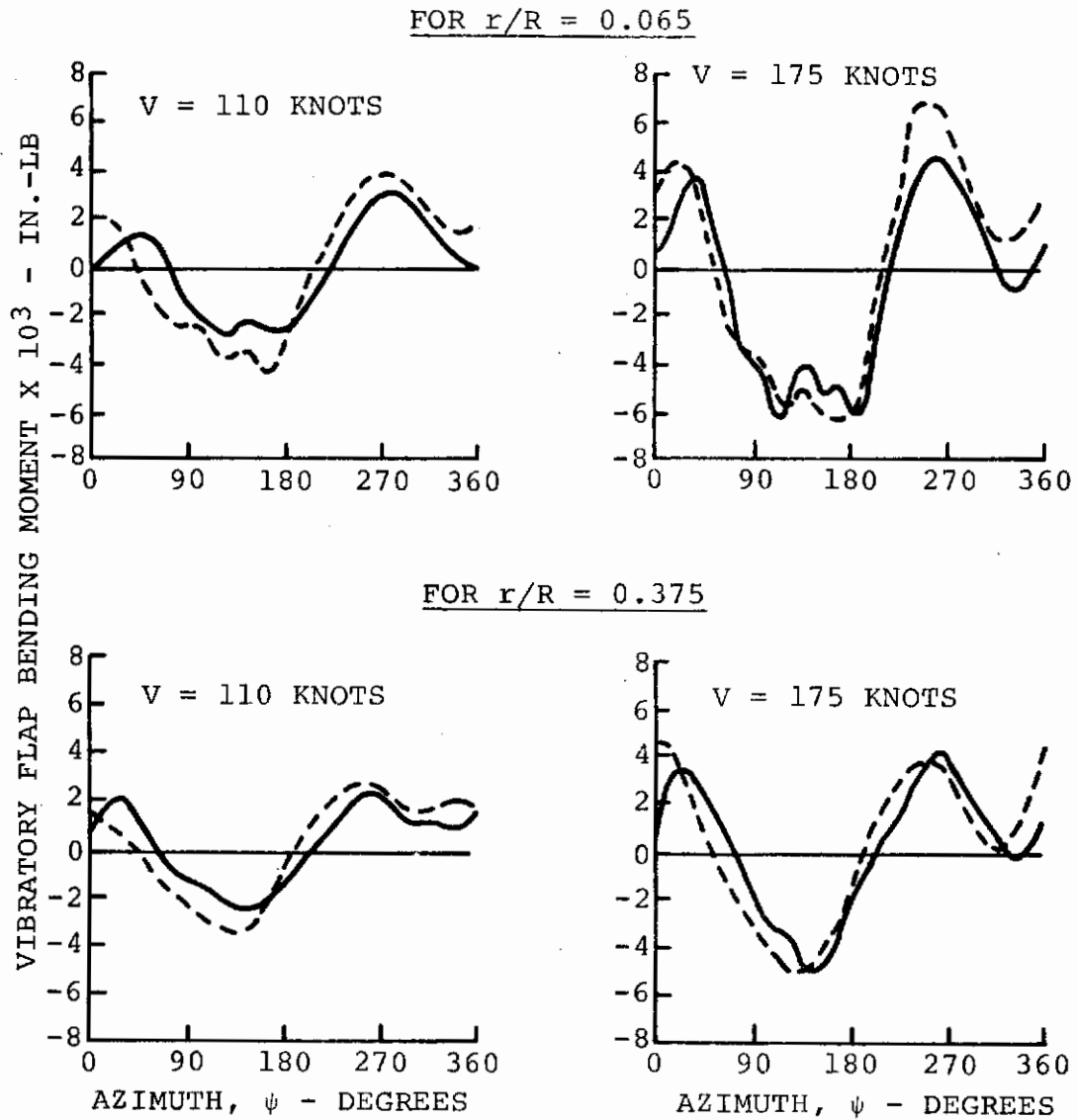Shaft Tilt on H-34 Rotor in Ames 40- by 60-Foot
Tunnel

FOR r/R = 0.065

V = 110 KNOTS

V = 175 KNOTS

FOR r/R = 0.375

V = 110 KNOTS

V = 175 KNOTS

VIBRATORY FLAP BENDING MOMENT X 10^3 - IN.-LB

AZIMUTH, ψ - DEGREES

AZIMUTH, ψ - DEGREES

Figure 47. Typical Test and Analytical Flap Bending Moment Waveforms For 5 Degree Forward Shaft Tilt on H-34 Rotor in Ames 40- by 60-Foot Tunnel
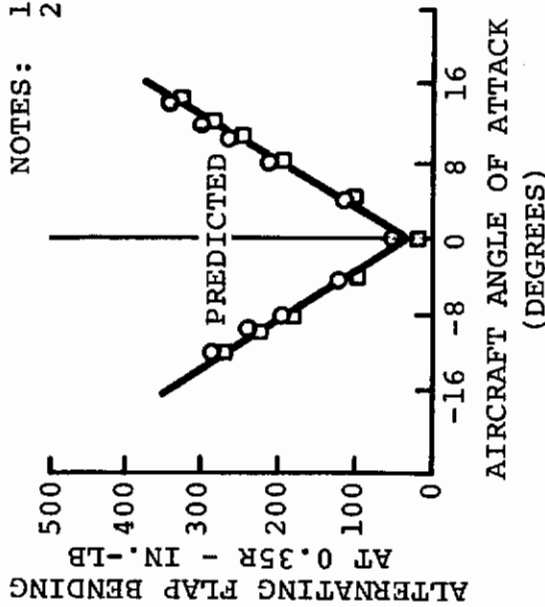
88

Figure 48. Theory and Test Flap Bending Moments for Tilt-Rotor Model 160 Performance Model

$\theta_t = 36°$
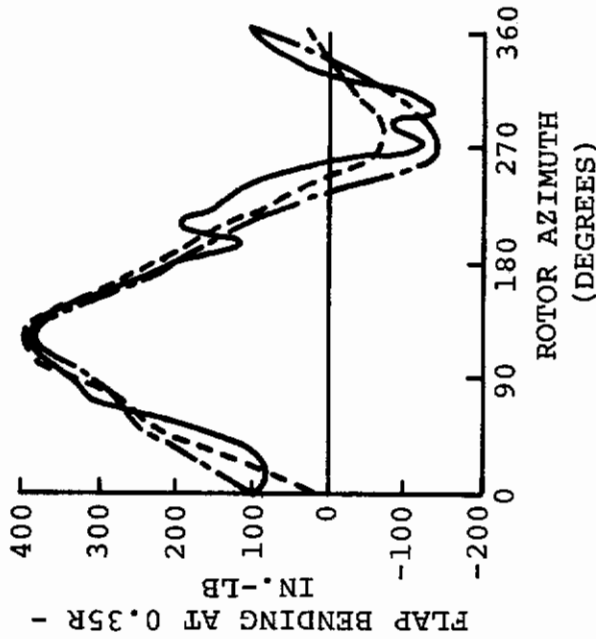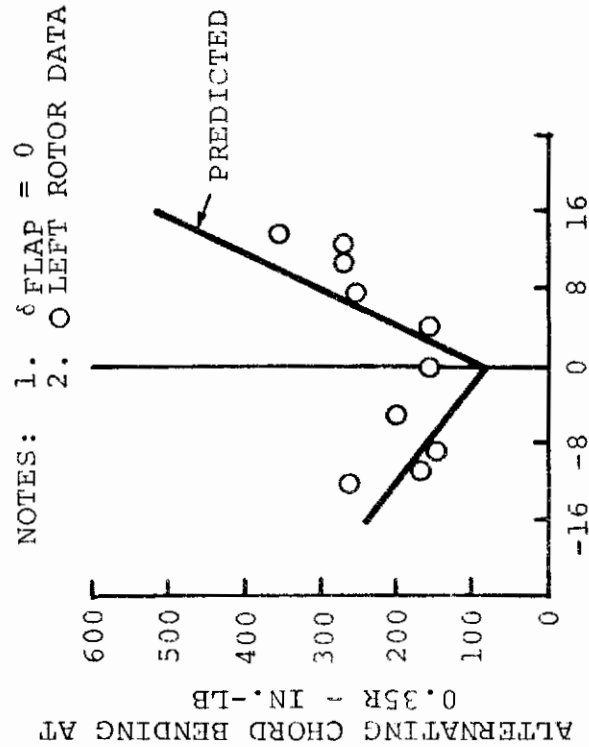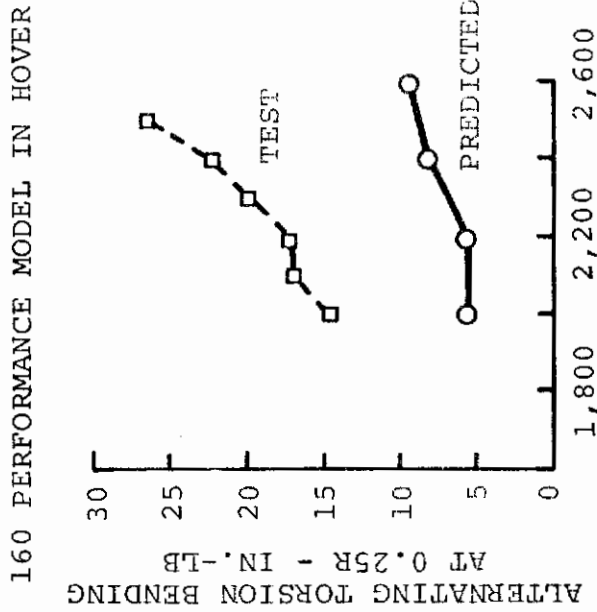
MEASURED AND PREDICTED ALTERNATING
CHORD BENDING PRODUCED BY AIRCRAFT
ANGLE OF ATTACK IN CRUISE AT θ_{75} =
30°, V_{TIP} = 570 FPS, AND V_{TUNNEL} = 220 FPS

ALTERNATING BLADE TORSION VS RPM
FOR i_N = 90°, θ_2 = 3°, AND
h/D = 0.39, 1.8

160 PERFORMANCE MODEL IN HOVER

TEST

PREDICTED

ROTOR SPEED - RPM

1,800   2,200   2,600

ALTERNATING TORSION BENDING
AT 0.25R - IN.-LB

0   5   10   15   20   25   30

NOTES: 1. δ_{FLAP} = 0
       2. O LEFT ROTOR DATA

PREDICTED

AIRCRAFT ANGLE OF ATTACK - DEGREES

-16   -8   0   8   16

ALTERNATING CHORD BENDING AT
0.35R - IN.-LB

0   100   200   300   400   500   600

Figure 49.   Theory and Test Chord Bending Moments and Torsion for
             Tilt-Rotor Model 160 Performance Model

90

- LIFTING LINE THEORY INCLUDING COMPRESSIBILITY AND STALL

THREE-DIMENSIONAL FLOW

VARIABLE CHORD AND AIRFOIL SECTION GEOMETRY
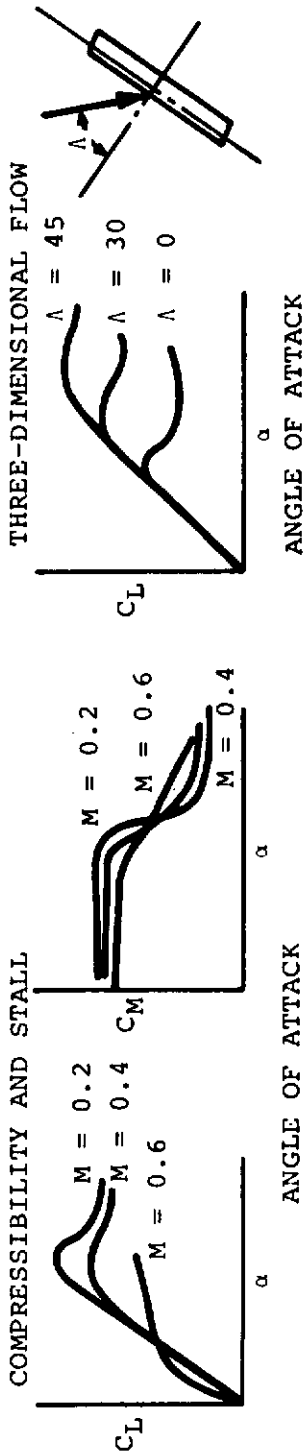
UNSTEADY EFFECTS FOR BOTH STALL AND UNSTALLED CONDITIONS
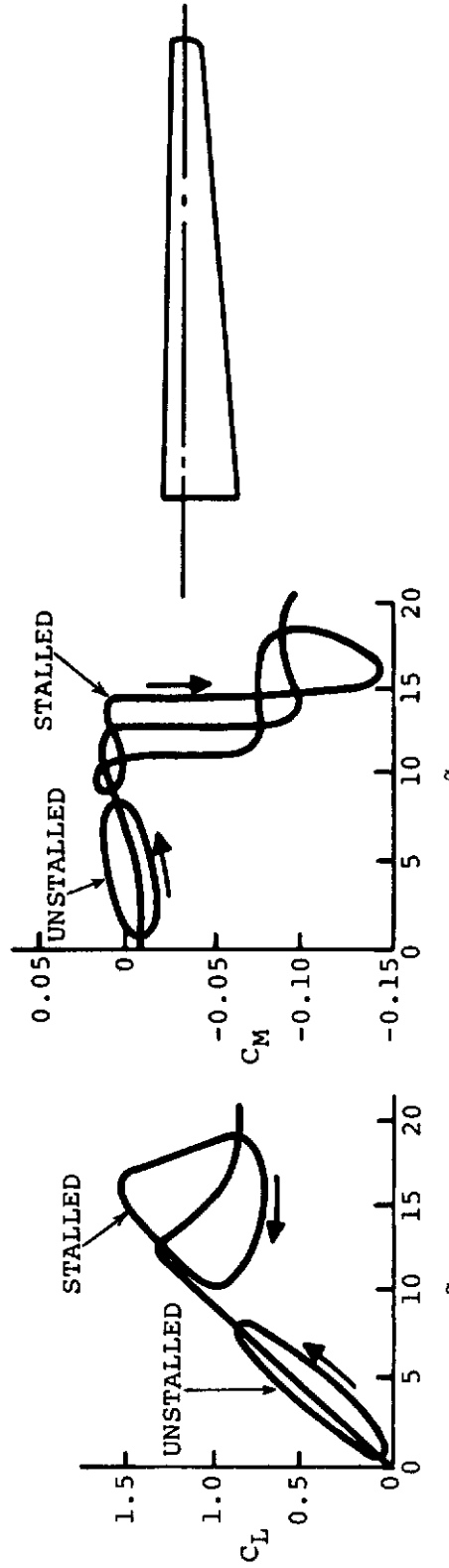
Figure 50. Current Capability in Aerodynamic Properties of Airfoils

91

- NONUNIFORM DOWNWASH INCLUDING RIGID WAKE

  RELATIVE WIND

  ROTOR BLADE

  TIP VORTEX WAKE

  ROTOR SHAFT

- ELASTIC FLAP AND PITCH DEFLECTIONS IN THE AIRLOADS

  FLAP

  TORSION

COMPATIBLE TIP AND ROOT VORTEX

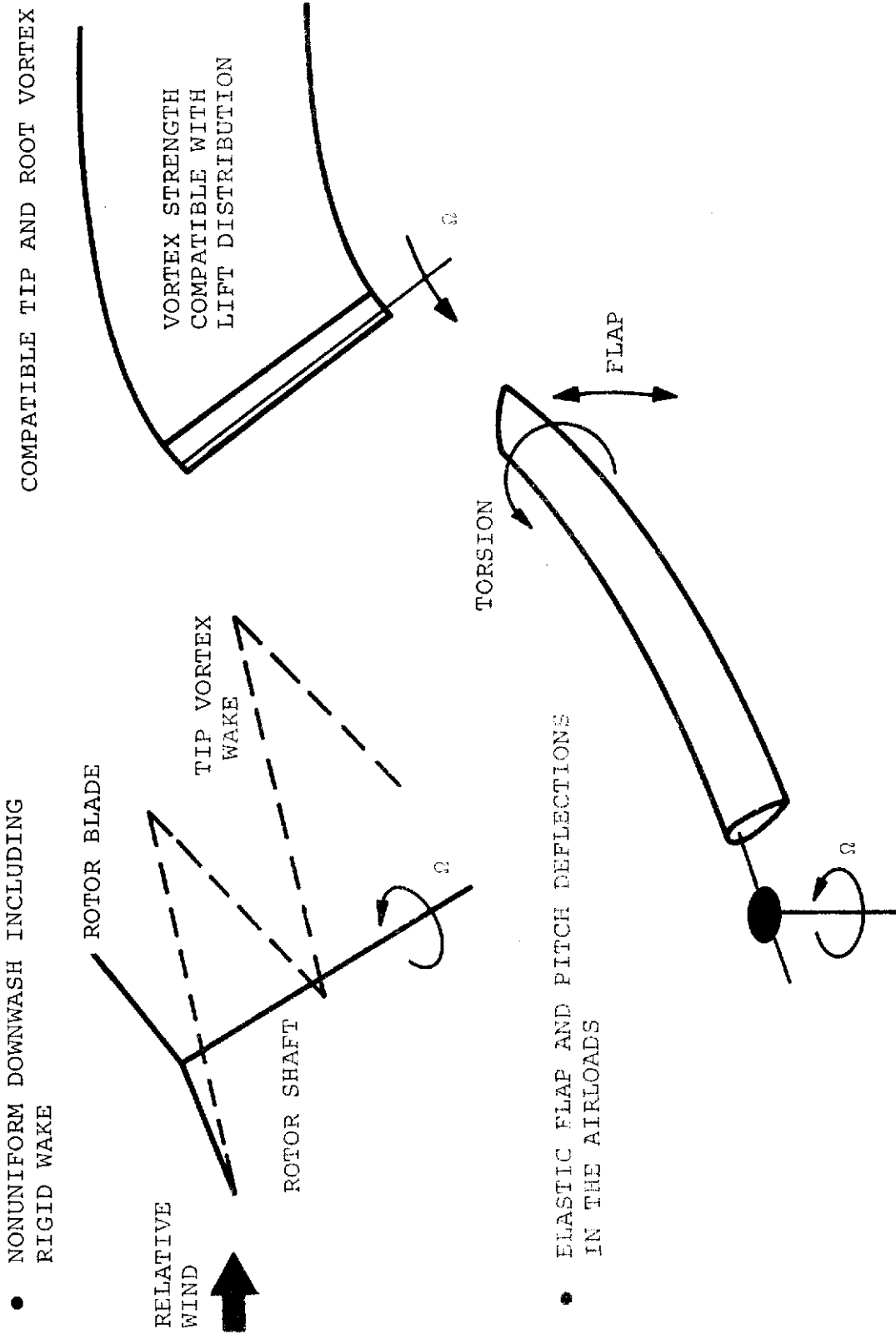VORTEX STRENGTH COMPATIBLE WITH LIFT DISTRIBUTION

Figure 51. Current Capability in Aerodynamic Effects of Downwash and Elasticity

92

accounts for both the articulated and hingeless rotor config-
urations, it does not account for those V/STOL rotor designs
whose root-end attachments, although hingeless in appearance,
are actually pinned with an effective angular spring about the
pin along with an effective linear spring acting outboard of
the pin axis. This is a potential reason for poor bending
moments for highly twisted rotors of this type. Still another
reason is the aerodynamic coupling between the flap and chord
bending motions which is not accounted for in the present
mathematical model and which is believed to be of particular
importance for soft-in-plane hingeless rotors. These major
deficiencies, along with many others of less importance, will
be removed in the mathematical model being developed under
this contract. This new model will employ the most advanced
concepts in dynamics, aerodynamics, and elasticity known at
this time for a prop/rotor blade.

PROGRAM USAGE

Utilization of this program requires the definition of a
flight condition, detailed rotor blade physical properties,
and gross aircraft properties. A trim analysis must be run
to define the control input, thrust, aircraft attitude, and
blade initial deflections. A blade idealization program is
required to lump the detailed blade properties into discrete
elements. For hover conditions an additional calculation
must be performed to correct the cyclic to account for the
downwash due to lift dissymmetry. For other conditions where
wing circulation passes through the rotor, another program
must be run to define the velocity distribution due to this
blade circulation. A review of the program usage is given in
Figure 52.

PROGRAM FLOW DIAGRAM

Figure 53 shows a simple block diagram of the current loads
program. The nonuniform downwash calculation is based upon
the initial deflections only. The airload calculations can
provide required thrust by altering the collective angle until
the required thrust is obtained. The program can provide up
to 10 iterations between the airloads and the coupled flap-
pitch response. The uncoupled lag response is determined by
the airload and coriolis calculations; the lag response is not
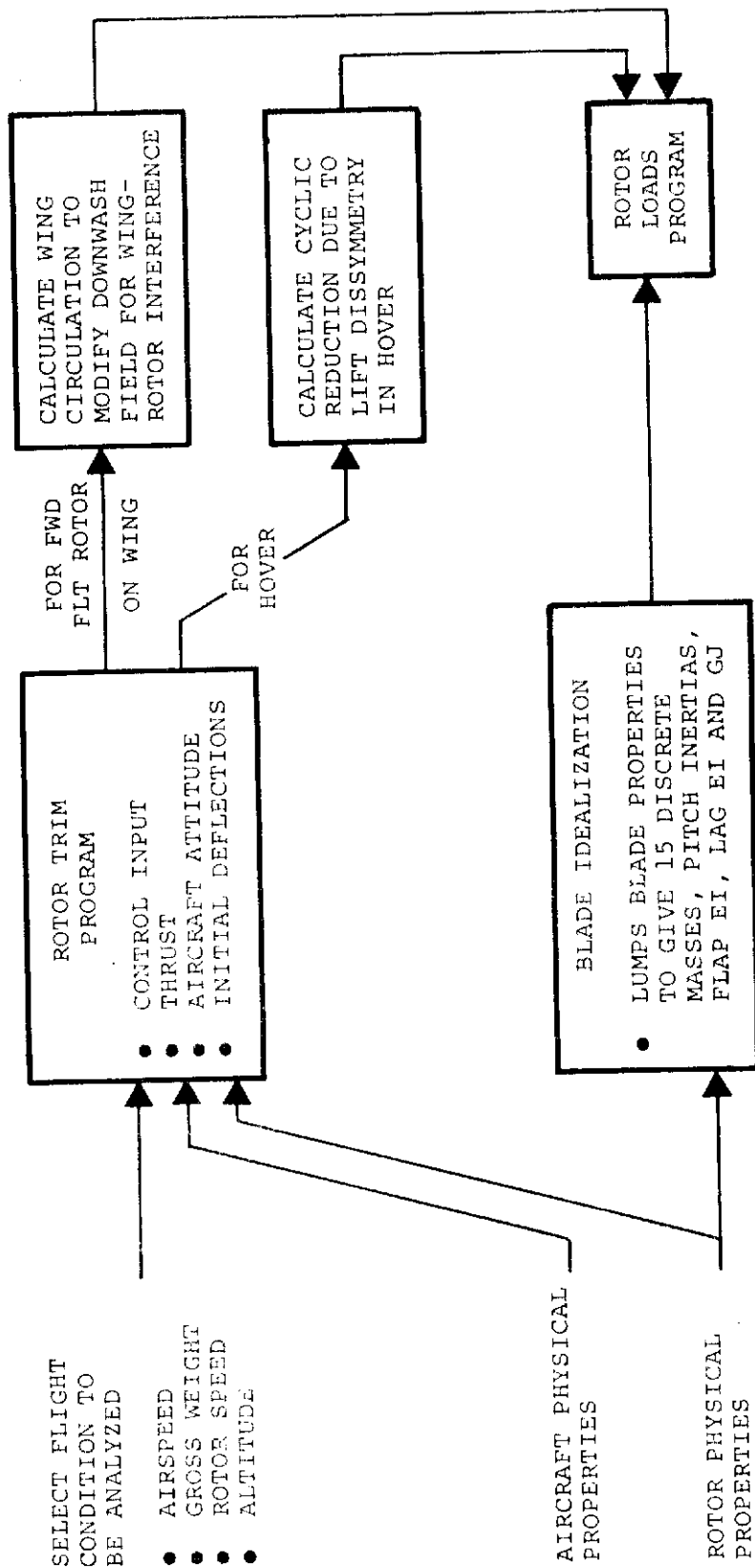used to alter the airloads or flap-pitch response.
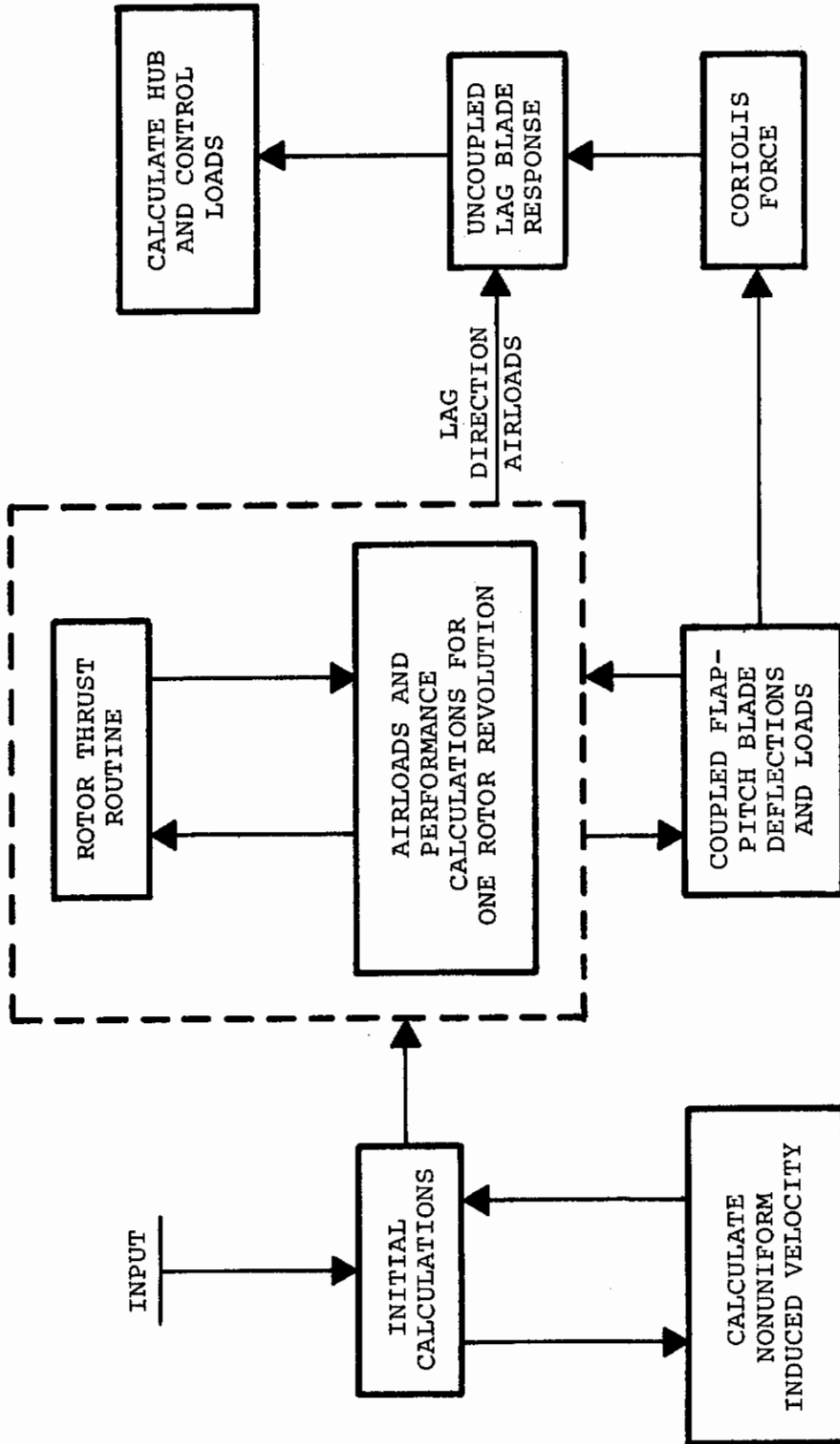
Figure 52. Program Usage

Figure 53. Flow Chart of Current Loads Program

MATHEMATICAL MODEL UNDER DEVELOPMENT

The mathematical model being developed under this contract will include modifications to the current model which will improve its prediction capabilities and enlarge its applicability to include V/STOL-type prop/rotor blades. These major modifications to the current mode include the following items.

BLADE IDEALIZATION

Number of Mass Stations

The model now has a prop/rotor blade idealization that includes 20 mass stations and 15 aerodynamic stations, thereby increasing the accuracy of the dynamic and aerodynamic force representations.

Coupled Flap-Chord-Pitch

A new solution technique considers a fully coupled analysis for flap bending, chord bending, and torsion. Specifically, the coupling includes dynamic, aerodynamic, and elastic forces involving the bending deflections normal and parallel to a section chord line with the section torsional deflections.

Other Improvements

The prop/rotor blade idealization now permits the inclusion of a large built-in twist angle, blade precone, blade prelag, variable vertical and horizontal neutral axes, variable shear center, and section inertias.

AERODYNAMICS

An advanced unsteady aerodynamic theory which has improved the prediction of pitch link loads in the stall regime of a helicopter rotor was reported in the May 1971 Annual Forum Meeting of the American Helicopter Society.

COMPUTER TECHNIQUES

There is a new digital computer program of the model that reflects the improved efficiency in coding techniques and data processing gained from experience with the current model.

APPROACH

Although the mathematical model under development contains the most recent advances in the field, only those items of importance are being selected in order to avoid generating an impractical computer program because of the inability to predict input data, long running time, or numerical convergence

96

problems. This limiting compromise follows from the fact that
the state of the art for a rotor aeroelastic analysis is de-
termined not by advanced theories in dynamics, aerodynamics,
and elasticity, but by the practical limits of computer time
and numerical tractability. A review of the additional capa-
bility under development is given in Figures 54 and 55.

PROGRAM FLOW DIAGRAM

Figure 56 shows the changes in the simple block diagram of
Figure 53. The program under development shows the coupled
flap-lag-pitch deflection calculations iterated with the
airloads. This allows the flap, lag, and pitch degrees of
freedom to be included in the airloads and includes all
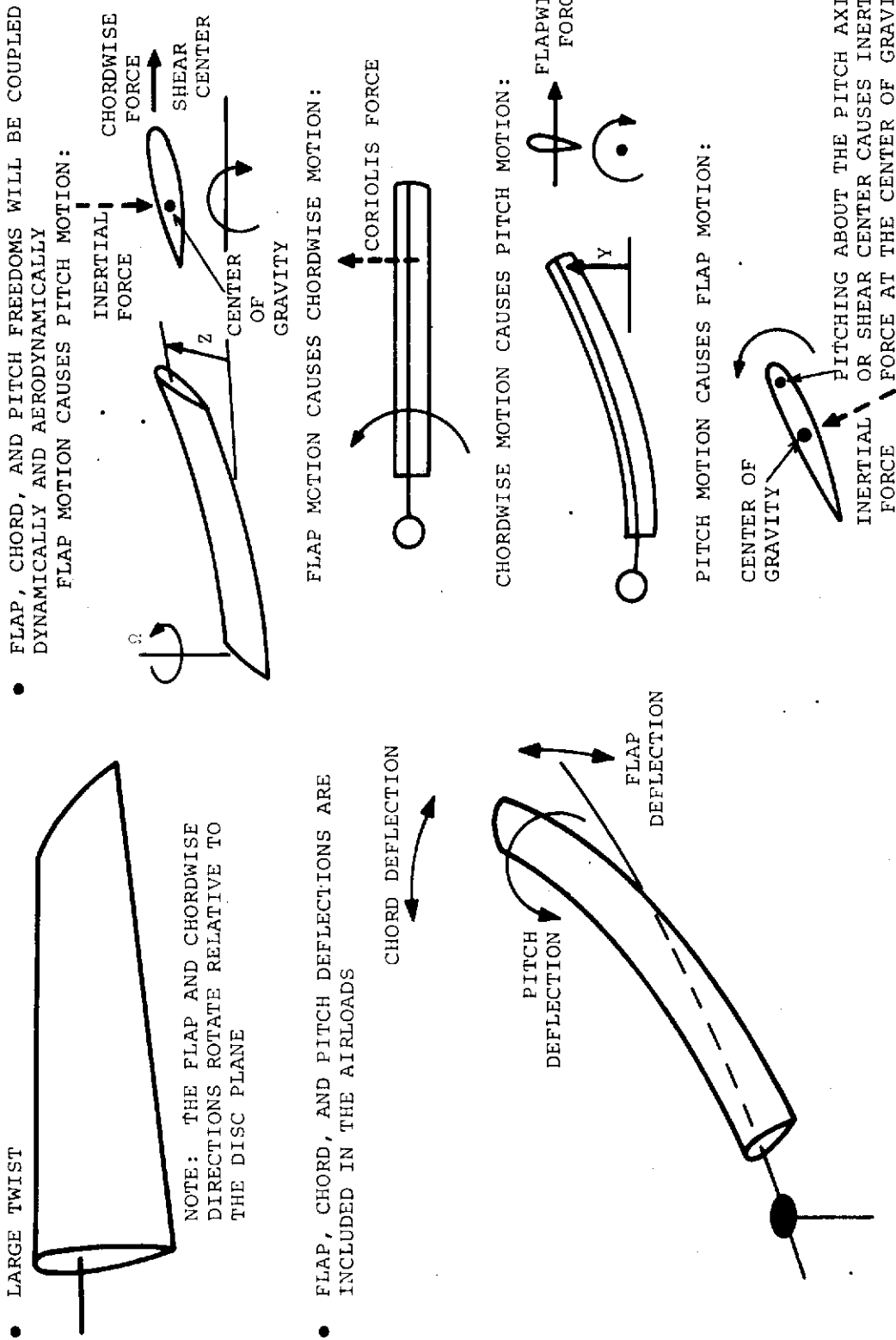significant couplings between flap, lag, and pitch.

- FLAP, CHORD, AND PITCH FREEDOMS WILL BE COUPLED DYNAMICALLY AND AERODYNAMICALLY

FLAP MOTION CAUSES PITCH MOTION:

INERTIAL FORCE

CHORDWISE FORCE

SHEAR CENTER

CENTER OF GRAVITY

FLAP MOTION CAUSES CHORDWISE MOTION:

CORIOLIS FORCE

CHORDWISE MOTION CAUSES PITCH MOTION:

FLAPWISE FORCE

PITCH MOTION CAUSES FLAP MOTION:

CENTER OF GRAVITY

PITCHING ABOUT THE PITCH AXIS INERTIAL OR SHEAR CENTER CAUSES INERTIAL FORCE AT THE CENTER OF GRAVITY

- LARGE TWIST

NOTE: THE FLAP AND CHORDWISE DIRECTIONS ROTATE RELATIVE TO THE DISC PLANE

- FLAP, CHORD, AND PITCH DEFLECTIONS ARE INCLUDED IN THE AIRLOADS

CHORD DEFLECTION

FLAP DEFLECTION

PITCH DEFLECTION

Figure 54. Coupling of Blade Motions in Improved Program

98
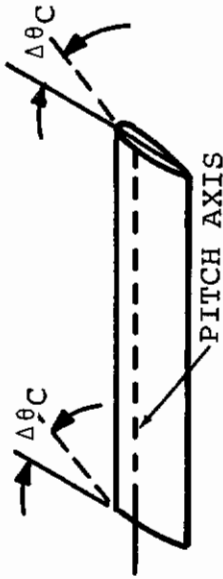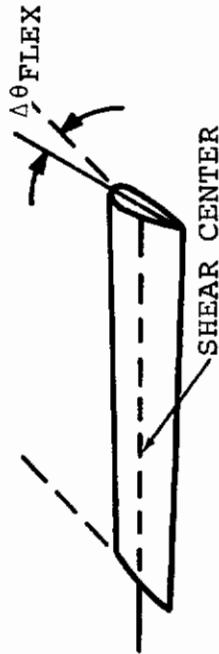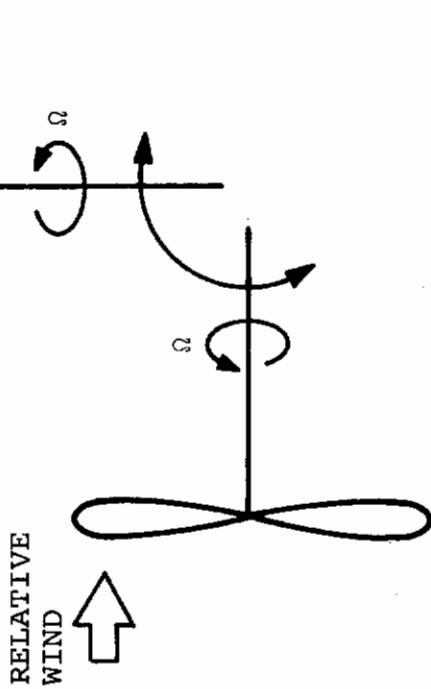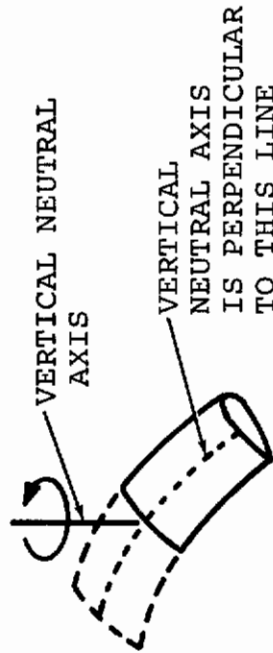
Figure 55. High Twist and Shaft Tilts in Improved Program

Figure 56. Flow Chart of Improved Loads Program

METHOD OF SOLUTION

All of the available published data indicates that the major-
ity of the members of the rotary-wing industry employ the
lumped-mass approach in solving the rotor loads problem for a
V/STOL prop/rotor blade. An alternative approach to the
solution of this problem is the modal analytical method which
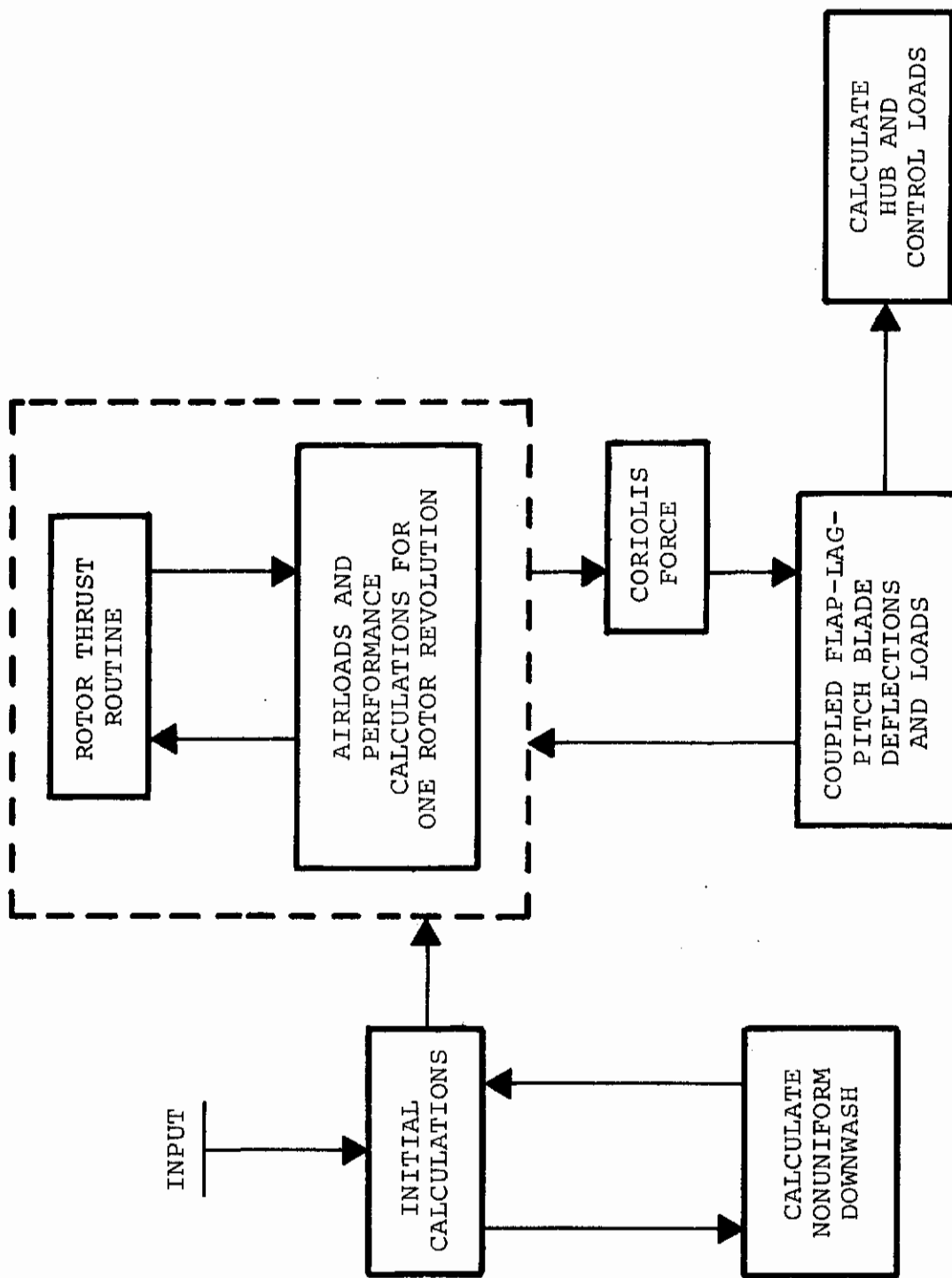employs the prop/rotor blade normal modes derived from a free
vibration analysis. The lumped-mass approach appears to have
an advantage over the modal analytical method in that it does
not require preknowledge of the blade normal modes, nor does
it encounter numerical convergence problems which are inherent
in the modal analysis. References 20 through 38 list the de-
tails of these analytical methods and their predictive capa-
bilities which vary in technique due to consideration of a
particular rotor system where experience has shown that a
particular mode of description or a particular parameter in
the dynamics, aerodynamics, or elasticity provides the best
correlation between theory and flight test data.

The typical rotor aeroelastic analysis first determines the
actual or equivalent flapping motion of the prop/rotor blade
by a step-by-step timewise integration of the inelastic flap-
ping equation of motion; the solution will converge to a
cyclic pattern when the steady-state flight condition is being
analyzed. This analysis can be refined further by introducing
the first flap bending normal mode and its associated equation
of motion, where now the two equations are integrated on the
basis of a set of starting boundary values determined from the
inelastic blade solution. When a steady-state condition is
being analyzed, the integration proceeds in small but finite
timewise steps; after a number of rotor revolutions, the pre-
dicted motions will become cyclic within a desired tolerance.
This is the usual solution sought, and the rotor performance,
loads, stress, and dynamic calculations are based on these
accepted cyclic motions. The airload calculations include
airfoil section geometry, compressibility, stall, 3-
dimensional flow, unsteady aerodynamics, and nonuniform down-
wash. The unsteady aerodynamic loads are calculated by various
modifications of the stall loads resulting from the airfoil
tables. The modifications typically include Theodorsen's shed
wake function or a derivative thereof, dynamic stall effects
based upon oscillating airfoil data, and yawed flow across the
blade. The nonuniform downwash calculations are based on shed
vortex data that ranges from tip vortex, tip and root vortex,
to multiple vortices immediately behind the blade. Several
different iterative schemes are used to establish vortex
strength as a function of calculated blade lift. Dissipation
of the vortex downstream is somewhat arbitrary in present
analytical techniques and the wake in most cases is assumed

101

rigid with drift relative to the hub and a resultant velocity
due to uniform inflow and aircraft speed. The solution for
the nonlinear aerodynamic loads and the coupled blade response
is performed in a series and the iteration between the air-
loads and blade response is used to obtain the final steady-
state solution.

PUBLISHED CORRELATION

Figures 57 through 65 summarize the available published data
on the loads-prediction capability typical of the industry.
This data includes the Kaman theory correlation with the CH-34
full-scale flight test conducted by NASA-Langley as reported
in Reference 35; the Sikorsky theory correlation with the
CH-34 full-scale tunnel test conducted by NASA-Ames as re-
ported in Reference 37; and the Sikorsky theory correlation
with the S-61F full-scale flight test conducted by Sikorsky
as reported in Reference 38. Generally speaking, the corre-
lation of theory with test data is fair to good, indicating
the obvious necessity for continued refinement of all theories
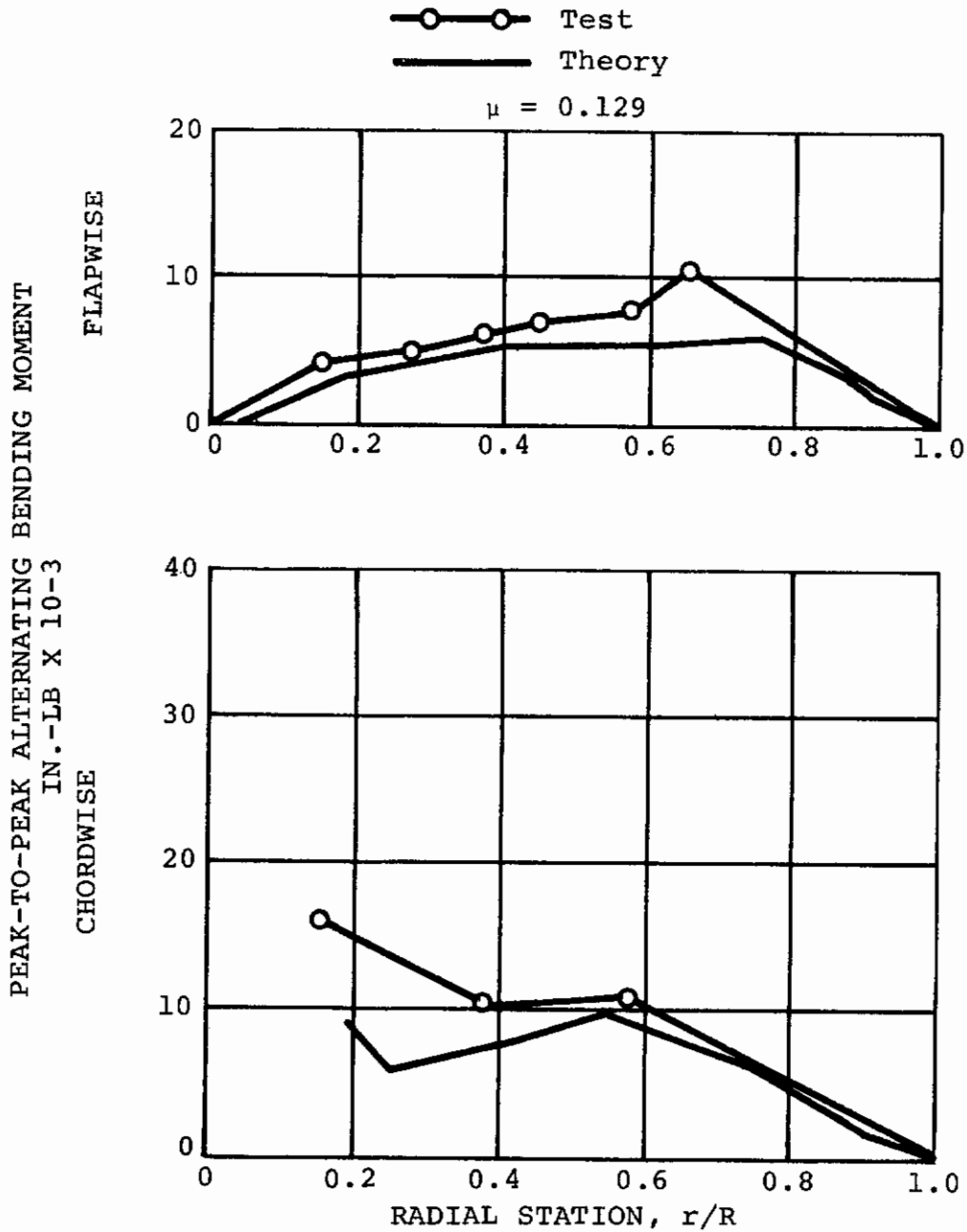presented herein.

REFERENCE 35

Figure 57. Transition Flight Moments from Sikorsky CH-34 Flight Data, NASA - Langley Test Data, and Kaman Theory

103
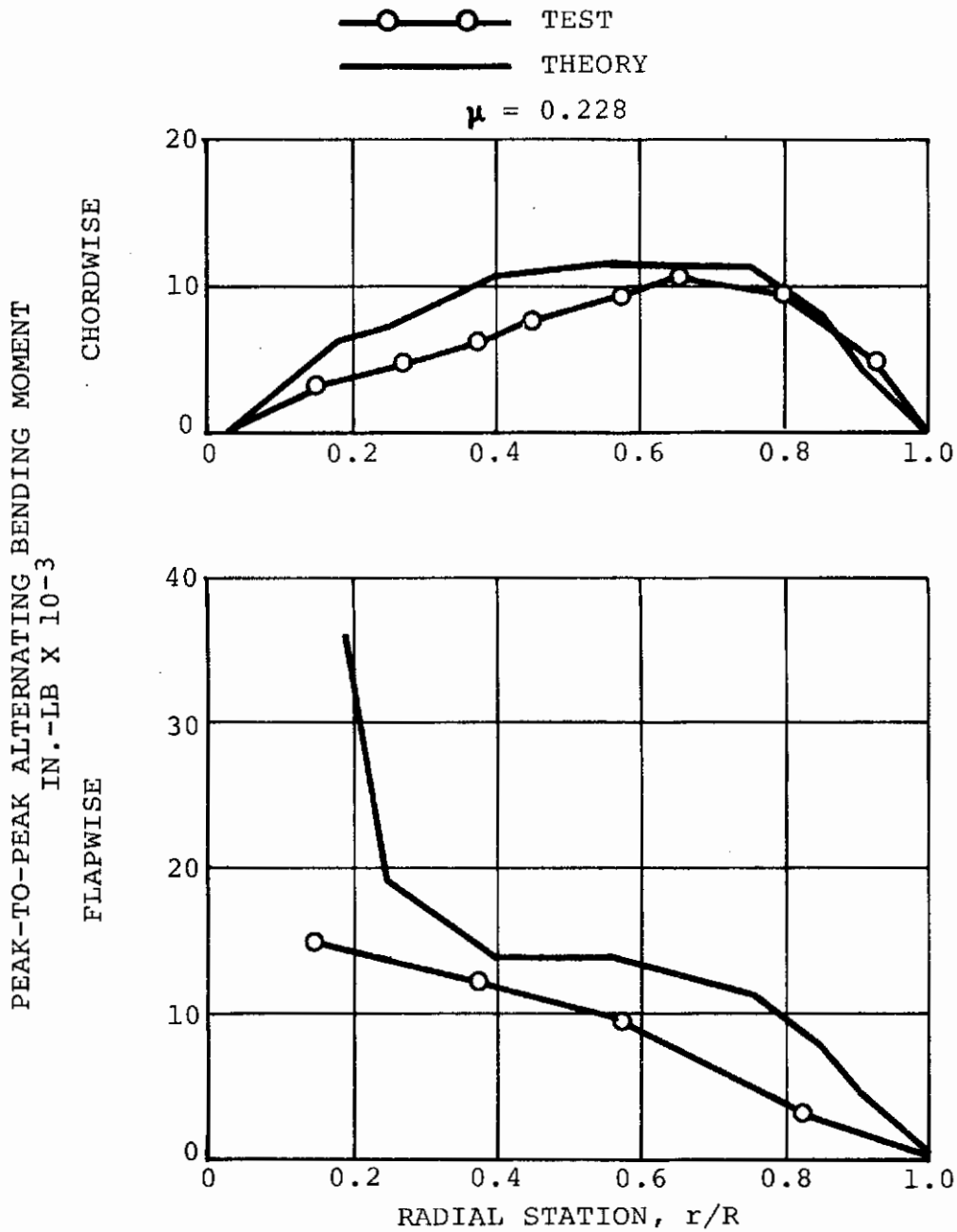
Figure 58. Cruise Flight Moments From Sikorsky CH-34 Flight
Data, NASA - Langley Test Data, and Kaman Theory
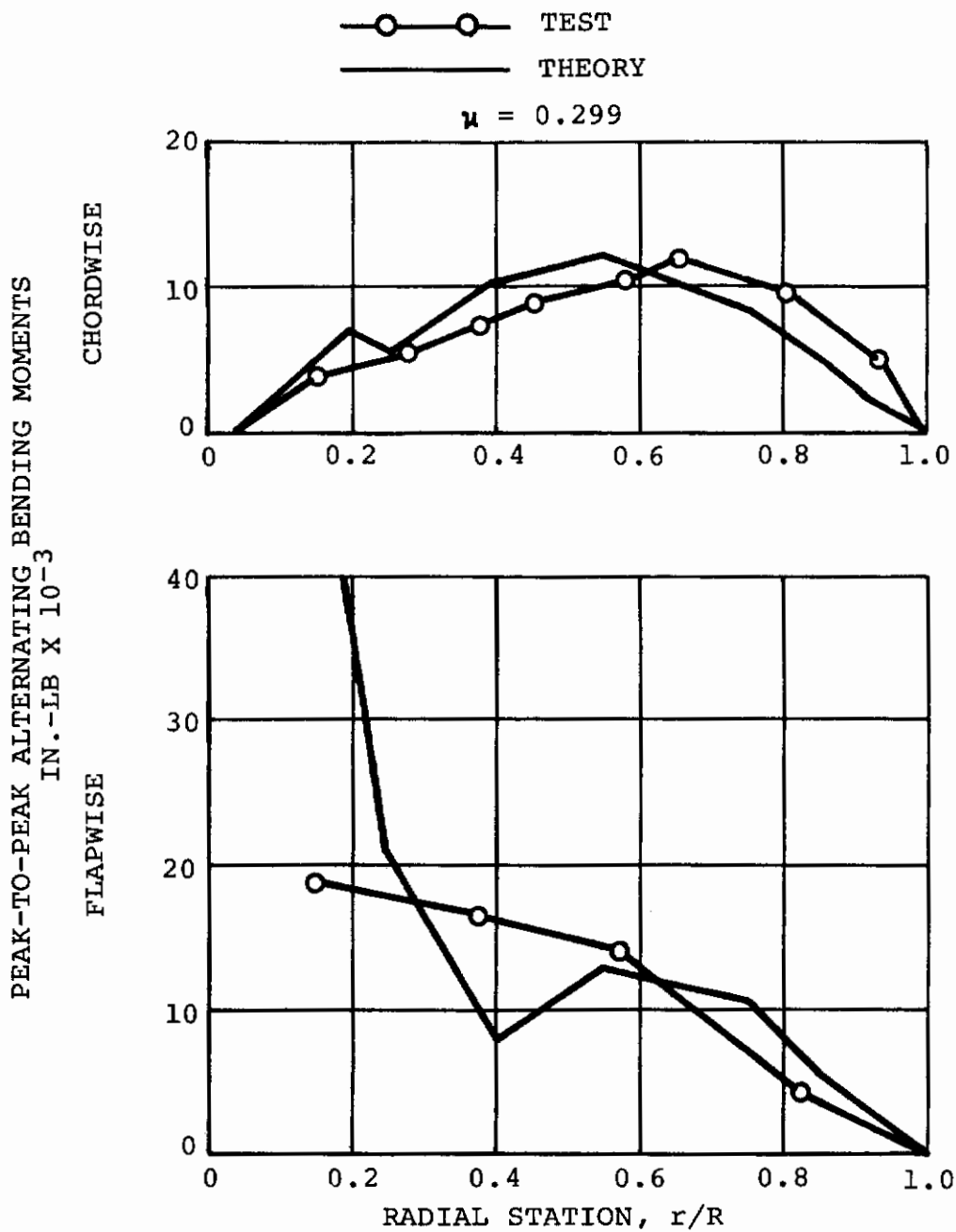
Figure 59. High-Speed Flight Moments From Sikorsky CH-34 Flight
Data, NASA - Langley Test Data, and Kaman Theory

105
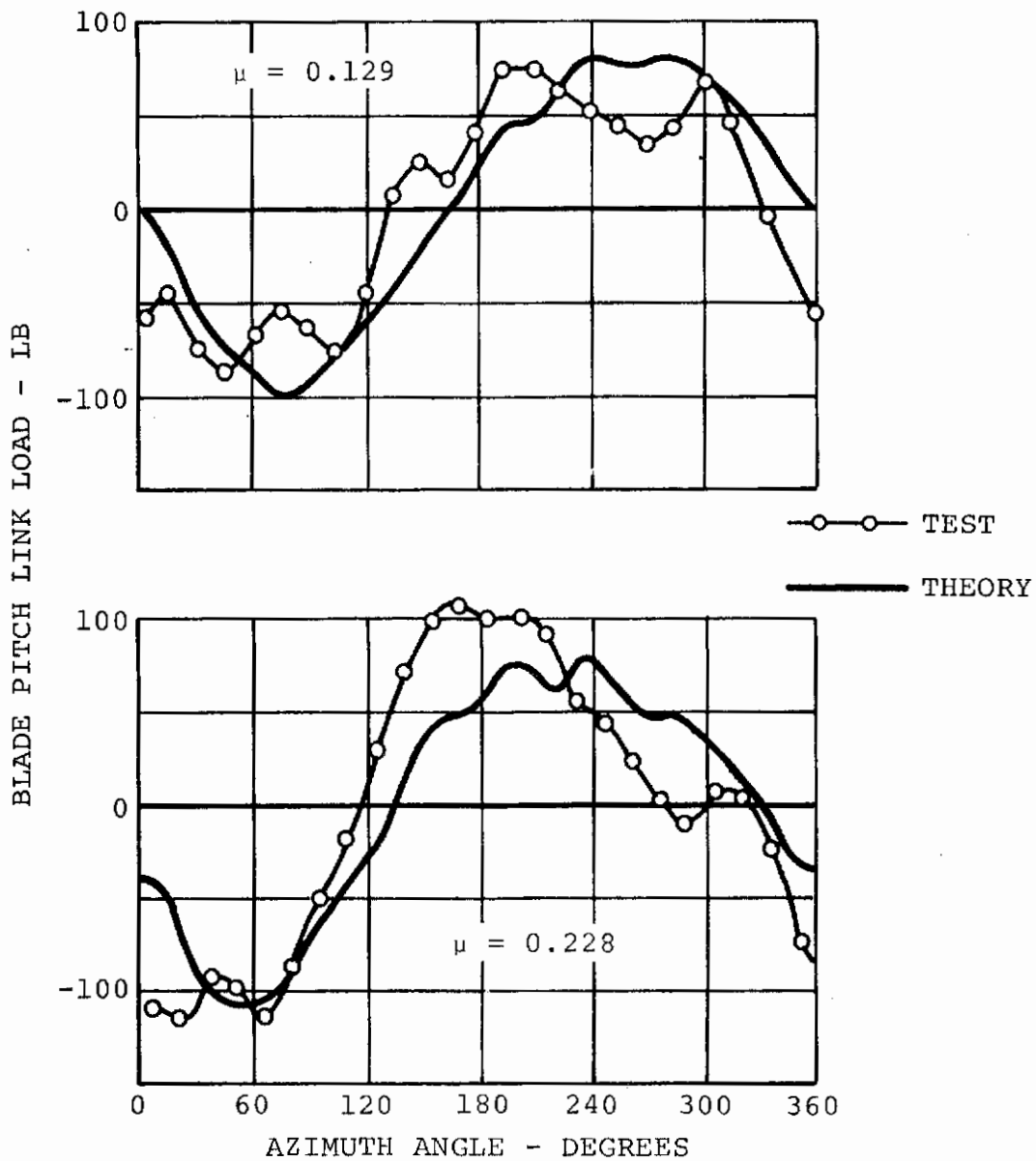
Figure 60. Cruise Pitch Link Loads From Sikorsky CH-34 Flight Data, NASA - Langley Test Data, and Kaman Theory

106
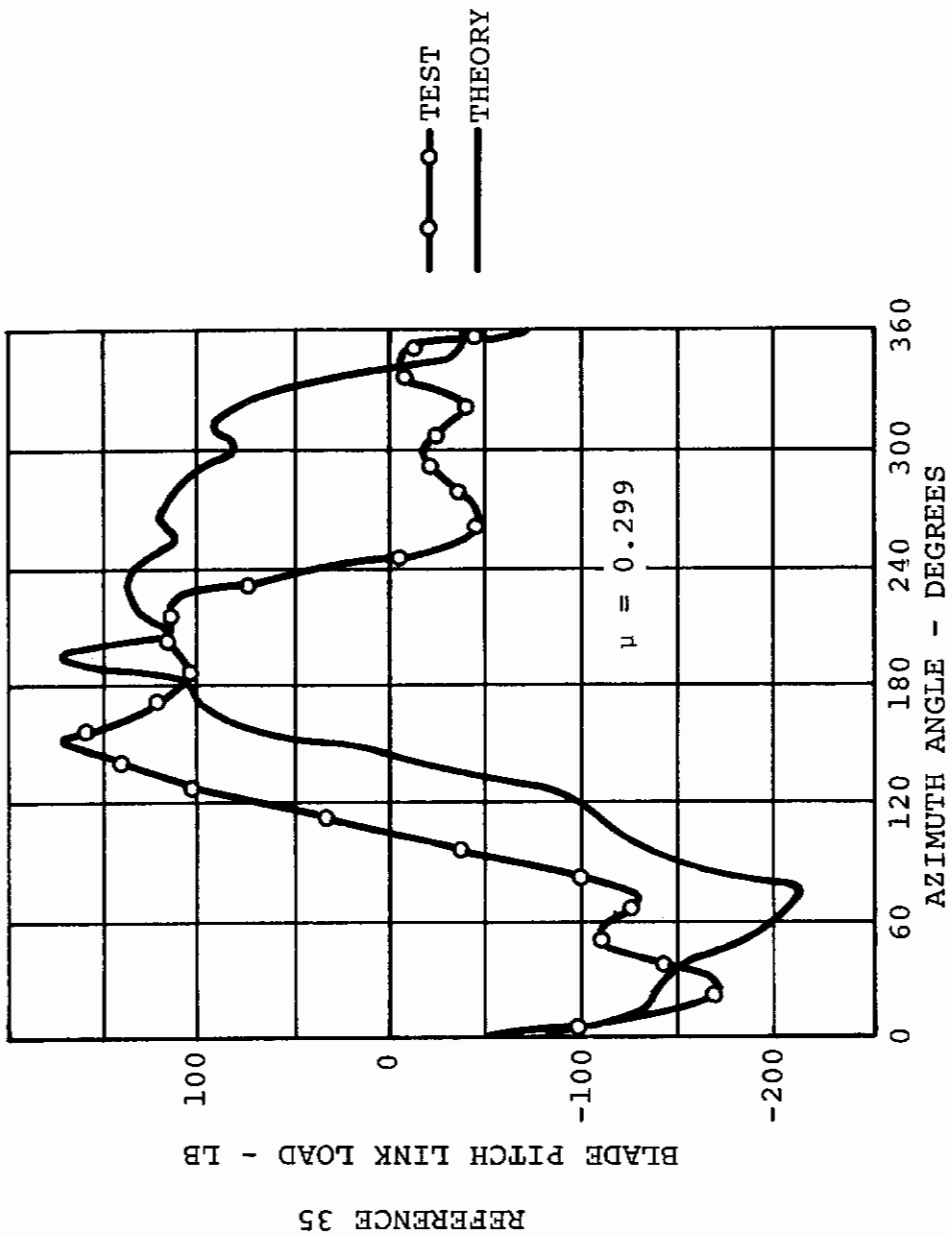
Figure 61. High-Speed Pitch Link Loads From
Sikorsky CH-34 Flight Data, NASA -
Langley Test Data, and Kaman Theory

107

———○——— TEST DATA

— — — — UNIFORM INFLOW THEORY

—■—·—■— VARIABLE INFLOW THEORY

V = 110 KNOTS
α_S = −5°
L = 8,300 LB

REFERENCE 37

VIBRATORY STRESS AMPLITUDE − PSI

FLAPWISE

CHORDWISE

TORSION

RADIAL STATION, r/R
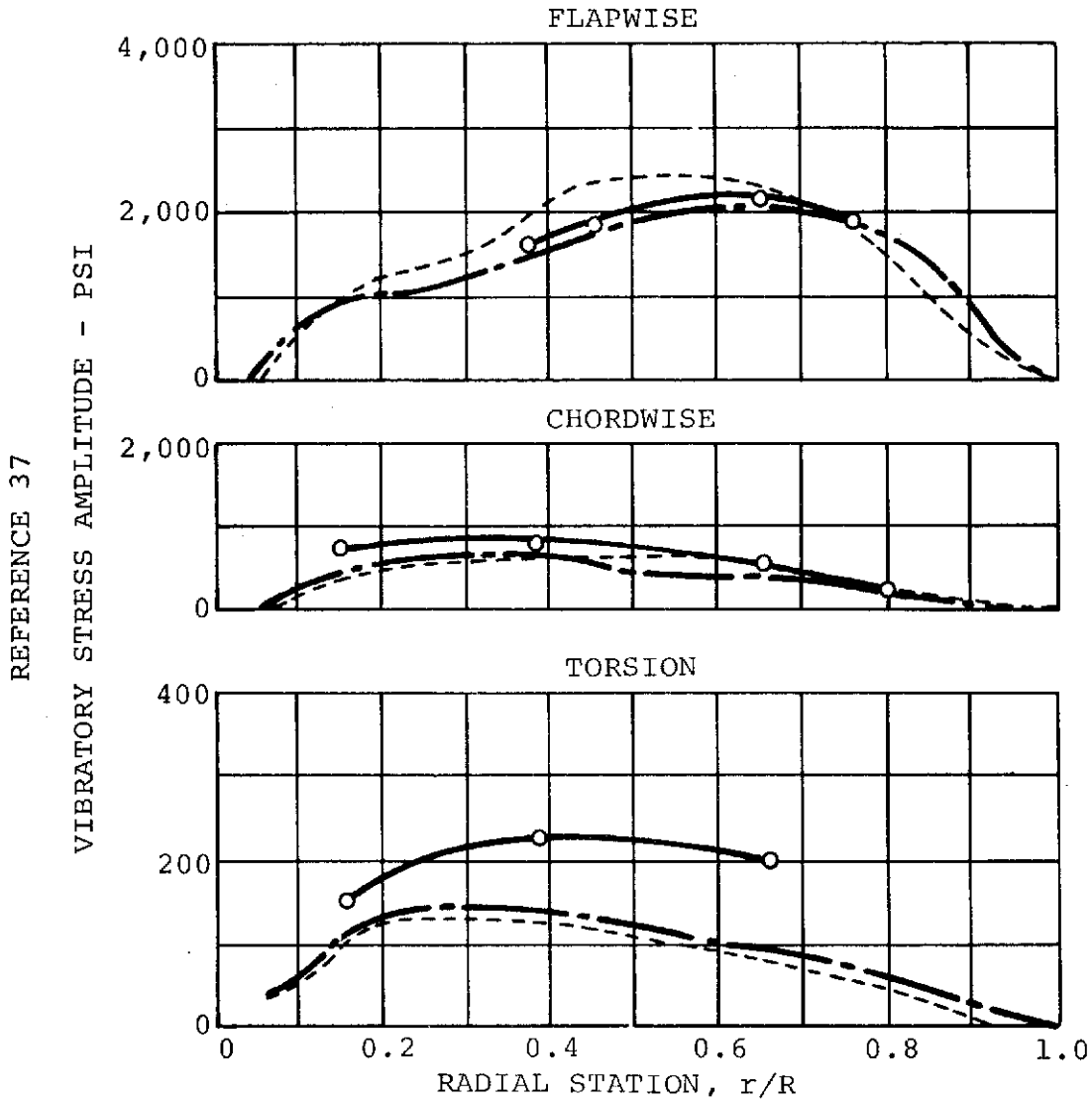
Figure 62. Transition Flight Loads From Sikorsky CH-34
Tunnel Data, NASA-Ames Test Data, and
Sikorsky Theory

Figure 63. Cruise Flight Loads From
Sikorsky CH-34 Tunnel Data,
NASA-Ames Test Data, and
Sikorsky Theory

109

TEST DATA

UNIFORM INFLOW THEORY

VARIABLE INFLOW THEORY

V = 175 KNOTS

α_s = -5°

L = 7,100 LB
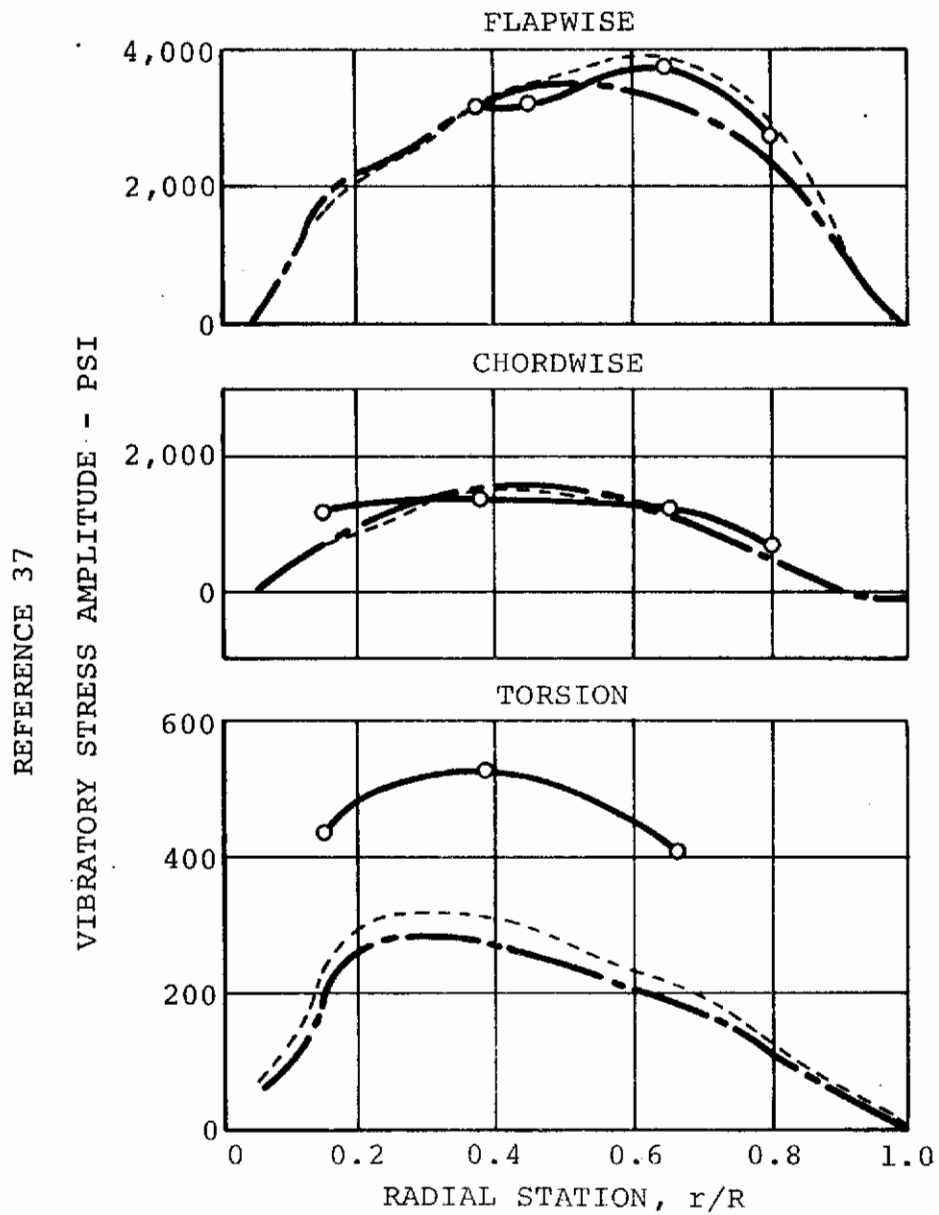
Figure 64.   High-Speed Flight Loads From
            Sikorsky CH-34 Tunnel Data,
            NASA-Ames Test Data, and
            Sikorsky Theory

110

FLAPWISE

CHORDWISE

V = 142 KNOTS

REFERENCE 38

VIBRATORY STRESS AMPLITUDE - PSI

RADIAL STATION, r/R

Figure 65. High-Speed Flight Moments From Sikorsky
S-61F Compound Full-Scale Flight Data

111

REFERENCES

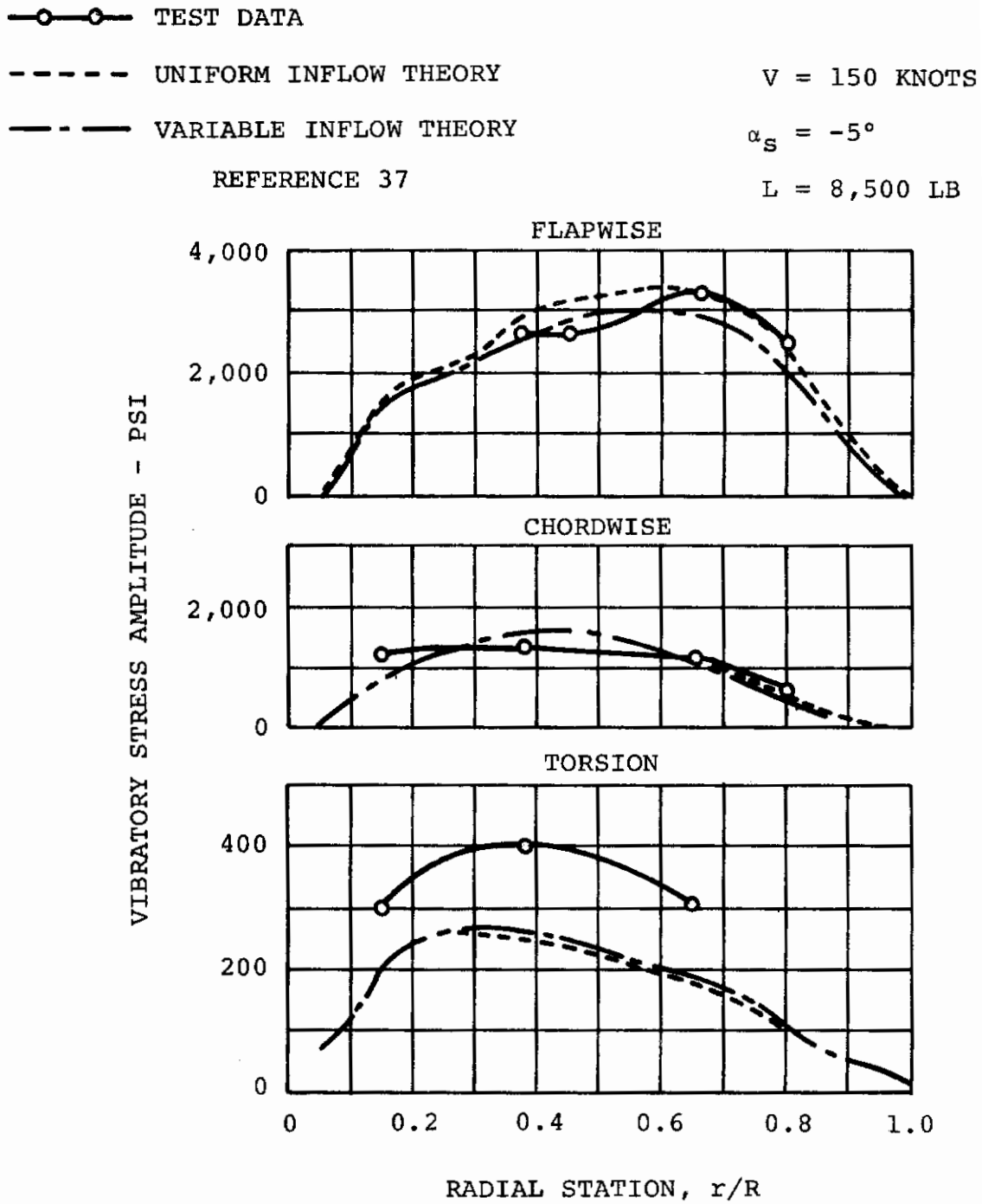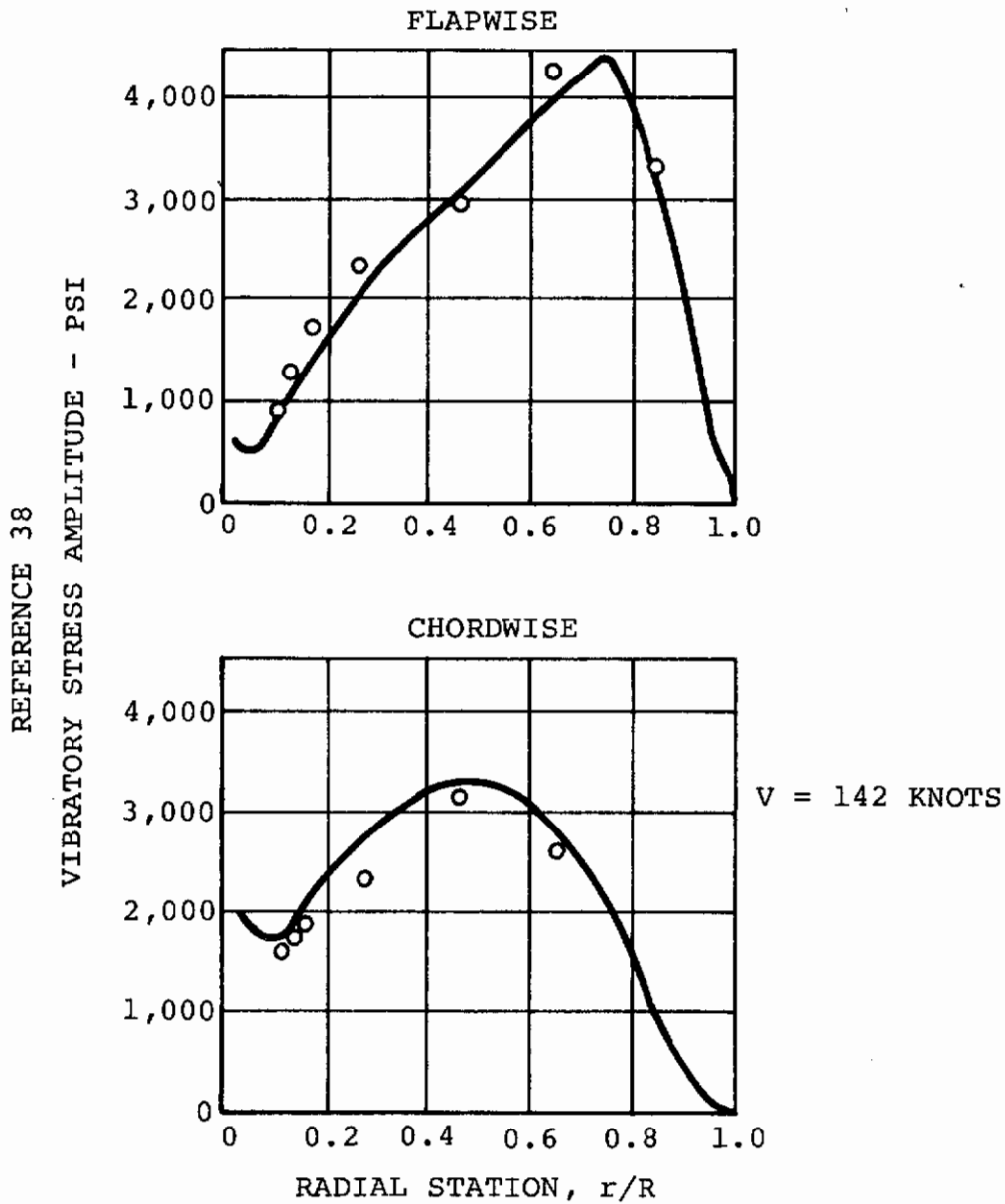1. Coleman, Robert P., and Feingold, Arnold M., THEORY OF SELF-EXCITED MECHANICAL OSCILLATIONS OF HELICOPTER ROTORS WITH HINGED BLADES, NACA T.N. 3844, 1957.

2. Gaffey, T. M., Yen, J. G., and Kvaternick, R. G., ANALYSIS AND MODEL TESTS OF THE PROP/ROTOR DYNAMICS OF A TILT-PROP/ROTOR VTOL AIRCRAFT, Presented at the Air Force V/STOL Technology and Planning Conference, Las Vegas, Nevada, September 1969.

3. Reed, Wilmer H. III, REVIEW OF PROPELLER-ROTOR WHIRL FLUTTER, NASA Technical Report, TR R-264, July 1967.

4. WIND TUNNEL TEST OF THE DYNAMICS AND AERODYNAMICS OF ROTOR SPIN-UP, STOPPING, AND FOLDING ON A SEMI-SPAN FOLDING TILT-ROTOR MODEL, AFFDL TR-71-62, Vol. VII.

5. FLUTTER AND DIVERGENCE TEST RESULTS ON A 1/22 DYNAMICALLY SCALED WINDMILLING MODEL OF THE M160, Boeing Document D8-2083, The Boeing Company, Vertol Division, Philadelphia, Pennsylvania.

6. Lytwyn, R. T., Miao, W., and Woitsch, W., AIRBORNE AND GROUND RESONANCE OF HINGELESS ROTORS, Proceedings of the 26th American Helicopter Society Forum, Preprint No. 414, June 1970.

7. Hohenemser, Kurt H., and Heaton, Paul W., Jr., AEROELASTIC INSTABILITY OF TORSIONALLY RIGID HELICOPTER BLADES, Journal of the American Helicopter Society, Vol. 12, No. 2, April 1967.

8. Johnston, J. F., and Cook, J. R., AH-56 VEHICLE DEVELOPMENT, American Helicopter Society, Preprint No. 574.

9. Hohenemser, Kurt H., and Perisho, Clarence H., ANALYSIS OF THE VERTICAL FLIGHT DYNAMIC CHARACTERISTICS OF THE LIFTING ROTOR WITH FLOATING HUB AND OFF-SET CONING HINGES, Journal of the American Helicopter Society, Vol. 3, No. 4, October 1958.

10. Miller, Rene H., and Ellis, Charles W., BLADE VIBRATION AND FLUTTER, Journal of the American Helicopter Society, Vol. 1, No. 3, July 1956.

11. DuWaldt, F. A., Gates, C. A., and Piziali, R. A., INVESTIGATION OF HELICOPTER ROTOR BLADE FLUTTER AND FLAPWISE BENDING RESPONSE IN HOVERING, WADC Technical Report 59-403, August 1959.

12. Daughaday, H., DuWaldt, F., and Gates, C., INVESTIGATION OF HELICOPTER BLADE FLUTTER AND LOAD AMPLIFICATION PROBLEMS, Journal of the American Helicopter Society, Vol. 2, No. 3, July 1957.

13. Goland, Leonard, and Perlmutter, A. A., A COMPARISON OF THE CALCULATED AND OBSERVED FLUTTER CHARACTERISTICS OF A HELICOPTER ROTOR BLADE HAVING BOTH CONTROL SYSTEM AND BLADE FLEXIBILITY, Forrestal Research Center, Princeton University, Report No. 333, December 1955.

14. Loewy, Robert G., A TWO-DIMENSIONAL APPROXIMATION TO THE UNSTEADY AERODYNAMICS OF ROTARY WINGS, Journal of the Aeronautical Sciences, Vol. 24, No. 2, February 1957.

15. Morduchow, M., and Hinchey, F. G., THEORETICAL ANALYSIS OF OSCILLATIONS IN HOVERING OF HELICOPTER BLADES WITH INCLINED AND OFFSET FLAPPING AND LAGGING HINGE AXES, NACA TN 2226, December 1950.

16. Pei Chi Chou, PITCH-LAG INSTABILITY OF HELICOPTER ROTORS, Journal of the American Helicopter Society, Vol. 3, No. 3, July 1958.

17. Blake, B. B., Burkam, J. E., and Loewy, R. G., RECENT STUDIES OF THE PITCH-LAG INSTABILITIES OF ARTICULATED ROTORS, Journal of the American Helicopter Society, Vol. 6, No. 3, July 1961.

18. Gaffey, Troy M., THE EFFECT OF POSITIVE PITCH-FLAP COUPLING (NEGATIVE δ_3) ON ROTOR BLADE MOTION STABILITY AND FLAPPING, American Helicopter Society, Preprint No. 227, May 1968.

19. Young, M. I., A THEORY OF ROTOR BLADE MOTION STABILITY IN POWERED FLIGHT, Journal of the American Helicopter Society, Vol. 9, No. 3, July 1965.

20. Daughaday, H., and Piziali, R. A., AN IMPROVED COMPUTATIONAL MODEL FOR PREDICTING THE UNSTEADY AERODYNAMIC LOADS OF ROTOR BLADES, Journal of the American Helicopter Society, October 1966.

21. Miller, R. H., UNSTEADY AIRLOADS ON HELICOPTER ROTOR BLADES, Journal of the Royal Aeronautical Society, April 1964.

22. Miller, R. H., ON THE COMPUTATION OF AIRLOADS ACTING ON ROTOR BLADES IN FORWARD FLIGHT, Journal of the American Helicopter Society, April 1962.

23. Blankenship, B. L., and Harvey, K. W., A DIGITAL ANALYSIS FOR HELICOPTER PERFORMANCE AND ROTOR BLADE BENDING MOMENTS, Journal of the American Helicopter Society, October 1962.

24. LaForge, S. V., EFFECT OF BLADE STALL ON ROTOR AND CONTROL SYSTEM LOADS, Hughes Tool Company, Aircraft Division, Report Number HTC-62-59, April 1963.

25. LaForge, S. V., EFFECTS OF BLADE STALL ON HELICOPTER ROTOR BLADE BENDING AND TORSIONAL LOADS, Hughes Tool Company, Aircraft Division, Report Number 347-V-1002 (HTC AD-64-8), May 1965.

26. Berman, A., RESPONSE MATRIX METHOD OF ROTOR BLADE ANALYSIS, Journal of the Aeronautical Sciences, Vol. 23, No. 2, February 1956.

27. Myklestad, N. O., VIBRATION ANALYSIS, McGraw-Hill Book Company, Inc., 1956.

28. Targoff, W., THE BENDING VIBRATIONS OF A TWISTED ROTATING BEAM, WADC Technical Report Number 56-27, December 1955.

29. Wood, E. R., and Hilzinger, K. D., A METHOD FOR DETER- MINING THE FULLY COUPLED AEROELASTIC RESPONSE OF HELICOPTER ROTOR BLADES, Proceedings of the Nineteenth Annual Forum of the American Helicopter Society, pp 28-37, May 1963.

30. Wood, E. R., Hilzinger, K. D., and Buffalano, A. C., AN AEROELASTIC STUDY OF HELICOPTER ROTOR SYSTEMS IN HIGH SPEED FLIGHT, Proceedings of CAL/TRECOM Symposium, June 1963.

31. Leone, P. F., THEORY OF ROTOR BLADE UNCOUPLED FLAP BENDING AEROELASTIC VIBRATIONS, Proceedings of the Tenth Annual Forum of the American Helicopter Society, pp 60-112, June 1954.

32. Leone, P. F., THEORY OF ROTOR BLADE UNCOUPLED LAG BENDING AEROELASTIC VIBRATIONS, Proceedings of the Eleventh Annual Form of the American Helicopter Society, pp 155- 172, May 1955.

33. Leone, P. F., THEORETICAL AND EXPERIMENTAL STUDY OF THE COUPLED FLAP BENDING AND TORSION AEROELASTIC VIBRATIONS OF A HELICOPTER ROTOR BLADE, Proceedings of the Thirteenth Annual Form of the American Helicopter Society, pp 92-110, May 1957.

34. Bisplinghoff, R. L., Ashley, H., and Halfman, R. L., AEROELASTICITY, Addison-Wesley Publishing Company, Inc., 1955.

35. Lemnlos, A., Smith, A., and Berman, A., THE AEROELASTIC BEHAVIOR OF ROTARY WINGS IN FORWARD FLIGHT, Kaman Aircraft Corp., Report Nos. R585, 585-1, 585-2, Vols. I, II, and III.

36. Davenport, F., DOWNWASH THEORY FOR TANDEM ROTORS, Journal of the American Helicopter Society, July 1964.

37. Rabbott, J. P., Jr., Lizak, A., and Paglino, V. M., A PRESENTATION OF MEASURED AND CALCULATED FULL-SCALE BLADE AERODYNAMIC AND STRUCTURAL LOADS, USAAVLABS Technical Report TR66-31, July 1966.

38. Fenaughty, R., and Beno, E. A., A STUDY OF MEASURED PARAMETRIC EFFECTS OF ROTOR LOADING ON BLADE AIRLOADS, BLADE RESPONSE, AND HUB FORCES ON A HIGH SPEED COMPOUND HELICOPTER, AIAA Paper 68-980, Fifth Annual Meeting, October 1968.

UNCLASSIFIED
_____
Security Classification

DOCUMENT CONTROL DATA - R & D
(Security classification of title, body of abstract and indexing annotation must be entered when the overall report is classified)

1. ORIGINATING ACTIVITY *(Corporate author)*	2a. REPORT SECURITY CLASSIFICATION
THE BOEING COMPANY, Vertol Division Boeing Center, P. O. Box 16858 Philadelphia, Pennsylvania 19142	Unclassified
	2b. GROUP

3. REPORT TITLE

V/STOL DYNAMICS AND AEROELASTIC ROTOR-AIRFRAME TECHNOLOGY
VOLUME I.   STATE-OF-THE-ART REVIEW OF V/STOL ROTOR TECHNOLOGY

4. DESCRIPTIVE NOTES *(Type of report and inclusive dates)*
Final Report, February 1971 - February 1972

5. AUTHOR(S) *(First name, middle initial, last name)*
H. R. Alexander
P. F. Leone

6. REPORT DATE	7a. TOTAL NO. OF PAGES	7b. NO. OF REFS
January 1973	115	38

8a. CONTRACT OR GRANT NO. F33615-71-C-1310	9a. ORIGINATOR'S REPORT NUMBER(S)
b. PROJECT NO. 1370	D210-10464-1
c. Task No. 137005	9b. OTHER REPORT NO(S) *(Any other numbers that may be assigned this report)* AFFDL-TR-72-40, Volume I
d.	

10. DISTRIBUTION STATEMENT

Distribution limited to U. S. Government agencies only; test and evaluation; statement applied 18 April 1972. Other requests for this document must be referred to the AF Flight Dynamics Laboratory, (FY), Wright-Patterson AFB, Ohio 45433.

11. SUPPLEMENTARY NOTES Volume I of a 3-volume report	12. SPONSORING MILITARY ACTIVITY Air Force Flight Dynamics Laboratory Air Force Systems Command Wright-Patterson Air Force Base, Ohio

13. ABSTRACT

The aeroelastic phenomena associated with prop/rotor systems are discussed and classified. It is concluded that an acceptable technology exists in several areas, including wing/rotor divergence, whirl flutter, aeromechanical instability, and air and ground resonance.

The technology is less successful in those areas where the flow through the rotor is significantly nonaxial, e.g., tilt-rotor transition regime and high-speed helicopter flight; also when forms of intermodal blade coupling exist due to finite deflections of the blades. It is believed that, in addition to collective deflections, finite cyclical deflections of the blades produce destabilizing coupling effects in some cases. Significantly large edgewise flow in combination with nonzero blade steady-state deflections is also seen to be destabilizing.

A minimum-complexity methodology which may be expected to correlate with currently identified phenomena is defined.

The methods contained in this report are intended to be used by designers to calculate with improved accuracy, the dynamic and aeroelastic response characteristics of rotor powered V/STOL aircraft. The essential new feature of these methods is that the coupled flap-pitch-lag blade deflections are taken into account. These calculations are essential if a high level of confidence is to be had in the results.

DD FORM 1473
1 NOV 65

UNCLASSIFIED
_____
Security Classification

UNCLASSIFIED
_____
Security Classification

14. KEY WORDS	LINK A		LINK B		LINK C	
	ROLE	WT	ROLE	WT	ROLE	WT
Stability in V/STOL aircraft						
Undesirable aeroelastic effects						
Rotor/airframe instabilities						
Wing/rotor divergence						
Whirl flutter						
Oscillatory behavior						
Blade instability mechanisms						
Blade vibratory loads						
Source of airloads						
Blade loads						
Mathematical model						
Industry review						

Security Classification